

Scientific Advisory Board

Ayşegül Akgün

Ege University, Medical School, Department of Nuclear Medicine, İzmir, Turkey

Esma Akın

The George Washington University, Medical School, Department of Diagnostic Radiology, Washington DC, USA

Claudine Als

Hopitiaux Robert Schuman Zitha Klinik, Médecine Nucléaire, Luxembourg

Vera Artiko

Clinical Center of Serbia, Center for Nuclear Medicine, Belgrade, Serbia

Nuri Arslan

Health Sciences University, Gülhane Medical School, Gülhane Training and Research Hospital, Clinic of Nuclear Medicine, Ankara, Turkey

Marika Bajc

Lund University Hospital, Clinic of Clinical Physiology, Lund, Sweden

Lorenzo Biassoni

Great Ormond Street Hospital for Children NHS Foundation Trust, Department of Radiology, London, United Kingdom

Hans Jürgen Biersack

University of Bonn, Department of Nuclear Medicine, Clinic of Radiology, Bonn, Germany

M. Donald Blafox

Albert Einstein College of Medicine, Department of Radiology, Division of Nuclear Medicine, New York, USA.

Patrick Bourguet

Centre Eugène Marquis, Department of Nuclear Medicine, Clinic of Radiology, Rennes, France

A. Cahid Civelek

NIH Clinical Center, Division of Nuclear Medicine, Bethesda, USA

Arturo Chiti

Humanitas University, Department of Biomedical Sciences; Humanitas Clinical and Research Center, Clinic of Nuclear Medicine, Milan, Italy

Josep Martin Comin

Hospital Universitari de Bellvitge, Department of Nuclear Medicine, Barcelona, Spain

Alberto Cuocolo

University of Naples Federico II, Department of Advanced Biomedical Sciences, Napoli, Italy

Tevfik Fikret Çermik

Health Sciences University, İstanbul Training and Research Hospital, Clinic of Nuclear Medicine, İstanbul, Turkey

Angelika Bischof Delaloye

University Hospital of Lausanne, Department of Radiology, Lausanne, Switzerland

Mustafa Demir

İstanbul University, Cerrahpaşa Medical School, Department of Nuclear Medicine, İstanbul, Turkey

Hakan Demir

Kocaeli University Medical School, Department of Nuclear Medicine, Kocaeli, Turkey

Peter Josef Ell

University College Hospital, Institute of Nuclear Medicine, London, United Kingdom

Tanju Yusuf Erdil

Marmara University, Pendik Training and Research Hospital, Clinic of Nuclear Medicine, İstanbul, Turkey

Türkan Ertay

Dokuz Eylül University, Medical School, Department of Nuclear Medicine, İzmir, Turkey

Jure Fettich

University Medical Centre Ljubljana, Department for Nuclear Medicine, Ljubljana, Slovenia

Christiane Franzius

Klinikum Bremen Mitte Center, Center for Modern Diagnostics, Bremen, Germany

Lars Friberg

University of Copenhagen Bispebjerg Hospital, Department of Nuclear Medicine, Copenhagen, Denmark

The Owner on Behalf of Turkish Society of Nuclear Medicine

Prof. Gamze Çapa Kaya, MD.

Dokuz Eylül University, Medical School, Department of Nuclear Medicine, İzmir, Turkey

Publishing Manager

Prof. Zehra Özcan, MD.

Ege University, Medical School, Department of Nuclear Medicine, İzmir, Turkey

E-mail: zehra.ozcan@yahoo.com

Editor in Chief

Prof. Zehra Özcan, MD.

Ege University, Medical School, Department of Nuclear Medicine, İzmir, Turkey

E-mail: zehra.ozcan@yahoo.com

ORCID ID: 0000-0002-6942-4704

Associate Editor

Associate Prof. Murat Fani Bozkurt, MD. Hacettepe University, Medical School, Department of Nuclear Medicine, Ankara, Turkey

E-mail: fanibozkurt@gmail.com

ORCID ID: 0000-0003-2016-2624

Prof. Tanju Yusuf Erdil, MD. Marmara University Medical School, Department of Nuclear Medicine, İstanbul, Turkey

E-mail: yerdil@marmara.edu.tr

ORCID ID: 0000-0002-5811-4321

Associate Prof. Nalan Selçuk, MD. Yeditepe University, Medical School, Department of Nuclear Medicine, İstanbul, Turkey

E-mail: nalanselcuk@yeditepe.edu.tr

ORCID ID: 0000-0002-3738-6491

Statistics Editors

Prof. Gül Ergör, MD.

Dokuz Eylül University, Medical School, Department of Public Health, İzmir, Turkey

E-mail: gulergor@deu.edu.tr

Prof. Sadettin Kılıçkap, MD.

Hacettepe University, Medical School, Department of Preventive Oncology, Ankara, Turkey

E-mail: skilickap@yahoo.com

English Language Editor

Didem Öncel Yakar, MD.

İstanbul, Turkey

Jørgen Frøkiær

Aarhus University Hospital, Clinic of Nuclear Medicine and PET, Aarhus, Denmark

Maria Lyra Georgosopoulou

University of Athens, 1st Department of Radiology, Aretaieion Hospital, Radiation Physics Unit, Athens, Greece

Gevorg Gevorgyan

The National Academy of Sciences of Armenia, H. Buniatian Institute of Biochemistry, Yerevan, Armenia

Seza Güleç

Florida International University Herbert Wertheim College of Medicine, Departments of Surgery and Nuclear Medicine, Miami, USA

Liselotte Højgaard

University of Copenhagen, Department of Clinical Physiology, Nuclear Medicine and PET, Rigshospitalet, Copenhagen, Denmark

Ora Israel

Tel Aviv University Sackler Medical School, Assaf Harofeh Medical Center, Clinic of Otolaryngology-Head and Neck Surgery, Haifa, Israel

Csaba Juhasz

Wayne State University Medical School, Children's Hospital of Michigan, PET Center and Translational Imaging Laboratory, Detroit, USA

Metin Kır

Ankara University, Medical School, Department of Nuclear Medicine, Ankara, Turkey

Irena Dimitrova Kostadinova

Alexandrovska University Hospital, Clinic of Nuclear Medicine, Sofia, Bulgaria

Lale Kostakoğlu

The Mount Sinai Hospital, Clinic of Nuclear Medicine, New York, USA

Rakesh Kumar

All India Institute of Medical Sciences, Department of Nuclear Medicine, New Delhi, India

Georgios S. Limouris

Athens University, Medical School, Department of Nuclear Medicine, Athens, Greece

Luigi Mansi

Second University of Naples, Medical School, Department of Nuclear Medicine, Naples, Italy

Yusuf Menda

University of Iowa Health Care, Carver College of Medicine, Department of Radiology, Iowa City, USA

Vladimir Obradović

University of Belgrade, Faculty of Organizational Sciences, Department of Human Development Theory, Business Administration, Organizational Studies, Belgrade, Serbia

Yekta Özer

Hacettepe University, Faculty of Pharmacy, Department of Radiopharmaceutical, Ankara, Turkey

Francesca Pons

Hospital Clinic, Clinic of Nuclear Medicine, Barcelona, Spain

Monica Rossleigh

Sydney Children's Hospital, Clinic of Nuclear Medicine, Sydney, Australia

Dragana Sobic Saranovic

University of Belgrade, Medical School, Departments of Radiology, Oncology and Cardiology, Belgrade, Serbia

Mike Sathegke

University of Pretoria, Steve Biko Academic Hospital, Department of Nuclear Medicine, Pretoria, South Africa

Kerim Sönmezoğlu

İstanbul University, Cerrahpaşa Medical School, Department of Nuclear Medicine, İstanbul, Turkey

Zsolt Szabo

The Johns Hopkins Hospital, Divisions of Radiology and Radiological Science, Baltimore, USA

Istvan Szilvasi

Semmelweis University, Medical School, Department of Nuclear Medicine, Budapest, Hungary

Berna Okudan Tekin

Ankara Numune Training and Research Hospital, Clinic of Nuclear Medicine, Ankara, Turkey

Mathew L. Thakur

Thomas Jefferson University, Department of Radiology, Pennsylvania, USA

Bülent Turgut

Cumhuriyet University, Medical School, Department of Nuclear Medicine, Sivas, Turkey

Gülin Uçmak

Health Sciences University, Ankara Oncology Training and Research Hospital, Clinic of Nuclear Medicine, Ankara, Turkey

Doğangün Yüksel

Pamukkale University, Medical School, Department of Nuclear Medicine, Denizli, Turkey

Turkish Society of Nuclear Medicine

Cinnah Caddesi Pilot Sokak No: 10/12 Çankaya 06650 Ankara, Turkey Phone: +90 312 441 00 45 Fax: +90 312 441 12 95 Web: www.tsnm.org E-mail: dernekmerkezi@tsnm.org

"Formerly Turkish Journal of Nuclear Medicine"

© The paper used to print this journal conforms to ISO 9706: 1994 standard (Requirements for Permanence). The National Library of Medicine suggests that biomedical publications be printed on acid-free paper (alkaline paper). Reviewing the articles' conformity to the publishing standards of the Journal, typesetting, reviewing and editing the manuscripts and abstracts in English, creating links to source data, and publishing process are realized by Galenos.

**Galenos Publishing House Owner and Publisher**

Erkan Mor

Publication Director

Nesrin Çolak

Web Coordinators

Soner Yıldırım

Turgay Akpınar

Web Assistant

Başak Büşra Yılmaz

Graphics Department

Ayda Alaca

Çiğdem Birinci

Project Coordinators

Eda Koluksa

Hatice Balta

Lütfiye Ayhan İrtem

Zeynep Altındağ

Project Assistants

Esra Semerci

Günay Selimoğlu

Sedanur Sert

Finance Coordinator

Sevinç Çakmak

Research&Development

Deniz Slepstov

Publisher Contact

Address: Molla Gürani Mah. Kaçamak Sk. No: 21/1

34093 İstanbul, Turkey

Phone: +90 (212) 621 99 25 Fax: +90 (212) 621 99 27

E-mail: info@galenos.com.tr/yayin@galenos.com.tr

Web: www.galenos.com.tr

Printing at: Özgün Ofset Ticaret Ltd. Şti.

Yeşilce Mah. Aytekin Sk. No: 21 34418 4. Levent, İstanbul, Turkey

Phone: +90 (212) 280 00 09

Printing Date: 10 October 2018

ISSN: 2146-1414 E-ISSN: 2147-1959

International scientific journal published quarterly.



Molecular Imaging and Radionuclide Therapy (formerly Turkish Journal of Nuclear Medicine) is the official publication of Turkish Society of Nuclear Medicine.

Focus and Scope

Molecular Imaging and Radionuclide Therapy (Mol Imaging Radionucl Ther, MIRT) is a double-blind peer-review journal published in English language. It publishes original research articles, reviews, editorials, short communications, letters, consensus statements, guidelines and case reports with a literature review on the topic, interesting images in the field of molecular imaging, multimodality imaging, nuclear medicine, radionuclide therapy, radiopharmacy, medical physics, dosimetry and radiobiology. MIRT is published three times a year (February, June, October). Audience: Nuclear medicine physicians, medical physicists, radiopharmaceutical scientists, radiobiologists.

The editorial policies are based on the "Recommendations for the Conduct, Reporting, Editing, and Publication of Scholarly Work in Medical Journals (ICMJE Recommendations)" by the International Committee of Medical Journal Editors (2016, archived at <http://www.icmje.org/>) rules.

Open Access Policy

This journal provides immediate open access to its content on the principle that making research freely available to the public supports a greater global exchange of knowledge.

Open Access Policy is based on rules of Budapest Open Access Initiative (BOAI) (<http://www.budapestopenaccessinitiative.org/>). By "open access" to [peer-reviewed research literature], we mean its free availability on the public internet, permitting any users to read, download, copy, distribute, print, search, or link to the full texts of these articles, crawl them for indexing, pass them as data to software, or use them for any other lawful purpose, without financial, legal, or technical barriers other than those inseparable from gaining access to the internet itself. The only constraint on reproduction and distribution, and the only role for copyright in this domain, should be to give authors control over the integrity of their work and the right to be properly acknowledged and cited.

This journal is licensed under a Creative Commons 3.0 International License.

Permission Requests

Permission required for use any published under CC-BY-NC license with commercial purposes (selling, etc.) to protect copyright owner and author rights). Republication and reproduction of images or tables in any published material should be done with proper citation of source providing authors names; article title; journal title; year (volume) and page of publication; copyright year of the article.

Instructions for Authors

Instructions for authors are published in the journal and on the website <http://mirt.tsnmjournals.org>

Manuscripts can only be submitted electronically through the Journal Agent website (<http://www.journalagent.com/mirt/?plng=eng>) after creating an account. This system allows online submission and review.

All published volumes in full text can be reached free of charge through the website <http://mirt.tsnmjournals.org>

Material Disclaimer

Scientific and legal responsibilities pertaining to the papers belong to the authors. Contents of the manuscripts and accuracy of references are also the author's responsibility. The Turkish Society of Nuclear Medicine, the Editor, the Editorial Board or the publisher do not accept any responsibility for opinions expressed in articles.

Financial expenses of the journal are covered by Turkish Society of Nuclear Medicine.

Correspondence Address

Editor-in-Chief, Prof. Zehra Özcan, MD,

Ege University, Medical School, Department of Nuclear Medicine, İzmir, Turkey

Phone: +90 312 441 00 45

Fax: +90 312 441 12 97

E-mail: editor@tsnmjournals.org

Web page: <http://mirt.tsnmjournals.org>

Publisher Corresponding Address

Galenos Yayınevi Tic. Ltd. Şti.

Address: Molla Gürani Mah. Kaçamak Sk. No: 21/1 34093

Fındıkzade, İstanbul, Turkey

Phone: +90 212 621 99 25

Fax: +90 212 621 99 27

E-mail: info@galenos.com.tr

The journal is printed on an acid-free paper.

INSTRUCTIONS TO AUTHORS

Molecular Imaging and Radionuclide Therapy (Mol Imaging Radionucl Ther, MIRT) publishes original research articles, short communications, reviews, editorials, case reports with a literature review on the topic, interesting images, consensus statements, guidelines, letters in the field of molecular imaging, multimodality imaging, nuclear medicine, radionuclide therapy, radiopharmacy, medical physics, dosimetry and radiobiology. MIRT is published by the Turkish Society of Nuclear Medicine three times a year (February, June, October). The journal is printed on an acid-free paper.

Molecular Imaging and Radionuclide Therapy does not charge any article submission or processing fees.

GENERAL INFORMATION

MIRT commits to rigorous peer review, and stipulates freedom from commercial influence, and promotion of the highest ethical and scientific standards in published articles. Neither the Editor(s) nor the publisher guarantees, warrants or endorses any product or service advertised in this publication. All articles are subject to review by the editors and peer reviewers. If the article is accepted for publication, it may be subjected to editorial revisions to aid clarity and understanding without changing the data presented.

Manuscripts must be written in English and must meet the requirements of the journal. The journal is in compliance with the uniform requirements for manuscripts submitted to biomedical journals published by the International Committee of Medical Journal Editors (NEJM 1997; 336:309-315, updated 2016). Manuscripts that do not meet these requirements will be returned to the author for necessary revision before the review. Authors of manuscripts requiring modifications have a maximum of two months to resubmit the revised text. Manuscripts returned after this deadline will be treated as new submissions.

It is the authors' responsibility to prepare a manuscript that meets ethical criteria. The Journal adheres to the principles set forth in the Helsinki Declaration October 2013 (<https://www.wma.net/policies-post/wma-declaration-of-helsinki-ethical-principles-for-medical-research-involving-human-subjects/>) and holds that all reported research involving "Human beings" conducted in accordance with such principles.

Reports describing data obtained from research conducted in human participants must contain a statement in the MATERIALS AND METHODS section indicating approval by the ethical review board (including the approval number) and affirmation that INFORMED CONSENT was obtained from each participant.

All manuscripts reporting experiments using animals must include a statement in the MATERIALS AND METHODS section giving assurance that all animals have received humane care in compliance with the Guide for the Care and Use of Laboratory Animals (www.nap.edu) and indicating approval by the ethical review board.

If the study should have ethical approval, authors asked to provide ethical approval in order to proceed the review process. If they provide approval, review of the manuscript will continue.

In case report(s) and interesting image(s) a statement regarding the informed consent of the patients should be included in the manuscript and the identity of the patient(s) should be hidden.

Subjects must be identified only by number or letter, not by initials or names. Photographs of patients' faces should be included only if scientifically relevant. Authors must obtain written consent from the patient for use of such photographs.

In cases of image media usage that potentially expose patients' identity requires obtaining permission for publication from the patients or their parents/guardians. If the proposed publication concerns any commercial product, the author must include in the cover letter a statement indicating that the author(s) has (have) no financial or other interest with the product or explaining the nature of any relations (including consultancies) between the author(s) and editor the manufacturer or distributor of the product.

All submissions will be screened by Crossref Similarity Check powered by "iThenticate". Manuscripts with an overall similarity index of greater than 25%, or duplication rate at or higher than 5% with a single source will be returned back to authors.

MANUSCRIPT CATEGORIES

1. Original Articles
2. Short Communications are short descriptions of focused studies with important, but very straightforward results.
3. Reviews address important topics in the field. Authors considering the submission of uninvited reviews should contact the editor in advance to determine if the topic that they propose is of current potential interest to the Journal. Reviews will be considered for publication only if they are written by authors who have at least three published manuscripts in the international peer reviewed journals and these studies should be cited in the review. Otherwise only invited reviews will be considered for peer review from qualified experts in the area.
4. Editorials are usually written by invitation of the editor by the editors on current topics or by the reviewers involved in the evaluation of a submitted manuscript and published concurrently with that manuscript.
5. Case Report and Literature Reviews are descriptions of a case or small number of cases revealing a previously undocumented disease process, a unique unreported manifestation or treatment of a known disease process, unique unreported complications of treatment regimens or novel and important insights into a condition's pathogenesis, presentation, and/or management. The journal's policy is to accept case reports only if it is accompanied by a review of the literature on the related topic. They should include an adequate number of images and figures.
6. Interesting Image
One of the regular parts of Molecular Imaging and Radionuclide Therapy is a section devoted to interesting images. Interesting image(s) should describe case(s) which are unique and include interesting findings adding insights into the interpretation of patient images, a condition's pathogenesis, presentation, and/or management.
7. Consensus Statements or Guidelines may be submitted by professional societies. All such submissions will be subjected to peer review, must be modifiable in response to criticisms, and will be published only if they meet the Journal's usual editorial standards.
8. Letters to the Editor may be submitted in response to work that has been published in the Journal. Letters should be short commentaries related to specific points of agreement or disagreement with the published work.

Note on Prior Publication

Articles are accepted for publication on the condition that they are original, are not under consideration by another journal, or have not been previously

INSTRUCTIONS TO AUTHORS

published. Direct quotations, tables, or illustrations that have appeared in copyrighted material must be accompanied by written permission for their use from the copyright owner and authors. Materials previously published in whole or in part shall not be considered for publication. At the time of submission, authors must report that the manuscript has not been published elsewhere. Abstracts or posters displayed at scientific meetings need not be reported.

MANUSCRIPT SUBMISSION PROCEDURES

MIRT only accepts electronic manuscript submission at the web site <http://www.journalagent.com/mirt/>. After logging on to the website Click the 'online manuscript submission' icon. All corresponding authors should be provided with a password and a username after entering the information required. If you already have an account from a previous submission, enter your username and password to submit a new or revised manuscript. If you have forgotten your username and/or password, please send an e-mail to the editorial office for assistance. After logging on to the article submission system please read carefully the directions of the system to give all needed information and attach the manuscript, tables and figures and additional documents.

All Submissions Must Include:

1. Completed Copyright Assignment & Disclosure of Potential Conflict of Interest Form; This form should be downloaded from the website (provided in the author section), filled in thoroughly and uploaded to the website during the submission.
2. All manuscripts describing data obtained from research conducted in human participants must be accompanied with an approval document by the ethical review board.
3. All manuscripts reporting experiments using animals must include approval document by the animal ethical review board.
4. All submissions must include the authorship contribution form which is signed by all authors.

Authors must complete all online submission forms. If you are unable to successfully upload the files please contact the editorial office by e-mail.

MANUSCRIPT PREPARATION

General Format

The Journal requires that all submissions be submitted according to these guidelines:

- Text should be double spaced with 2.5 cm margins on both sides using 12-point type in Times Roman font.
- All tables and figures must be placed after the text and must be labeled.
- Each section (abstract, text, references, tables, figures) should start on a separate page.
- Manuscripts should be prepared as a word document (*.doc) or rich text format (*.rtf).
- Please make the tables using the table function in Word.
- Abbreviations should be defined in parenthesis where the word is first mentioned and used consistently thereafter.
- Results should be expressed in metric units. Statistical analysis should be done accurately and with precision. Please consult a statistician if necessary.

- Authors' names and institutions should not be included in the manuscript text and should be written only in the title page.

Title Page

The title page should be a separate form from the main text and should include the following:

- Full title (in English and in Turkish). Turkish title will be provided by the editorial office for the authors who are not Turkish speakers.
- Authors' names and institutions.
- Short title of not more than 40 characters for page headings.
- At least three and maximum eight keywords. (in English and in Turkish). Do not use abbreviations in the keywords. Turkish keywords will be provided by the editorial office for the authors who are not Turkish speakers. If you are not a native Turkish speaker, please reenter your English keywords to the area provided for the Turkish keywords. English keywords should be provided from <http://www.nlm.nih.gov/mesh> (Medical Subject Headings) while Turkish keywords should be provided from <http://www.bilimterimleri.com>.
- Word count (excluding abstract, figure legends and references).
- Corresponding author's e-mail and address, telephone and fax numbers.
- Name and address of person to whom reprint requests should be addressed.

Original Articles

Authors are required to state in their manuscripts that ethical approval from an appropriate committee and informed consents of the patients were obtained.

Original Articles should be submitted with a structured abstract of no more than 250 words. All information reported in the abstract must appear in the manuscript. The abstract should not include references. Please use complete sentences for all sections of the abstract. Structured abstract should include background, objective, methods, results and conclusions. Turkish abstract will be provided by the editorial office for the authors who are not Turkish speakers. If you are not a native Turkish speaker, please reenter your English abstract to the area provided for the Turkish abstract.

- Introduction
- Materials and Methods
- Results
- Discussion
- Study Limitations
- Conclusion

May be given for contributors who are not listed as authors, or for grant support of the research.

References should be cited in numerical order (in parentheses) in the text and listed in the same numerical order at the end of the manuscript on a separate page or pages. The author is responsible for the accuracy of references. Examples of the reference style are given below. Further examples will be found in the articles describing the Uniform Requirements for Manuscripts Submitted to Biomedical Journals (Ann Intern Med.1988; 208:258-265, Br Med J. 1988; 296:401-405). The titles of journals should be abbreviated according to the style used in the Index Medicus. Journal Articles and Abstracts: Surnames and initials of author's name, title of the article, journal name, date, volume number, and pages. All authors should be listed regardless of number. The citation of unpublished papers, observations or personal communications is not permitted. Citing an abstract is

INSTRUCTIONS TO AUTHORS

not recommended. Books: Surnames and initials of author's names, chapter title, editor's name, book title, edition, city, publisher, date and pages.

Sample References

Journal Article: Sayit E, Söylev M, Capa G, Durak I, Ada E, Yilmaz M. The role of technetium-99m-HMPAO-labeled WBC scintigraphy in the diagnosis of orbital cellulitis. *Ann Nucl Med* 2001;15:41-44.

Erselcan T, Hasbek Z, Tandogan I, Gumus C, Akkurt I. Modification of Diet in Renal Disease equation in the risk stratification of contrast induced acute kidney injury in hospital inpatients. *Nefrologia* 2009 doi: 10.3265/Nefrologia.2009.29.5.5449.en.full.

Article in a journal published ahead of print: Ludbrook J. Musculo-venous pumps in the human lower limb. *Am Heart J* 2009;00:1-6. (accessed 20 February 2009).

Lang TF, Duryea J. Peripheral Bone Mineral Assessment of the Axial Skeleton: Technical Aspects. In: Orwoll ES, Bliziotes M (eds). *Osteoporosis: Pathophysiology and Clinical Management*. New Jersey, Humana Press Inc, 2003;83-104.

Books: Greenspan A. *Orthopaedic Radiology a Practical Approach*. 3th ed. Philadelphia, Lippincott Williams Wilkins 2000, 295-330.

Website: Smith JR. 'Choosing Your Reference Style', *Online Referencing* 2(3), <http://orj.sagepub.com> (2003, accessed October 2008).

- Tables

Tables must be constructed as simply as possible. Each table must have a concise heading and should be submitted on a separate page. Tables must not simply duplicate the text or figures. Number all tables in the order of their citation in the text. Include a title for each table (a brief phrase, preferably no longer than 10 to 15 words). Include all tables in a single file following the manuscript.

- Figure Legends

Figure legends should be submitted on a separate page and should be clear and informative.

- Figures

Number all figures (graphs, charts, photographs, and illustrations) in the order of their citation in the text. At submission, the following file formats are acceptable: AI, EMF, EPS, JPG, PDF, PPT, PSD, TIF. Figures may be embedded at the end of the manuscript text file or loaded as separate files for submission. All images MUST be at or above intended display size, with the following image resolutions: Line Art 800 dpi, Combination (Line Art + Halftone) 600 dpi, Halftone 300 dpi. Image files also must be cropped as close to the actual image as possible.

Short Communications:

Short communications should be submitted with a structured abstract of no more than 200 words. These manuscripts should be no longer than 2000 words, and include no more than two figures and tables and 20 references. Other rules which the authors are required to prepare and submit their manuscripts are the same as described above for the original articles.

Review Articles:

- Title page (see above)

- Abstract: Maximum 250 words; without structural divisions; in English and in Turkish. Turkish abstract will be provided by the editorial office for the authors who are not Turkish speakers. If you are not a native Turkish speaker, please reenter your English abstract to the area provided for the Turkish abstract.

- Text

- Conclusion

- Acknowledgements (if any)

- References

Editorial:

- Title page (see above)

- Abstract: Maximum 250 words; without structural divisions; in English and in Turkish. Turkish abstract will be provided by the editorial office for the authors who are not Turkish speakers. If you are not a native Turkish speaker, please reenter your English abstract to the area provided for the Turkish abstract.

- Text

- References

Case Report and Literature Review

- Title page (see above)

- Abstract: Approximately 100-150 words; without structural divisions; in English and in Turkish. Turkish abstract will be provided by the editorial office for the authors who are not Turkish speakers. If you are not a native Turkish speaker, please re-enter your English abstract to the area provided for the Turkish abstract.

- Introduction

- Case report

- Literature Review and Discussion

- References

Interesting Image:

No manuscript text is required. Interesting Image submissions must include the following:

Title Page: (see Original article section)

Abstract: Approximately 100-150 words; without structural divisions; in English and in Turkish. Turkish abstract will be provided by the editorial office for the authors who are not Turkish speakers. If you are not a native Turkish speaker, please re-enter your English abstract to the area provided for the Turkish abstract.

Image(s): The number of images is left to the discretion of the author. (See Original article section)

Figure Legend: Reference citations should appear in the legends, not in the abstract. Since there is no manuscript text, the legends for illustrations should be prepared in considerable detail but should be no more than 500 words total. The case should be presented and discussed in the Figure legend section.

References: Maximum eight references (see original article section).

Letters to the Editor:

- Title page (see above)

- Short comment to a published work, no longer than 500 words, no figures or tables.

- References no more than five.

Consensus Statements or Guidelines: These manuscripts should typically be no longer than 4000 words and include no more than six figures and tables and 120 references.

INSTRUCTIONS TO AUTHORS

Proofs and Reprints

Proofs and a reprint orders are sent to the corresponding author. The author should designate by footnote on the title page of the manuscript the name and address of the person to whom reprint requests should be directed. The manuscript when published will become the property of the journal.

Archiving

The editorial office will retain all manuscripts and related documentation (correspondence, reviews, etc.) for 12 months following the date of publication or rejection.

Submission Preparation Checklist

As part of the submission process, authors are required to check off their submission's compliance with all of the following items, and submissions may be returned to authors that do not adhere to these guidelines.

1. The submission has not been previously published, nor is it before another journal for consideration (or an explanation has been provided in Comments to the Editor).
2. The submission file is in Microsoft Word, RTF, or WordPerfect document file format. The text is double-spaced; uses a 12-point font; employs italics, rather than underlining (except with URL addresses); and the location for all illustrations, figures, and tables should be marked within the text at the appropriate points.
3. Where available, URLs for the references will be provided.
4. All authors should be listed in the references, regardless of the number.
5. The text adheres to the stylistic and bibliographic requirements outlined in the Author Guidelines, which is found in About the Journal.
6. English keywords should be provided from <http://www.nlm.nih.gov/mesh> (Medical Subject Headings), while Turkish keywords should be provided from <http://www.bilimterimleri.com>
7. The title page should be a separate document from the main text and should be uploaded separately.
8. The "Affirmation of Originality and Assignment of Copyright/The Disclosure Form for Potential Conflicts of Interest Form" and Authorship Contribution Form should be downloaded from the website, filled thoroughly and uploaded during the submission of the manuscript.

TO AUTHORS

Copyright Notice

The author(s) hereby affirms that the manuscript submitted is original, that all statement asserted as facts are based on author(s) careful investigation and

research for accuracy, that the manuscript does not, in whole or part, infringe any copyright, that it has not been published in total or in part and is not being submitted or considered for publication in total or in part elsewhere. Completed Copyright Assignment & Affirmation of Originality Form will be uploaded during submission. By signing this form;

1. Each author acknowledges that he/she participated in the work in a substantive way and is prepared to take public responsibility for the work.
2. Each author further affirms that he or she has read and understands the "Ethical Guidelines for Publication of Research".
3. The author(s), in consideration of the acceptance of the manuscript for publication, does hereby assign and transfer to the Molecular Imaging and Radionuclide Therapy all of the rights and interest in and the copyright of the work in its current form and in any form subsequently revised for publication and/or electronic dissemination.

Privacy Statement

The names and email addresses entered in this journal site will be used exclusively for the stated purposes of this journal and will not be made available for any other purpose or to any other party.

Peer Review Process

1. The manuscript is assigned to an editor, who reviews the manuscript and makes an initial decision based on manuscript quality and editorial priorities.
2. For those manuscripts sent for external peer review, the editor assigns at least two reviewers to the manuscript.
3. The reviewers review the manuscript.
4. The editor makes a final decision based on editorial priorities, manuscript quality, and reviewer recommendations.
5. The decision letter is sent to the author.

Contact Address

All correspondence should be directed to the Editorial Office:

Cinnah Caddesi Pilot Sokak No:10/12 06650 Çankaya / Ankara, Turkey

Phone: +90 312 441 00 45

Fax: +90 312 441 12 97

E-mail: info@tsnmjournals.org

Original Articles

- 99** Unexpected False-positive I-131 Uptake in Patients with Differentiated Thyroid Carcinoma
Diferansiyel Tiroid Karsinomlu Hastalarda Beklenmeyen Yanlış Pozitif I-131 Tutulumu
Aylin Oral, Bülent Yazıcı, Cenk Eraslan, Zeynep Burak; İzmir, Turkey
- 107** ^{18}F -FDG PET/CT in Patients with Parenchymal Changes Attributed to Radiation Pneumonitis
Radyasyon Pnömonisine Bağlı Parankimal Değişiklikleri Olan Hastalarda ^{18}F -FDG PET/CT
Anastas Krassenov Demirev, Irena Dimitrova Kostadinova, Iliya Rumenov Gabrovski; Sofia, Bulgaria
- 113** Benchmarking of a Simple Scintigraphic Test for Gastro-oesophageal Reflux Disease That Assesses Oesophageal Disease and Its Pulmonary Complications
Basit Bir Yöntem Olan Gastro-özefageal Reflü Sintigrafisi ile Özefagus Hastalığı ve Pulmoner Komplikasyonların Değerlendirilmesi
Leticia Burton, Gregory L. Falk, Stephen Parsons, Mel Cusi, Hans Van Der Wall; Sydney, Australia
- 121** I-131 mIBG Scintigraphy Curie Versus SIOPEN Scoring: Prognostic Value in Stage 4 Neuroblastoma
I-131 mIBG Sintigrafisi Curie ve SIOPEN Skorlarının Evre 4 Nöroblastomada Prognostik Değerinin Karşılaştırılması
Saima Riaz, Humayun Bashir, Saadiya Javed Khan, Abid Qazi; Lahore, Pakistan
- 126** Diagnostic Value of ^{18}F -FDG PET/CT in Patients with Carcinoma of Unknown Primary
Primeri Bilinmeyen Kanselerde ^{18}F -FDG PET/CT'nin Tanısal Değeri
Arzu Cengiz, Sibel Göksel, Yakup Yürekli; Aydın, Turkey
- Interesting Images**
- 133** Incidental ^{18}F -FDG Uptake of the Pubic Ramus and Abdominal Muscles due to Athletic Pubalgia During Acute Prostatitis
Akut Prostatit Sırasında Ramus Pubis ve Abdominal Kaslarda Atletik Pubaljiye Bağlı İncidental ^{18}F -FDG Tutulumu
Olivier Rager, Marlise Picarra, Emmanouil Astrinakis, Valentina Garibotto, Gaël Amzalag; Geneva, Switzerland
- 136** Synchronous Hepatocellular Carcinoma and Cholangiocellular Carcinoma on ^{18}F -FDG PET/CT
 ^{18}F -FDG PET/CT'de Senkron Hepatosellüler Karsinoma ve Kolanjiyosellüler Karsinoma
Ezgi Başak Erdoğan, Hacı Mehmet Türk, Ertuğrul Tekçe, Mehmet Aydın; İstanbul, Turkey
- 138** ^{18}F -FDG PET/CT Findings of Non-Hodgkin Lymphoma Involving the Whole Genitourinary System
Ürogenital Sistemin Tamamını Tutan Non-Hodgkin Lenfomada ^{18}F -FDG PET/CT Bulguları
Aylin Oral, Bülent Yazıcı, Özgür Ömür; İzmir, Turkey
- 141** Masking Effect of Radiopharmaceutical Dose Extravasation During Injection on Myocardial Perfusion Defects During SPECT Myocardial Perfusion Imaging: A Potential Source of False Negative Result
SPECT Miyokard Perfüzyon Sintigrafisi Sırasında Radyofarmasötik Doz Ekstravazasyonunun Miyokard Perfüzyon Defektlerini Maskeleyen Etkisi: Olası Bir Yanlış Negatif Sonuç Nedeni
Mohsen Qutbi; Tehran, Iran
- 144** Colonic Malignant Melanoma: ^{18}F -FDG PET/CT Findings
Kolonda Malign Melanoma: ^{18}F -FDG PET/CT Bulguları
Eser Kaya, Tamer Aksoy, Ahmet Levent Güner, Hakan Temiz, Erkan Vardareli; İstanbul, Turkey
- 146** Lung Perfusion Imaging in Tetralogy of Fallot: A Case Report
Fallot Tetralojisinde Akciğer Perfüzyon Görüntüleme: Bir Olgu Sunumu
Artor Niccoli Asabella, Alessandra Cimino, Corinna Altini, Valentina Lavelli, Giuseppe Rubini; Bari, Italy



Unexpected False-positive I-131 Uptake in Patients with Differentiated Thyroid Carcinoma

Diferansiye Tiroid Karsinomlu Hastalarda Beklenmeyen Yanlış Pozitif I-131 Tutulumu

✉ Aylin Oral¹, ✉ Bülent Yazıcı¹, ✉ Cenk Eraslan², ✉ Zeynep Burak¹

¹Ege University Faculty of Medicine, Department of Nuclear Medicine, İzmir, Turkey

²Ege University Faculty of Medicine, Department of Radiology, İzmir, Turkey

Abstract

Objective: Radioiodine is the most specific radionuclide for differentiated thyroid carcinoma (DTC) imaging. Despite its high specificity and sensitivity, false-positive I-131 uptake could be seen on whole body scan (WBS) that may lead to misdiagnosis and unnecessary radioiodine treatment. In this study, we aimed to present the I-131 WBS and concomitant single photon emission computed tomography/computed tomography (SPECT/CT) images of unexpected false-positive radioiodine uptake along with the patients' clinical outcomes and the contribution of SPECT/CT imaging.

Methods: I-131 WBSs of 1507 patients with DTC were retrospectively reviewed, and anticipated I-131 uptakes (like in breasts or thymus) were excluded from the study. The unexpected false-positive I-131 uptakes with concomitant SPECT/CT imaging were included in the study.

Results: Twenty-one patients had 23 unexpected I-131 uptakes on WBS and concomitant SPECT/CT imaging. The vast majority (87%) of these cases were seen on post-therapeutic I-131 WBS. Most of the false-positive I-131 uptakes could be explained by SPECT/CT and radiologic findings, and were secondary to non-thyroid conditions (bronchiectasis, lung infection, subcutaneous injection into gluteal fatty tissue, aortic calcification, benign bone cyst, vertebral hemangioma, recent non-thyroid surgical procedure site, rotator cuff injury, mature cystic teratoma and ovarian follicle cyst). However, the possible reasons of 9 false-positive I-131 uptakes could not be explained by radiologic findings.

Conclusion: We suggest that false-positive I-131 uptake and its underlying mechanisms (inflammation, trapping, increased perfusion, etc.) must be kept in mind in patients with thyroid cancer and unexpected findings must be considered together with serum thyroglobulin levels, SPECT/CT and radiologic findings in order to avoid misdiagnosis and unnecessary radioiodine treatment.

Keywords: I-131, radioiodine, scintigraphy, SPECT/CT, thyroid, cancer

Öz

Amaç: Radyoaktif iyot diferansiye tiroid karsinomu (DTK) görüntülemesinde kullanılan en yüksek özgüllüğe sahip radyonüklididir. Duyarlılık ve özgüllüğü yüksek olmakla birlikte I-131 tüm vücut tarama sintigrafisinde (TVTS) yanlış pozitif I-131 tutulumu görülebilmekte ve bu durum tanınal güçlüklerle ve gereksiz tedavi uygulanmasına neden olabilmektedir. Bu çalışmada I-131 TVTS'de izlenen beklenmedik yanlış pozitif I-131 tutulumlarına ait TVTS ve tek foton emisyon bilgisayarlı tomografisi/bilgisayarlı tomografi (SPECT/BT) görüntüleme bulguları ile hastaların klinik sonuçlarının ve SPECT/BT görüntülemenin katkısının sunulması amaçlanmıştır.

Yöntem: Kliniğimizde takipli 1507 DTK tanılı hastaya ait I-131 TVTS'leri retrospektif olarak incelendi ve alışılmamış yanlış pozitif I-131 tutulumları (timüs, meme gibi) çalışma dışında bırakıldı. Eş zamanlı SPECT/BT görüntüleri olan ve beklenen alanlar dışında izlenen yanlış pozitif I-131 tutulumları çalışmaya dahil edildi.

Address for Correspondence: Aylin Oral MD, Ege University Faculty of Medicine, Department of Nuclear Medicine, İzmir, Turkey
Phone: +90 505 265 62 77 E-mail: draylinoral@yahoo.com ORCID ID: orcid.org/0000-0001-8014-4327

Received: 15.02.2018 **Accepted:** 03.07.2018

©Copyright 2018 by Turkish Society of Nuclear Medicine
Molecular Imaging and Radionuclide Therapy published by Galenos Yayınevi.

Bulgular: Yirmi bir hastada 23 adet eş zamanlı SPECT/BT ile lokalize edilen, beklenmedik yanlış pozitif I-131 tutulumu saptandı. Bulguların büyük çoğunluğu (%87) post-terapötik TVTS'de izlendi. Yanlış pozitif tutulumların çoğunun eş zamanlı SPECT/BT ve radyolojik bulgular ile tiroid dışı nedenlere (bronşektazi, akciğer enfeksiyonu, gluteal yağlı dokuya subkutan enjeksiyon, aort kalsifikasyonu, benign kemik kisti, vertebral hemanjiom, yakın zamanlı tiroid dışı cerrahi girişim, rotator kılıf yaralanması, matür kistik teratom ve overde follikül kisti) bağlı olduğu anlaşıldı. Dokuz hastada ise yanlış pozitif iyot tutulumu radyolojik görüntüleme bulguları ile açıklanamadı.

Sonuç: Tiroid kanserli hastalarda yanlış pozitif I-131 tutulumunun izlenebileceği ve altta yatan mekanizmaları (enflamasyon, kanlanma artışı, kistik lezyonda tutulum vb.) akılda tutularak, beklenmeyen I-131 tutulumlarının serum tiroglobulin düzeyi, SPECT/BT ve radyolojik verilerle birlikte değerlendirilerek gereksiz tedavilerin önüne geçilmesi gerektiği sonucuna varılmıştır.

Anahtar kelimeler: I-131, radyoaktif iyot, sintigrafi, SPECT/BT, tiroid, kanser

Introduction

Differentiated thyroid carcinoma (DTC), including papillary and follicular thyroid cancer, represents over 90% of all thyroid cancer cases (1). The primary treatment of choice in DTC is surgery (1,2). DTC patients, except microcarcinomas with no extension beyond the thyroid capsule and without lymph node or distant metastasis, receive radioiodine treatment after surgery (3). Radioiodine is the most specific (>90%) radionuclide for DTC imaging (3). Post-therapeutic I-131 whole body scan (WBS) is used for restaging while diagnostic I-131 WBS is used for the follow-up of DTC patients. Despite its high specificity and sensitivity, false-positive I-131 uptake could be seen on I-131 WBS (4,5,6,7,8,9,10). Functional (residual or metastatic) thyroid tissue is not the only tissue that accumulates radioiodine, but also salivary glands, liver, breasts and thymus could accumulate radioiodine. Also, gastrointestinal and urinary system can be visualized in radioiodine scans due to iodine excretion. In addition to these organs and systems, unexpected and false-positive radioiodine accumulation could be seen on I-131 WBS which might lead to misdiagnosis and unnecessary radioiodine treatment (8,9). Further imaging modalities are usually required to explain the unexpected I-131 uptake, but it is difficult to guide further examinations due to the absence of anatomical location data on planar imaging protocols. In such cases, single photon emission computed tomography/computed tomography (SPECT/CT) hybrid imaging is a very useful modality to determine the exact anatomic localization of the I-131 avid foci that was detected on I-131 WBS. CT component of the hybrid imaging not only improves attenuation correction, but also improves the planar data interpretation by offering the opportunity to differentiate between abnormal and physiologic structures, and sometimes low dose CT images help to diagnose the underlying pathology.

In this study, we aimed to present the imaging findings [I-131 WBS, SPECT/CT, magnetic resonance imaging (MRI), etc.], and clinical outcomes of patients as well as the contribution of SPECT/CT imaging in unexpected false-positive I-131 accumulation, and to discuss the underlying etiology of these cases.

Materials and Methods

Patients

From May 2012 to April 2015, 1507 DTC patients' radioiodine scans were retrospectively reviewed. Radioiodine contaminations and expected physiologic I-131 uptakes like in the breasts or thymus were excluded from the study. Concomitant SPECT/CT imaging was performed to determine the exact anatomical localization of the I-131 avid foci on WBS and to exclude contaminations and expected physiologic I-131 uptakes. The unexpected I-131 uptakes on WBS were determined as false-positive for DTC; if non-thyroid pathologies were demonstrated by SPECT/CT and/or radiologic imaging, or no anatomic pathologies were detected by concomitant SPECT/CT or further radiologic imagings with low serum thyroglobulin (Tg) levels and negative follow-up diagnostic I-131 scans. According to these parameters, 21 patients with 23 unexpected false-positive I-131 uptakes were included in the study.

Follow-up Protocol

In order to prevent thyroid remnants from stunning, diagnostic I-131 WBSs were not performed before the administration of therapeutic dose. Radioiodine therapy was performed according to the guideline for radioiodine therapy of DTC (11). In the presence of abnormal findings on post-therapeutic or diagnostic I-131 WBS, concomitant SPECT/CT imaging was performed. Afterwards, further diagnostic investigations were performed in patients with abnormal laboratory or imaging findings and in patients with persistent disease, repetitive radioiodine therapies were administered at least 3 months after I-131 WBS.

Imaging Protocol

Planar I-131 WBS was performed in both anterior and posterior projections using dual-head gamma-camera (Infinia Hawkeye 4[®], GE Healthcare) with high-energy, parallel-hole collimators. Continuous acquisition mode was used at a table speed of 8 cm/min with a 1,024x256 matrix. The photopeak was 364 keV with a $\pm 10\%$ window. Additional images were required in case of unexpected iodine uptakes or accumulations that give an impression

of physiologic uptake (scanning after drinking a glass of water to wash out physiologic uptake in the esophagus) or contamination (scanning after removing the contamination and taking off the stained clothes). Additional spot views are performed using a 256x256 matrix for 5 min/view.

Imaging with SPECT/CT requires a long scanning time. Therefore, in our department SPECT/CT (Infinia Hawkeye 4[®], GE Healthcare) is not performed routinely. SPECT/CT imaging is performed for specific sites which are determined by a nuclear medicine physician based on the WBS and additional spot images. Emission SPECT images are acquired with a matrix size of 128x128, and the photopeak was 364 keV with a $\pm 10\%$ window. A total image of 60 frames is acquired over 360° with an acquisition time of 40 s/frame, angular step of 6, and zooming factor of 1. After SPECT acquisition, a CT scan is acquired for attenuation correction with a low-dose, 4-slice helical CT scanner. The CT parameters are 140 kV and 2.5 mAs. The images are reconstructed with conventional iterative algorithm, ordered subset expectation maximization and fused with CT images by using software (Xeleris[®], GE Healthcare) for multiplanar reformatted image display.

Results

Twenty-one patients with 23 unexpected false-positive I-131 uptakes were reviewed. The vast majority (87%) of unexpected findings were seen in post-therapeutic I-131 WBS after first ablation treatment, while the rest (13%) were seen on diagnostic WBSs.

The study included 21 patients with a median age of 58 (range 28-77 years) and a female/male ratio of 2.5:1. Nineteen patients had papillary thyroid carcinoma while 2 patients had follicular thyroid carcinoma. The histologic subtypes of papillary thyroid carcinoma were conventional in 10 (48%), follicular variant in 8 (38%) patients and 1 (5%) patient had oncocyctic variant of papillary thyroid carcinoma.

Out of the 23 unexpected findings, the number of lesions located in the cranial, thoracic, abdominal and pelvic regions were 1, 15, 1 and 6, respectively. One of the patients had false-positive I-131 uptakes in both the thoracic and pelvic regions. Also, one patient had 2 false-positive uptakes in the thoracic region, one of them in the lung and the other on the rib. The locations and possible etiologies of unexpected false-positive iodine uptakes are listed in Table 1.

Evaluation of the unexpected uptakes in the thoracic region (n=15), which was the most common region of false-positive I-131 uptakes in our study, revealed that 14 of them were focal uptakes while one was a mild and diffuse uptake like a thick band in the lung. On SPECT/CT images, 5, 2, 2, 1 and 5 of the false-positive uptakes in the thoracic region were located in the lung parenchyma, vascular structures, inflamed soft tissue, anterior mediastinum and bones, respectively.

Serum Tg levels of the patients with unexpected I-131 uptakes in the lung parenchyma were low (0.3-19 ng/mL) in terms of lung metastasis. In two patients with focal activity accumulation in the lung parenchyma, it was remarkable that on CT images there were findings concordant with bronchiectasis on the same area of I-131 uptake on SPECT/CT images (Figure 1). In 2 cases, no pathology was detected that could explain the I-131 uptake in the lungs. In one case, while there was a mild and diffuse I-131 uptake that was shaped like a thick band on the left lung in SPECT/CT images, no pathologic finding was found on this area on CT images (Figure 2). On inquiry, the patient had a history of using antibiotics due to lung infection approximately one month ago. The radioiodine uptake was thought to be secondary to the previous lung infection.

The concomitant SPECT/CT imaging of five of the unexpected I-131 uptakes in the thoracic region demonstrated that I-131 involvements were localized to the bone. Serum Tg levels of these patients were low (0.3-11.9 ng/mL) for bone metastasis. In 4 cases, the activity accumulations were located to the ribs. However, no etiology that could cause I-131 involvement was determined. Focal I-131 uptake of one case was located to the clavicle. This patient has been reported as a case-report earlier, in whom the focal I-131 uptake corresponded to a hypodense area in the left clavicle on CT images (4). An MRI revealed that the finding belonged to a benign lesion, a simple bone cyst.

One patient was treated with high dose I-131 because of multiple lung metastases with a serum Tg level of 279 ng/mL. On post-therapeutic I-131 WBS, besides the lung metastases, an intense I-131 uptake was determined at the posterior upper zone of the right hemi-thorax (Figure 3). SPECT/CT images demonstrated that the uptake was adjacent to the right scapula, and localized to skin/subcutaneous soft tissue. Moreover, surgical sutures were present in this area. It was understood that the patient had an operation due to a soft tissue lesion adjacent to the scapula before radioactive iodine (RAI) treatment, the pathology report of that lesion was interpreted as spindle-cell mesenchymal tumor. Following the second RAI treatment, the patient had no pathologic findings on I-131 WBSs and no clinical complaints. At the end of 3-years of follow-up period, the patient still has a mildly elevated serum Tg level (7.5 ng/mL) with thyroid-stimulating hormone stimulation.

Serum Tg levels of other 4 unexpected focal I-131 uptakes in the thoracic region were between 0.2 and 8 ng/mL. On SPECT/CT images, 2 of these 4 patients had focal I-131 uptake that was in accordance with aortic wall calcification and one patient had focal I-131 uptake in the anterior mediastinum without any density change on CT images. The other patient had an I-131 accumulation on the left shoulder on planar WBS that was adjacent to the left humeral head on SPECT/CT images. On inquiry, it was learned that the patient had a history of rotator cuff tear of

the left shoulder. It was thought that the I-131 uptake was secondary to this condition.

When the unexpected uptakes in the pelvic region (n=6), which was the second most common region of false-positive I-131 uptakes in our study, were further evaluated, it was remarkable that all unexpected findings were identified on post-therapeutic scans with low serum Tg levels (0.2-4.6 ng/dL).

On SPECT/CT images, the I-131 uptakes of 2 patients correlated to the ovaries. One of these patients was operated due to an ovarian-origin lesion and was diagnosed with mature cystic teratoma without thyroid tissue. This patient has been presented as a case report earlier (5). In the other case with I-131 uptake in the ovary, an ovarian hypo-dense cystic area was monitored on SPECT/CT images (Figure 4). Pelvic ultrasound (USG) demonstrated no pathology except a follicle cyst and it was thought that the I-131 uptake in the ovary was secondary to this cystic lesion.

Focal activity accumulation was observed in the pelvic region in 3 patients on posterior image of post-therapeutic I-131 WBS (Figure 5). It was hard to distinguish those activities from urinary contamination, so additional planar spot images were obtained. If the pelvic uptakes were persistent then concomitant SPECT/CT imaging was performed. On SPECT/CT images, it was found that the uptakes were localized to gluteal adipose tissue and it was evident that they matched with old injection sites in subcutaneous fatty tissue on CT images. On inquiry, all 3 cases had a history of gluteal injections within the last 2 months. Therefore, no further examination was required for these patients.

On post-therapeutic I-131 WBS, a patient had focal I-131 uptakes in the left hemithorax and posterior pelvic region. The patient's serum Tg level was low (3.7 ng/dL) for metastasis. The thoracic radioiodine uptake corresponded to the rib, and no pathologic finding was found on CT images. The uptake in the posterior pelvic region corresponded to the fifth lumbar vertebra on SPECT/CT.

Table 1. Localization sites and possible etiologies of false positive I-131 uptakes

Patient no	I-131 WBS (post-therapeutic/diagnostic)	SPECT/CT region	Localization of unusual I-131 uptake	Tg* (ng/mL)	Follow-up Tg** (ng/mL)	Etiology
1	Post-therapeutic	Thoracic	Soft tissue	3.2	<0.2	Rotator cuff injury
2	Post-therapeutic	Thoracic	Soft tissue	279	7.5	Inflammation after surgery
3	Post-therapeutic	Thoracic	Vascular structure	8	<0.2	Aortic calcification
4	Post-therapeutic	Thoracic	Vascular structure	1.4	<0.2	Aortic calcification
5	Post-therapeutic	Thoracic	Mediastinum	0.2	<0.2	Undetermined
6	Post-therapeutic	Thoracic	Lung	0.3	<0.2	Bronchiectasis
7	Post-therapeutic	Thoracic	Lung	10	<0.2	Bronchiectasis
8	Post-therapeutic	Thoracic	Lung	8	0.7	Lung infection
9	Post-therapeutic	Thoracic	Lung	19	1.9	Undetermined
10	Diagnostic	Thoracic	Lung	0.3	<0.2	Undetermined
10	Diagnostic	Thoracic	Bone-rib	0.3	<0.2	Undetermined
11	Post-therapeutic	Thoracic	Bone-rib	11.9	1.0	Undetermined
12	Post-therapeutic	Thoracic	Bone-rib	3.4	<0.2	Undetermined
13	Post-therapeutic	Thoracic	Bone-clavicle	2.4	<0.2	Benign bone cyst
14	Post-therapeutic	Thoracic	Bone-rib	3.7	0.3	Undetermined
14	Post-therapeutic	Pelvic	Bone-vertebrae	3.7	0.3	Vertebral hemangioma
15	Post-therapeutic	Pelvic	Soft tissue	0.2	<0.2	Subcutaneous injection site
16	Post-therapeutic	Pelvic	Ovary	1.4	<0.2	Mature cystic teratoma
17	Post-therapeutic	Pelvic	Ovary	7.2	<0.2	Follicle cyst
18	Post-therapeutic	Pelvic	Soft tissue	2.2	<0.2	Subcutaneous injection site
19	Post-therapeutic	Pelvic	Soft tissue	0.6	<0.2	Subcutaneous injection site
20	Post-therapeutic	Abdominal	Soft tissue	5.2	<0.2	Undetermined
21	Diagnostic	Head	Bone-calvarium	0.5	0.2	Undetermined

*Serum thyroglobulin level at false positive uptake on I-131 WBS, **Serum thyroglobulin level at follow-up I-131 whole body scan. WBS: Whole body scan, SPECT/CT: Single photon emission computed tomography/computed tomography, Tg: Thyroglobulin

On MRI images there was a hyper-intense lesion on T1 and T2-weighted sequences in accordance with hemangioma in the fifth lumbar vertebra.

In a patient with a focal I-131 uptake on the right abdominal region, the uptake was found to correlate with soft tissue at the intercostal area adjacent to the liver on SPECT/CT

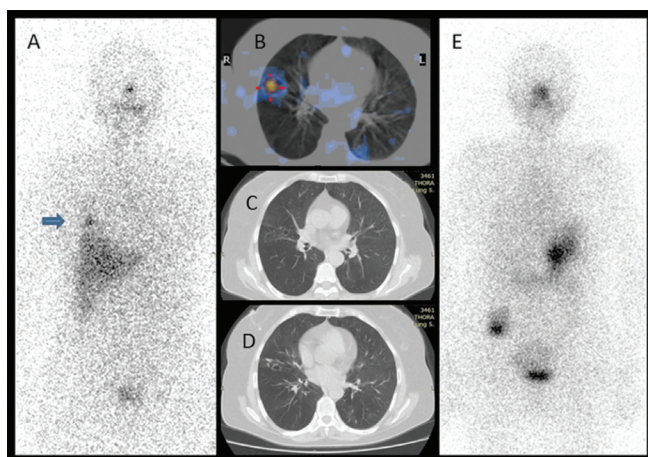


Figure 1. There was I-131 uptake at the lower zone of the right hemithorax on the anterior image of post-therapeutic I-131 whole body scan (A, arrow). The focal activity accumulation in the lung parenchyma on fused single photon emission computed tomography/computed tomography (CT) image (B), and findings on CT images (C, D) were concordant with bronchiectasis. The diagnostic I-131 scan (E) did not reveal any pathologic uptake and the serum thyroglobulin level was low (<0.2 ng/mL)

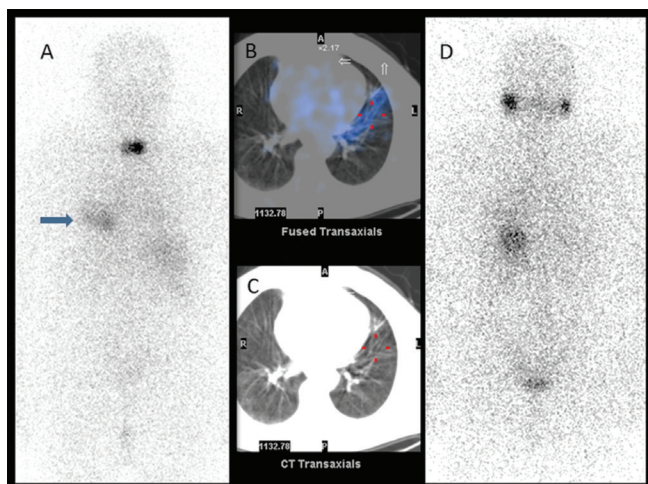


Figure 2. A mild diffuse I-131 uptake at the lower zone of the left hemithorax (arrow) was seen on posterior image of post-therapeutic I-131 whole body scan (A) in addition to residual thyroid tissue. The uptake in the left lung parenchyma was shaped like a thick band that could be compatible with the trajectory of a previous lung infection that was detected on fused single photon emission computed tomography/computed tomography images (B), and no pathologic finding was found on this area on computed tomography images (C). On diagnostic I-131 scan (D) there wasn't any pathologic uptake and the serum thyroglobulin level was low (0.7 ng/mL)

images. However, no etiology that can explain I-131 uptake could be detected by abdominal CT or USG.

During diagnostic I-131 WBS of one patient, focal activity accumulation was identified in the cranium on posterior planar image. On SPECT/CT, an activity was detected at the right parieto-occipital area. There wasn't any density change on CT images. No etiology could be found by 2 cranial MRIs obtained with an interval of 6 months.

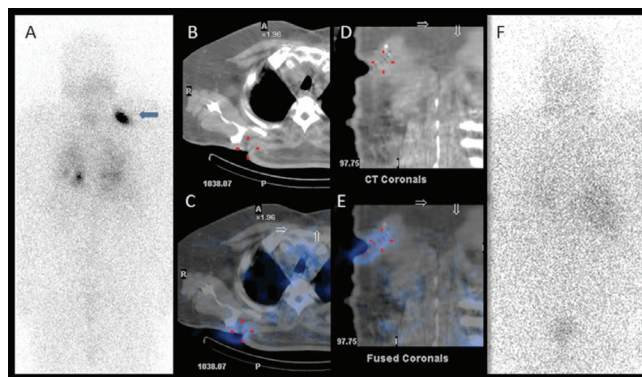


Figure 3. An intense I-131 uptake was identified at the upper zone of the right hemithorax (arrow) on posterior image of post-therapeutic I-131 whole body scan (A) in addition to lung metastasis. On axial computed tomography (CT) (B) and fused single photon emission computed tomography (SPECT)/CT images (C), the finding was adjacent to the right scapula, and localized to the skin/subcutaneous soft tissue. In addition, on coronal CT (D) and SPECT/CT images (E) surgical sutures related to a non-thyroidal soft tissue excision prior to radioiodine treatment were detected. On follow-up I-131 scan (F) there wasn't any pathologic uptake but the patient still had a mildly elevated serum thyroglobulin level (7.5 ng/mL) with thyroid-stimulating hormone stimulation

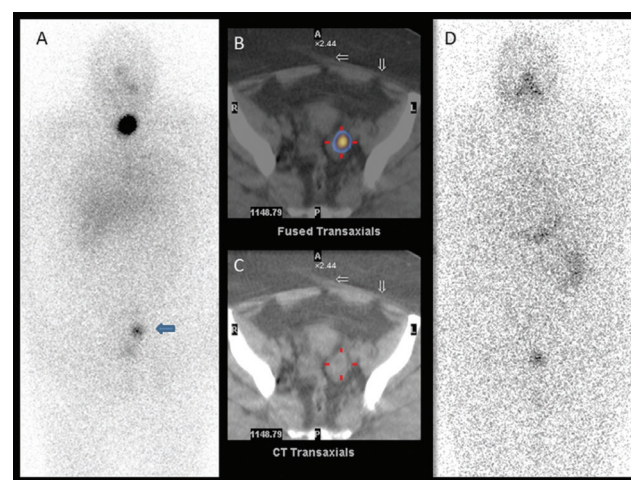


Figure 4. On anterior image of post-therapeutic I-131 whole body scan (A), in addition to residual thyroid tissue, there was a focal I-131 accumulation over the left side of the bladder (arrow). Fused single photon emission computed tomography/computed tomography (CT) image (B) showed that the I-131 uptake was localized to the left ovary and a hypodense cystic area in the left ovary was identified on CT image (C). The follow-up diagnostic I-131 scan (D) was normal and the thyroglobulin level was undetectable (<0.2 ng/mL)

Tg values were determined during follow-up diagnostic I-131 WBS in all cases, and varied between <0.2 and 1.9 ng/mL except the case with lung metastasis (stimulated Tg: 7.5 ng/mL, unstimulated Tg <0.2 ng/mL). There was no pathologic finding on diagnostic I-131 WBSs, and patients are being followed-up for 1-3 years as disease-free. All of the patients' unstimulated Tg levels remain low (0.2 ng/mL).

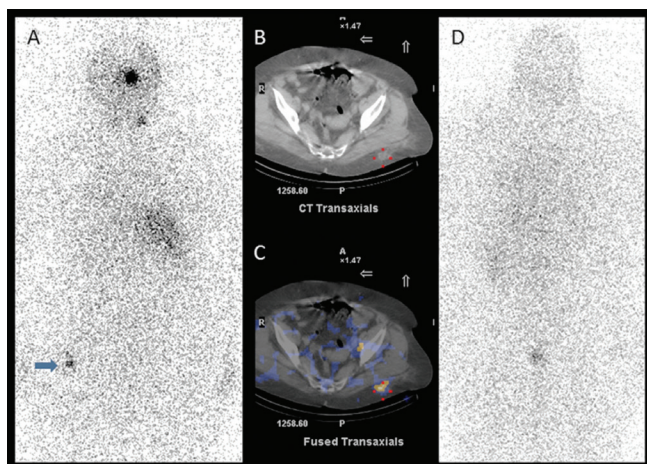


Figure 5. On posterior image of post-therapeutic I-131 whole body scan (A), in addition to residual thyroid tissue, there was a mild focal I-131 accumulation in the pelvic region (arrow). On axial computed tomography (CT) (B) and fused single photon emission computed tomography (SPECT)/CT (C) images, it was clear that the activity was located in the posterior gluteal soft tissue and there were density changes in the fatty tissue due to previous subcutaneous injections. The follow-up diagnostic I-131 scan (D) was normal and the thyroglobulin level was undetectable (<0.2 ng/mL)

Discussion

Sodium iodide symporter expression is one of the well-known mechanisms that is responsible for RAI uptake in tissues. The physiologic I-131 uptake in the thymus, breast, salivary gland and gastrointestinal system in addition to the thyroid tissue is explained with this mechanism. In addition, false-positive uptake might be encountered in I-131 WBSs by mechanisms such as metabolism of I-131-labeled thyroid hormones (liver uptake), retention and contamination of physiologic secretions and body fluids containing radioiodine (saliva, tears, sweat, urine, blood, exudate, transudate, gastric and mucosal secretions, etc.), uptake and retention of radioiodine in inflamed tissues. Nevertheless, mechanism of the uptake of activity observed in a group of patients is not completely understood yet (8,9).

Increased perfusion and vasodilation, and enhanced capillary permeability in pulmonary infections are suggested to cause I-131 accumulation (8). Although rare, false-positive I-131 uptake secondary to active or inactive lung

infections has been reported in the literature (12,13). Also, in this study, an accumulation of activity that was attributed to infection was observed in a patient with a previous history of lung infection.

Accumulation of bronchial secretions in bronchiectasis causes I-131 uptake (8). Focal I-131 accumulations that might be confused with lung metastasis due to bronchiectasis had been reported in the literature (14,15). Also, observation of activity accumulation in the bronchiectasis area in 2 patients in this study supports this finding.

To identify the exact localization of an uptake site on planar I-131 WBS is difficult due to the lack of anatomic landmarks. SPECT/CT, the hybrid imaging modality that combines SPECT scan with CT scan, is very useful to determine the exact anatomic location of the I-131 avid foci that is detected on I-131 WBS. Further imaging modalities are usually required to explain unexpected I-131 uptakes. CT component of the hybrid imaging improves the planar data interpretation by offering the opportunity to differentiate between abnormal and physiologic structures. Sometimes low dose CT component of SPECT/CT imaging helps to diagnose the underlying pathology. Maruoka et al. (16) reported that the interpretation was altered to be physiologic or benign uptake in 38% of patients with the addition of SPECT/CT. Also SPECT/CT imaging helps for choosing the optimal imaging modality (USG, MRI, contrast enhanced CT, etc.) if the CT component fails to determine the underlying etiology of an uptake site.

Three patients with I-131 uptake in the gluteal fatty tissue had a recent history of gluteal injection. This finding was thought to be secondary to the probable inflammation due to injection into the fatty tissue instead of the intramuscular area. False-positive I-131 uptake has been reported in the literature in the gluteal fatty tissue secondary to a granuloma due to foreign material (17).

Post-therapeutic imaging of the patient with a history of partial rotator cuff tear, and of the patient who received RAI following a previously performed surgery for a skin lesion suggested that transudate and inflammation that were produced due to tissue injury might be the possible etiology of the false-positive radioiodine uptake.

The etiology of focal I-131 uptake in the area of an aortic wall calcification is not entirely known. A false-positive uptake of I-131 has been reported in a case with aortic aneurysm in the literature (18). The aorta diameter was normal in the case presented herein, and this finding was thought to be secondary to atherosclerosis and a possible inflamed plaque corresponding to this area.

The incidence of vertebral hemangiomas is reported as approximately 11%, more frequently in the thoracic vertebrae in autopsy series. In this present study, the I-131 uptake in the lumbar vertebrae on SPECT/CT images in one case was compatible with a hemangioma as detected by MRI. The I-131 uptake in hemangiomas is

attributed to intravascular blood pooling and enhanced capillary permeability. A thoracic focal activity uptake in the posterior planar image secondary to a hemangioma has been previously reported in the literature (19).

In our study, ovarian I-131 accumulation was observed in 2 patients. One of them was diagnosed with mature cystic teratoma and has been previously reported as a case report (5). The other patient had no pathology except an ovarian follicle cyst. Functional follicle cysts have been reported to demonstrate I-131 accumulation in the literature (20). Also, there are several studies published in the literature reporting false-positive I-131 accumulation in cystic structures (7,8,21,22). Radioiodine enters cysts by passive diffusion and is trapped in the cyst (8). In this paper, a case with I-131 accumulation due to a benign bone cyst in the clavicle is also included, who has been previously reported (4).

In this study, the possible etiology of 9 false-positive I-131 uptakes in 8 patients remained unclear. I-131 uptakes in the remaining patients were mostly associated with inflammation. The radioiodine uptakes in the undetermined group were thought to be secondary to inflammation that could not be demonstrated by radiologic findings. This might be explained by recovery of the possible temporary and mild inflammation within the time period between radioiodine uptake and further radiologic examination (<4 weeks).

Evaluation of false-positive uptake in the neck area is important since it may be confused with residual thyroid tissue or metastatic lymph nodes. However, the contribution of adequate patient history (presence of metastatic disease, serum Tg values, findings of previous imaging studies and etc.) obtained from the clinician is very helpful on the evaluation of I-131 WBSs. SPECT/CT examination has significant importance to prevent unnecessary examinations and treatment, if available for the evaluation of unexpected radioiodine uptake.

The importance of prevention of unnecessary treatments has also been emphasized in the literature, by taking false-positive uptake rates and laboratory findings (Tg), clinical and imaging data into consideration in addition to I-131 WBS findings of a particular patient (6,14,23).

Conclusion

Unexpected radioiodine uptake secondary to various extra-thyroidal reasons (inflammation, increased blood supply, trapping in the cystic lesion, etc.) should be kept in mind while interpreting I-131 WBSs, especially in post-therapeutic scans due to the higher dose applied. In patients with notably discordant clinical and laboratory data, accurate localization of radioiodine uptake is important. At this point, SPECT/CT imaging is the method of choice to both localize the unexpected foci and aid differential diagnosis. It is concluded that the unexpected finding should be

enlightened by using different imaging models (MRI, USG, etc.) according to the specifications of the tissue thus preventing unnecessary treatment.

Ethics

Ethics Committee Approval: No ethics committee approval required since the study was retrospective.

Informed Consent: Written informed consent was obtained from each patient included in this study.

Peer-review: Externally peer-reviewed.

Authorship Contributions

Surgical and Medical Practices: A.O., B.Y., Concept: A.O., Z.B., Design: A.O., Z.B., Data Collection or Processing: A.O., B.Y., Analysis or Interpretation: A.O., C.E., Literature Search: A.O., Writing: A.O.

Conflict of Interest: No potential conflict of interest was disclosed by any authors.

Financial Disclosure: The authors declared that this study received no financial support.

References

1. American Thyroid Association (ATA) Guidelines Taskforce on Thyroid Nodules and Differentiated Thyroid Cancer, Cooper DS, Doherty GM, Haugen BR, Kloos RT, Lee SL, Mandel SJ, Mazzaferri EL, McIver B, Pacini F, Schlumberger M, Sherman SI, Steward DL, Tuttle RM. Revised American Thyroid Association management guidelines for patients with thyroid nodules and differentiated thyroid cancer. *Thyroid* 2009;19:1167-1214.
2. Schlumberger MJ. Papillary and follicular thyroid carcinoma. *N Engl J Med* 1998;338:297-306.
3. Lind P. Differentiated Thyroid Carcinoma. In: Ell PJ, Gambhir SS, (eds). *Nuclear Medicine in Clinical Diagnosis and Treatment*. 3rd ed. Edinburgh, Churchill Livingstone, 2004;145-164.
4. Yazici B, Oral A, Eraslan C, Argin M, Ömür Ö. False-Positive I-131 Uptake in a Benign Bone Lesion on Post-therapy Scan. *Clin Nucl Med* 2016;41:63-65.
5. Yazici B, Oral A, Omur O, Yazici A. Radioiodine uptake in an ovarian mature teratoma detected with SPECT/CT. *Clin Nucl Med* 2015;40:157-160.
6. Garger YB, Winfeld M, Friedman K, Blum M. In Thyroidectomized Thyroid Cancer Patients, False-Positive I-131 Whole Body Scans Are Often Caused by Inflammation Rather Than Thyroid Cancer. *J Investig Med High Impact Case Rep* 2016;4:2324709616633715.
7. Buton L, Morel O, Gault P, Illouz F, Rodien P, Rohmer V. False-positive iodine-131 whole-body scan findings in patients with differentiated thyroid carcinoma: report of 11 cases and review of the literature. *Ann Endocrinol (Paris)* 2013;74:221-230.
8. Oh JR, Ahn BC. False-positive uptake on radioiodine whole-body scintigraphy: physiologic and pathologic variants unrelated to thyroid cancer. *Am J Nucl Med Mol Imaging* 2012;2:362-385.
9. Shapiro B, Rufini V, Jarwan A, Geatti O, Kearfott KJ, Fig LM, Kirkwood ID, Gross MD. Artifacts, anatomical and physiological variants, and unrelated diseases that might cause false-positive whole-body I-131 scans in patients with thyroid cancer. *Semin Nucl Med* 2000;30:115-132.
10. Çayır D, Araz M, Apaydın M, Çakal E. Inguinal Endometriosis Visualized on I-131 Whole Body Scan. *Mol Imaging Radionucl Ther* 2018;27:52-54.
11. Luster M, Clarke SE, Dietlein M, Lassmann M, Lind P, Oyen WJ, Tennvall J, Bombardieri E; European Association of Nuclear Medicine

- (EANM). Guidelines for radioiodine therapy of differentiated thyroid cancer. *Eur J Nucl Med Mol Imaging* 2008;35:1941-1159.
12. Pina JS, Meyer CA, Billingsley JL, Matlock JP, Horan MP, Knodel DH. Inflammatory diseases of the lung causing false-positive ¹³¹I whole body scans in the evaluation of papillary thyroid carcinoma. Two case reports. *Chest* 1996;110:565-567.
 13. Bakheet SM, Hammami MM, Powe J, Bazarbashi M, Al Suhaibani H. Radioiodine uptake in inactive pulmonary tuberculosis. *Eur J Nucl Med* 1999;26:659-662.
 14. Gargya A, Chua E. Focal bronchiectasis causing abnormal pulmonary radioiodine uptake in a patient with well-differentiated papillary thyroid carcinoma. *Case Rep Endocrinol* 2012;2012:452758.
 15. Jong I, Taubman K, Schlicht S. Bronchiectasis simulating pulmonary metastases on iodine-131 scintigraphy in well-differentiated thyroid carcinoma. *Clin Nucl Med* 2005;30:688-689.
 16. Maruoka Y, Abe K, Baba S, Isoda T, Sawamoto H, Tanabe Y, Sasaki M, Honda H. Incremental diagnostic value of SPECT/CT with ¹³¹I scintigraphy after radioiodine therapy in patients with well-differentiated thyroid carcinoma. *Radiology* 2012;265:902-909.
 17. Gültekin SS, Dilli A, Arıkök AT, Bostancı H, Hasdemir AO. The false-positive radioiodine I-131 uptake in the foreign body granuloma located in gluteal adipose tissue. *Radiol Oncol* 2012;46:28-31.
 18. Mena Bares LM, Vallejo Casas JA, Moreno Ortega E, del Real Nuñez R, Maza Muret FR, Latre Romero JM. I-131 visualization of thoracic aortic aneurysm after radioiodine administration for thyroid carcinoma. *Clin Nucl Med* 2008;33:553-554.
 19. Laguna R, Silva F, Vazquez-Sellés J, Orduña E, Flores C. Vertebral hemangioma mimicking a metastatic bone lesion in well-differentiated thyroid carcinoma. *Clin Nucl Med* 2000;25:611-613.
 20. Jang HY, Kim BH, Kim WJ, Jeon YK, Kim SS, Kim YK, Kim IJ. False-positive radioiodine uptake in a functional ovarian cyst in a patient treated with total thyroidectomy for papillary cancer. *Intern Med* 2013;52:2321-2323.
 21. Omür O, Ozbek SS, Akgün A, Yazici B, Mutlukoca N, Ozcan Z. False-positive I-131 accumulation in a hepatic hydatid cyst. *Clin Nucl Med* 2007;32:930-932.
 22. Bural GG, Peel RL, Mountz JM. Benign epithelial cyst mimicking thyroid cancer metastasis: a false-positive finding on post-therapy I-131 scan. *Clin Nucl Med* 2012;37:88-90.
 23. Carlisle MR, Lu C, McDougall IR. The interpretation of ¹³¹I scans in the evaluation of thyroid cancer, with an emphasis on false positive findings. *Nucl Med Commun* 2003;24:715-735.



¹⁸F-FDG PET/CT in Patients with Parenchymal Changes Attributed to Radiation Pneumonitis

Radyasyon Pnömonisine Bağlı Parankimal Değişiklikleri Olan Hastalarda ¹⁸F-FDG PET/BT

✉ Anastas Krassenov Demirev¹, ✉ Irena Dimitrova Kostadinova¹, ✉ Iliya Rumenov Gabrovski²

¹Acibadem City Clinic Cancer Center, Clinic of Nuclear Medicine, Sofia, Bulgaria

²The Queen Giovanna Hospital, Sofia, Bulgaria

Abstract

Objectives: Radiation pneumonitis (RP) can be an adverse complication of radiotherapy (RT) and can limit the application of the already planned radiation dose. It is often associated with RT of lung carcinoma and is occasionally caused by radiation therapy of breast carcinoma and lymphomas located in the mediastinum. Positron emission tomography/computed tomography (PET/CT) emerges lately as a prospective modality for early diagnostics of RP. The aim of this study was to summarize the initial data from diagnostic application of PET/CT in patients suspicious of RP and to derive criteria, which can help differentiate RP from early recurrence of the disease and/or residual tumor.

Methods: The current study included 23 patients who had metabolic (PET) and anatomical (CT) changes consistent with RP. We additionally defined metabolic activity (SUV_{max}) in the lung parenchyma of 20 patients without RT.

Results: All patients had increased metabolic activity in the lung parenchyma involved in the irradiated area with a mean SUV_{max} 3.45 (ranging between 1 and 7.1). The control group had a physiological background metabolic activity- SUV_{max} 0.61 +/- 0.11.

Conclusion: Metabolic changes in patients suspicious of RP involved diffusely increased metabolic activity coinciding with the anatomical changes in the irradiated area. Three out of 23 patients had a proven recurrence of the primary neoplastic process in the irradiated area. The metabolic changes in those patients involved an increase in metabolic activity at follow-up or lack of tendency towards normalization after chemotherapy, which implied the existence of viable tumor cells. Our initial experience in the diagnostic application of ¹⁸F-FDG PET/CT in patients suspicious of RP allows us to summarize the following: PET/CT is a reliable imaging modality in the diagnostics of RP. Through its sequential use, we can differentiate inflammatory changes related to RP from early recurrence of the primary neoplastic process.

Keywords: ¹⁸F-FDG PET/CT, radiation pneumonitis, radiotherapy, hybrid imaging

Öz

Amaç: Radyasyon pnömonisi (RP) radyoterapinin (RT) yan etkisi olarak görülebilir ve planlanmış olan radyasyon dozunun uygulanmasını engelleyebilir. Sıklıkla akciğer karsinomu için uygulanan RT'ye bağlıdır ancak meme kanseri ve mediastinal lenfoma için uygulanan RT ile de oluşabilir. Son zamanlarda pozitron emisyon tomografi/bilgisayarlı tomografi (PET/BT), RP'nin erken tanısı için kullanılmaktadır. Bu çalışmanın amacı RP şüphesi olan hastalarda tanısal PET/BT uygulamasının ilk verilerini özetlemek ve RP'yi erken nüks ve/veya rezidü tümörden ayırt etmede kullanılabilecek kriterler oluşturmaktır.

Yöntem: Bu çalışmaya RP ile uyumlu metabolik (PET) ve anatomik (BT) değişiklikleri olan 23 hasta dahil edilmiştir. Buna ek olarak RT almamış 20 hastanın akciğer parankiminde metabolik aktiviteyi (SUV_{max}) değerlendirdik.

Address for Correspondence: Anastas Krassenov Demirev MD, Acibadem City Clinic Cancer Center, Clinic of Nuclear Medicine, Sofia, Bulgaria
Phone: +00359884918238 E-mail: demirevanastas@gmail.com ORCID ID: orcid.org/0000-0001-5591-924X

Received: 30.03.2018 **Accepted:** 13.07.2018

©Copyright 2018 by Turkish Society of Nuclear Medicine
Molecular Imaging and Radionuclide Therapy published by Galenos Yayınevi.

Bulgular: Tüm hastalarda radyasyon uygulanmış alanlarda akciğer parankiminde metabolik aktivite artmıştı (ortalama SUV_{max} 3,45, aralık 1-7,1). Kontrol grubunda fizyolojik metabolik aktivite mevcuttu (SUV_{max} 0,61 +/- 0,11).

Sonuç: RP şüphesi olan hastalardaki metabolik değişiklikler anatomik olarak radyasyon uygulanmış alanlara denk gelen diffüz artmış metabolik aktiviteyi içermekteydi. Yirmi üç hastanın üçünde bu bölgede primer neoplastik sürecin kanıtlanmış nüksü vardı. Bu hastalardaki metabolik değişiklikler arasında, canlı tümör hücrelerinin varlığını ima eder şekilde, takip sürecinde metabolik aktivitede artış ya da kemoterapi sonrası normale dönme eğiliminin olmaması bulundu. RP şüphesi olan hastalarda ¹⁸F-FDG PET/BT'nin tanısal uygulamasında ilk deneyimlerimiz doğrultusunda PET/BT'nin RP tanısında güvenilir bir görüntüleme yöntemi olduğu sonucuna vardık. Sürekli kullanımı ile RP'ye bağlı enflamatuvar değişiklikleri primer neoplastik sürecin erken nüksünden ayırt edebiliriz.

Anahtar kelimeler: ¹⁸F-FDGPET/BT, radyasyon pnömonisi, radyoterapi, hibrid görüntüleme

Introduction

Radiation pneumonitis (RP) is an unfavorable complication that sometimes limits the course of radiotherapy (RT). It is most commonly associated with radiation therapy for lung cancer, and less frequently with other tumors such as breast cancer and mediastinal lymphoma, respectively in about 5-50%, 5-10%, and 1-5% of the cases (1,2). RP is an inflammatory reaction in the affected area of the pulmonary parenchyma. The acute stage is observed most frequently from 6 to 12 weeks after RT and symptoms include cough, shortness of breath, fever and changes in pulmonary function (3,4,5,6,7). Its chronic form occurs most often in the span of 6 to 12 months and can last up to 2 years after RT, a process associated with the development of fibrosis (8,9,10,11,12,13,14,15). Frequency and severity depend on a number of parameters, such as age, irradiated area, radiotherapeutic regimen, administered cumulative dose - most often at values above 20 Gray and almost always at doses above 40 Gray, as well as previous or concomitant chemotherapy. All of the above mentioned factors may increase drastically the effect of RT (4,11,12,15,16,17,18,19,20). Changes, attributed to RP and visualized by computed tomography (CT), are also divided into early and late ones, respectively, acute inflammatory reactions including matt glass type/ infiltrative parenchymal changes and late or chronic ones (most of the cases) resulting in fibrosis (21,22). The loss of local pulmonary blood perfusion, characteristic of RP, can be visualized and quantified by conventional scintigraphy, but this method lacks sufficient specificity (23).

¹⁸F-FDG positron emission tomography (PET)/CT, a more recent and promising approach for early diagnostics and monitoring of patients with RP, offers a possibility for visualization of metabolic changes. Since they appear earlier than anatomical ones, detected by CT, it de facto improves the diagnostic algorithm (24,25).

The aim of this study is to summarize our initial data on the use of ¹⁸F-FDG PET/CT in the diagnostics of patients with parenchymal changes attributed to RP and to derive criteria for its differentiation from early recurrence, residual tumor tissue and/or metastatic lesions, thus helping us to discriminate better between inflammatory and neoplastic processes.

Materials and Methods

This retrospective study includes 23 (n=23) patients who underwent RT in the thoracic area involving the parenchyma of the lung, and showed computer-tomographic data of RP between 2012 to 2016 in two university hospitals located in Sofia, Bulgaria. Their age range was 42-80 years (mean 62 and median 61 years). A control group comprised of 23 patients without pulmonary disease and/or neoplastic process in the thoracic area who did not undergo RT, was also evaluated. Of the patients with parenchymal and metabolic changes, 19 were women and 4 were men. Seven of them had lung cancer, 3 had Hodgkin's lymphoma, 12 had breast carcinoma, and 1 had carcinoma of the submandibular gland and mediastinal lymphatic metastases. In 13/23 patients, serial PET/CT (pre-and post-RT) studies were performed-in 9 of the patients before and up to 6 months after RT and in 4 of the patients before and after 6 months post-RT. The remaining 10 patients underwent a single ¹⁸F-FDG PET/CT study up to- or over 6 months after completion of RT. The total radiation dose administered in patients suspected of RP varied between 20-60 Gray. 19/23 of the patients had chemotherapy prior to or concomitant with RT-the type of which depended on the histology, location and stage of the disease. 16/23 of the patients underwent 3D conformal RT (linear accelerator), 1 underwent intensity modulated radiation therapy (IMRT) linear accelerator and the remaining 6 patients underwent 2D conformal RT (using a Co-60 source)-data is summarized in Table 1. ¹⁸F-FDG PET/CT studies were conducted according to the European Association of Nuclear Medicine guidelines and included a whole body PET and CT scan performed approximately 60 minutes after intravenous injection of ¹⁸F-FDG with activity of up to 3 MBq/kg per patient. The CT part of the study was conducted on a 16 slice computer tomography. The quantitative accumulation of ¹⁸F-FDG was measured with the standardized accumulation ratio of SUV_{max}.

Declaration of informed consent was signed by all patients stating that they give their full consent for their data to be used in scientific publications-above all it is a retrospective study of procedures already approved and executed.

Informed consent was obtained from each patient prior to PET/CT scanning procedure. The written document stated that the patient agrees her or his personal information as

well as results from the scanning procedure be used in scientific studies and surveys.

Results

All 23 patients had increased metabolic activity in the lung parenchyma involved in the RT field with a mean metabolic activity of SUV_{max} of 3.36 (+/- 1.7). Patients from the control group had physiological background metabolic activity with a mean SUV_{max} of 0.61 (+/- 0.07). In 16/23 of the patients (70%), CT changes included limited areas of consolidated lung tissue (interpreted as fibrosis). In the remaining 7/23 patients (30%) infiltrative and/or matt glass type changes were observed. Infiltrative/matt glass type CT changes were also characterized by a higher metabolic activity seen on the PET study, and were observed in patients studied up to 6 months after RT (Figure 1A, 1B). In 3/23 of the patients followed up serially with PET/CT

after RT and chemotherapy, the higher metabolic activity persisted. Mean SUV_{max} remained at a mean value of 3.5 (+/- 0.8), and did not decrease (showed no trend towards decrease) to the background metabolic activity of the controls. Subsequently, those 3 cases were diagnosed with recurrence (Figure 2A, 2B).

Discussion

According to recent studies, RP is becoming less and less frequent, mainly due to technological advances in RT and the increasing knowledge of its etiology (26,27). However, it still remains as a complication that may interfere with quality of life in cancer patients. More importantly, it can limit the application of the proper radio-therapeutic dose (28). Early and adequate diagnostics with ¹⁸F-FDG PET/CT hybrid imaging allows eventual modification of the RT

Table 1. Includes patients' age, sex, primary malignancy, area involved in radiotherapy, fraction, cumulative dose, radiation techniques used

Number	Patient	Diagnosis	Area involved	Fraction/Gray	Total/Gray	Radiation technique
1	M, 80	Lung carcinoma	Lymph nodes-tracheal bifurcation	2	60	3D conformal
2	F, 54	Breast carcinoma	Left supraclavicular region, left breast	2	60	3D conformal
3	M, 58	Hodgkin lymphoma	Mediastinal lymph nodes	1.8	30.6	3D conformal
4	F, 74	Breast carcinoma	Thoracic wall, left breast, supraclavicular region, left axilla	2	50	2D conformal Co-60
5	F, 42	Breast carcinoma	Right breast, parasternal, supraclavicular and axillary region	2	50	2D conformal Co-60
6	F, 57	Breast carcinoma	Left thoracic wall, left supraclavicular region	2	50	3D conformal
7	F, 72	Breast carcinoma	Left thoracic wall	2	50	2D conformal Co-60
8	F, 45	Lung carcinoma	Right thoracic wall	2	60	IMRT
9	F, 73	Breast carcinoma	Right thoracic wall	2	50	3D conformal
10	F, 59	Lung carcinoma	Left lung	3	30	2D conformal Co-60
11	F, 77	Breast carcinoma	Right thoracic wall	2	50	2D conformal Co-60
12	F, 58	Breast carcinoma	Right thoracic wall	2	50	2D conformal Co-60
13	M, 64	Carcinoma of submandibular gland	Mediastinal lymph nodes	2	50	3D conformal
14	F, 67	Breast carcinoma	Left breast	2	50	3D conformal
15	F, 65	Lung carcinoma	Mediastinum	3	30	3D conformal
16	F, 56	Breast carcinoma	Right thoracic wall	2	50	3D conformal
17	F, 46	Hodgkin lymphoma	Mediastinum	2	20	3D conformal
18	F, 55	Hodgkin lymphoma	Mediastinum	2	30	3D conformal
19	F, 63	Lung carcinoma	Lung	2	60	3D conformal
20	F, 64	Lung carcinoma	Lung	2	60	3D conformal
21	F, 57	Breast carcinoma	Right breast	2	50	3D conformal
22	F, 61	Breast carcinoma bilateral	Right supraclavicular region	2	50	3D conformal
23	F, 72	Lung carcinoma	Mediastinum	2	60	3D conformal

F: Female, M: Male

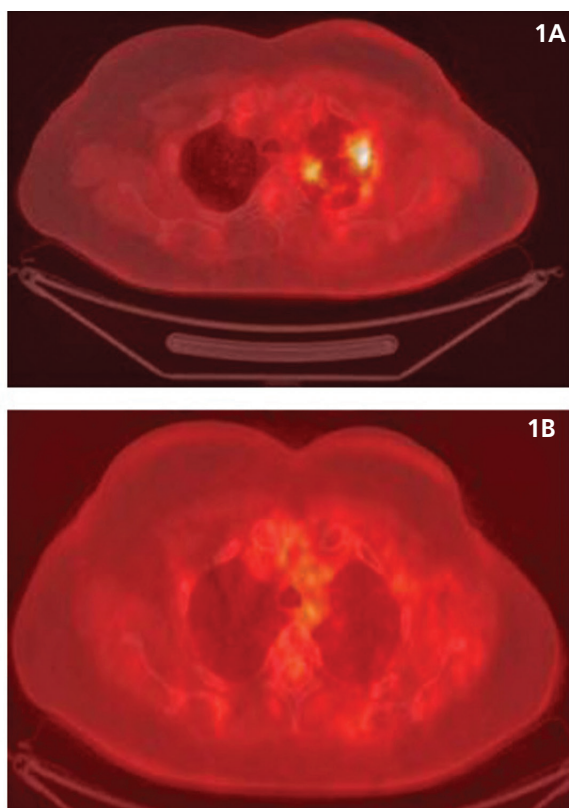


Figure 1. A) Metabolically active parenchymal changes located in the upper left lobe of the lung apex-the study was conducted up to 6 months after completion of radiotherapy (upper row). B) Follow-up study conducted 6 months after completion of radiotherapy-no significantly increased metabolic activity in the lung parenchyma along with anatomical changes that almost completely resolved-evidence of the inflammatory nature of the changes (bottom line)

protocol and, if necessary, initiation of an adequate therapy, in order to prevent chronic disease. On the other hand, this method also allows for visualization of early recurrence and differentiation from RP, if performed sequentially (29).

Hicks et al. (30) described the characteristic PET/CT changes in 2004, as an increased ¹⁸F-FDG accumulation that is the result of an active metabolic process, due to inflammatory post-radio-therapeutic changes. These changes were later characterized and quantified by Guerrero et al. (31) and defined on a scale of 0 to 3, with a linear relationship between radiation dose and metabolic activity of ¹⁸F-FDG in the involved lung parenchyma. However, in each of the studied patients, this metabolic response varies significantly depending on location, timing (i.e. concomitant or prior to radiation) as well as chemotherapy and RT regimen (4,20). However, these changes vary significantly between patients, depending on: location of the neoplastic process, presence of concurrent or sequential chemotherapy and type of radiation technique (4,20). The summary of the data in Table 1 is important since it gives an overview of the types of applied radiation techniques a significant part of

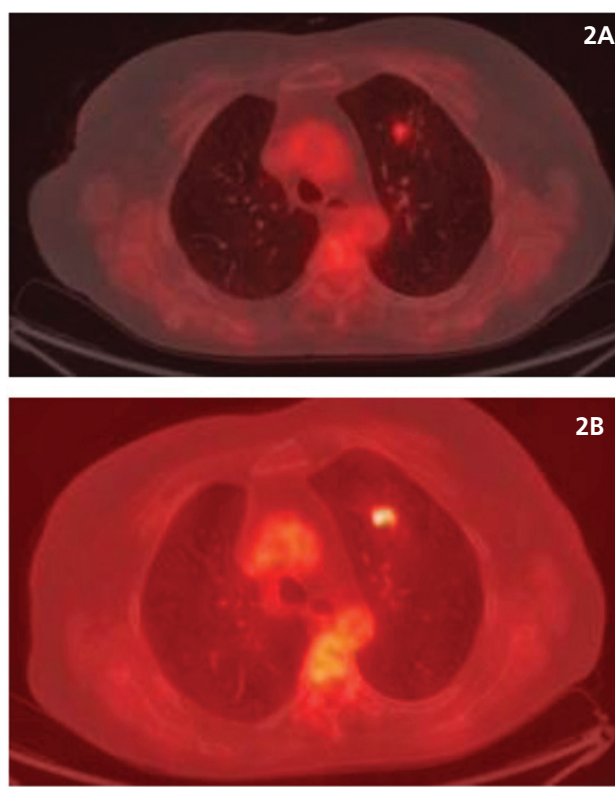


Figure 2. A) focal zone of increased metabolic activity in the left lobe parenchyma-visualized 14 months after completion of radiotherapy (upper row). B) shows significantly increased metabolic activity in the area seen on the previous study, the study was performed 20 months after completion of radiotherapy-subsequently, disease recurrence was diagnosed (bottom line)

the studied population, for example, (6/23 patients were) was treated in a 2D conformal technique with a Co-60 (Cobalt 60) teletherapy on a Co-60 unit in a 2D mode. The majority of patients (16/23) were treated with a linear accelerator in a 3D mode (conformal technique) and only one patient (1/23) underwent IMRT (3D mode-linear accelerator). The cumulative radiation dose exceeded 20 Gray in almost everyone in our patient group, a factor which contributes to the development of pulmonary injury (as stated previously) (4,9). Several studies have reported the benefits of significantly lower toxicity in the surrounding tissue after 3D radiation planning using a linear accelerator vs. 2D planning techniques (in the case of Co-60 unit) (32,33). IMRT is even superior to the previous two (2D and 3d conformal techniques) in terms of pulmonary toxicity (34). This, we consider, is one of the reasons for the higher prevalence of inflammatory and metabolically active changes involving the lung, in our relatively small group of patients. Instead of concentrating on the various reasons etiology of RP, we decided to investigate what part of those changes -1486260889 were as associated with inflammation and what part represented recurrence/metastatic spread of the main neoplastic process. After

quantification of the metabolic activity in the irradiated lung and its comparison to normal pulmonary tissue, we were able to show that there is a statistically significant difference between the two ($p < 0.0001$ - unpaired t-test). It was important to determine the physiological background metabolic activity of the lungs in order to derive criteria for the differentiation of recurrence from inflammation. In patients with confirmed disease recurrence, changes involved increased metabolic activity or lack of tendency towards normalization long after the completion of RT and chemotherapy due to the presence of vital tumor cells, a trend also observed by other authors (31). Metabolic changes attributed to pneumonitis also involved diffuse metabolic activity overlapping with the irradiated area. On the contrary, alterations consistent with recurrence were characterized by focal metabolic activity against a background of consolidated/fibrotic changes (showing no significant increase in size or anatomic change on CT images) not entirely overlapping with the involved/irradiated area of the lung. Based on our initial diagnostic experience, we recommend that all patients with increased metabolic activity in the area of the involved/irradiated volume of the lung should be followed-up by serial ¹⁸F-FDG PET/CT in 3 to 6 months, in order to detect early recurrence and initiate adequate and timely therapy. Several other authors also offer the same diagnostic and follow-up strategy along with verification of these findings (31).

Conclusion

Based on our initial experience with PET/CT in patients with parenchymal changes attributed to RP, we concluded that this modality is adequate and reliable in such circumstances. Its implementation in the follow-up process can help discriminate between early recurrence of the neoplastic process and inflammatory processes.

Ethics

Ethics Committee Approval: Declaration of informed consent was signed by all patients stating that they give their full consent for their data to be used in scientific publications-above all it is a retrospective study of procedures already approved and executed.

Informed Consent: Declaration signed.

Peer-review: Externally and internally peer-reviewed.

Authorship Contributions

Surgical and Medical Practices: A.K.D., Concept: A.K.D., Design: A.K.D., Data Collection or Processing: A.K.D., I.R.G., I.D.K., Analysis or Interpretation: A.K.D., I.D.K., Literature Search: A.K.D., Writing: A.K.D.

Conflict of Interest: No conflict of interest was declared by the authors.

Financial Disclosure: The authors declared that this study received no financial support.

References

1. Mehta V. Radiation pneumonitis and pulmonary fibrosis in non-small-cell lung cancer: Pulmonary function, prediction, and prevention. *Int J Radiat Oncol Biol Phys* 2005;63:5-24.
2. Marks LB, Yu X, Vujaskovic Z, Small W Jr, Folz R, Anscher MS. Radiation-induced lung injury. *Semin Radiat Oncol* 2003;13:333-345.
3. Yue J, Shi Q, Xu T, Jeter M, Chen TY, Komaki R, Gomez DR, Pan T, Cleeland CS, Liao Z, Wang XS. Patient-reported lung symptoms as an early signal of impending radiation pneumonitis in patients with non-small cell lung cancer treated with chemoradiation: an observational study. *Qual Life Res* 2018; 27:1563-1570.
4. Deng G, Liang N, Xie J, Luo H, Qiao L, Zhang J, Wang D, Zhang J. Pulmonary toxicity generated from radiotherapeutic treatment of thoracic malignancies. *Oncol Lett* 2017;14:501-511.
5. Shapiro SJ, Shapiro SD, Mill WB, Campbell EJ. Prospective study of long-term pulmonary manifestations of mantle irradiation. *Int J Radiat Oncol Biol Phys* 1990;19:707-714.
6. Gibson PG, Bryant DH, Morgan GW, Yeates M, Fernandez V, Penny R, Breit SN. Radiation-induced lung injury: a hypersensitivity pneumonitis? *Ann Intern Med* 1988;109:288-291.
7. Kharofa J, Gore E. Symptomatic Radiation Pneumonitis in Elderly Patients Receiving Thoracic Irradiation. *Clin Lung Cancer* 2013;14:283-287.
8. Choi YW, Munden RF, Erasmus JJ, Park KJ, Chung WK, Jeon SC, Park CK. Effects of Radiation Therapy on the Lung: Radiologic Appearances and Differential Diagnosis. *RadioGraphics*. 2004;24:985-997.
9. Zhao J, Day RM, Jin JY, Quint L, Williams H, Ferguson C, Yan L, King M, Albsheer A, Matuszak M, Kong FS. Thoracic radiation-induced pleural effusion and risk factors in patients with lung cancer. *Oncotarget*. 2017;8:97623-97632.
10. Agrawal S. Clinical relevance of radiation pneumonitis in breast cancers. *South Asian J Cancer* 2013;2:19-20.
11. Morgan GW, Breit SN. Radiation and the lung: a reevaluation of the mechanisms mediating pulmonary injury. *Int J Radiat Oncol Biol Phys* 1995;31:361-369.
12. Karpathiou G, Giatromanolaki A, Koukourakis MI, Mihailidis V, Sivridis E, Bouros D, Froudarakis ME. Histological Changes After Radiation Therapy in Patients with Lung Cancer: A Prospective Study. *Anticancer Res*. 2014;34:3119-3124
13. Zhang XJ, Sun JG, Sun J, Ming H, Wang XX, Wu L, Chen ZT. Prediction of radiation pneumonitis in lung cancer patients: a systematic review. *J Cancer Res Clin Oncol* 2012;138:2103-2116.
14. Williams JP, Johnston CJ, Finkelstein JN. Treatment for Radiation-Induced Pulmonary Late Effects: Spoiled for Choice or Looking in the Wrong Direction? *Current Drug Targets* 2010;11:1386-1394.
15. Giridhar P, Mallick S, Rath GK, Julka PK. Radiation induced lung injury: prediction, assessment and management. *Asian Pac J Cancer Prev* 2015;16:2613-2617.
16. Davis SD, Yankelevitz DF, Henschke CI. Radiation effects on the lung: clinical features, pathology, and imaging findings. *AJR Am J Roentgenol* 1992;159:1157-1164.
17. Fennessy JJ. Irradiation damage to the lung. *J Thorac Imaging* 1987;2:68-79.
18. Movsas B, Raffin TA, Epstein AH, Link CJ Jr. Pulmonary radiation injury. *Chest* 1997;111:1061-1076.
19. Chargari C, Riet F, Mazevet M, Morel E, Lepechoux C, Deutsch E. Complications of thoracic radiotherapy. *Presse Med* 2013;42:342-351.
20. Parashar B, Edwards A, Mehta R, Pasmantier M, Wernicke AG, Sabbas A, Kerestez RS, Nori D, Chao KS. Chemotherapy significantly increases the risk of radiation pneumonitis in radiation therapy of advanced lung cancer. *Am J Clin Oncol* 2011;34:160-164.
21. Choi YW, Munden RF, Erasmus JJ, Park KJ, Chung WK, Jeon SC, Park CK. Effects of radiation therapy on the lung: radiologic

- appearances and differential diagnosis. *Radiographics* 2004;24:985-997.
22. Ikezoe J, Takashima S, Morimoto S, Kadowaki K, Takeuchi N, Yamamoto T, Nakanishi K, Isaza M, Arisawa J, Ikeda H, et al. CT appearance of acute radiation-induced injury in the lung. *AJR Am J Roentgenol* 1988;150:765-770.
 23. Farr KP, Møller DS, Khalil AA, Kramer S, Morsing A, Grau C. Loss of lung function after chemo-radiotherapy for NSCLC measured by perfusion SPECT/CT: Correlation with radiation dose and clinical morbidity. *Acta Oncol*. 2015;54:1350-1354.
 24. Hassaballa HA, Cohen ES, Khan AJ, Ali A, Bonomi P, Rubin DB. Positron emission tomography demonstrates radiation-induced changes to nonirradiated lungs in lung cancer patients treated with radiation and chemotherapy. *Chest* 2005;128:1448-1452.
 25. McCurdy MR, Castillo R, Martinez J, Al Hallack MN, Lichter J, Zouain N, Guerrero T. [¹⁸F]-FDG uptake dose-response correlates with radiation pneumonitis in lung cancer patients. *Radiother Oncol* 2012;104:52-57.
 26. Besson N, Pernin V, Zefkili S, Kirova YM. Evolution of radiation techniques in the treatment of mediastinal lymphoma: from 3D conformal radiotherapy (3DCRT) to intensity-modulated RT (IMRT) using helical tomotherapy (HT): a single-centre experience and review of the literature. *Brish J Radiol*. 2016;89:20150409.
 27. Yamashita H, Takahashi W, Haga A, Nakagawa K. Radiation pneumonitis after stereotactic radiation therapy for lung cancer. *World J Radiol* 2014;6:708-715.
 28. Makimoto T, Tsuchiya S, Hayakawa K, Saitoh R, Mori M. Risk Factors for Severe Radiation Pneumonitis in Lung Cancer. *J Clin Oncol* 1999;29:192-197.
 29. Bury T, Corhay JL, Duysinx B, Daenen F, Ghaye B, Barthelemy N, Rigo P, Bartsch P. Value of FDG-PET in detecting residual or recurrent nonsmall cell lung cancer. *Eur Respir J* 1999;14:1376-1380.
 30. Hicks RJ, Mac Manus MP, Matthews JP, Hogg A, Binns D, Rischin D, Ball DL, Peters LJ. Early FDG-PET imaging after radical radiotherapy for non-small-cell lung cancer: Inflammatory changes in normal tissues correlate with tumor response and do not confound therapeutic response evaluation. *Int J Radiat Oncol Biol Phys* 2004;60:412-418.
 31. Guerrero T, Johnson V, Hart J, Pan T, Khan M, Luo D, Liao Z, Ajani J, Stevens C, Komaki R. Radiation pneumonitis: Local dose versus [¹⁸F]-fluorodeoxyglucose uptake response in irradiated lung. *Int J Radiat Oncol Biol Phys*. 2007;68:1030-1035.
 32. Ahmad N, Attia G, El-Ghoneimy E, Radwan A, El-Badawy S. Conventional (2D) Versus Conformal (3D) Techniques in Radiotherapy for Malignant Pediatric Tumors: Dosimetric Perspectives. *J Egypt Natl Canc Inst* 2009;21:309-314.
 33. Deng JY, Wang C, Shi XH, Jiang GL, Wang Y, Liu Y, Zhao KL. Reduced toxicity with three-dimensional conformal radiotherapy or intensity-modulated radiotherapy compared with conventional two-dimensional radiotherapy for esophageal squamous cell carcinoma: a secondary analysis of data from four prospective clinical trials. *Dis Esophagus* 2017;30:1-7.
 34. Hu X, He W, Wen S, Feng X, Fu X, Liu Y, Pu K. Is IMRT Superior or Inferior to 3DCRT in Radiotherapy for NSCLC? A Meta-Analysis. *PLoS One*. 2016;11:e0151988.



Benchmarking of a Simple Scintigraphic Test for Gastro-oesophageal Reflux Disease That Assesses Oesophageal Disease and Its Pulmonary Complications

Basit Bir Yöntem Olan Gastro-özefageal Reflü Sintigrafisi ile Özefagus Hastalığı ve Pulmoner Komplikasyonların Değerlendirilmesi

✉ Leticia Burton¹, ✉ Gregory L. Falk², ✉ Stephen Parsons³, ✉ Mel Cusi⁴, ✉ Hans Van Der Wall⁴

¹CNI Molecular Imaging, Sydney, Australia

²Sydney Heartburn Clinic, Sydney, Australia

³University of New South Wales, Sydney, Australia

⁴University of Notre Dame, Sydney, Australia

Abstract

Objectives: Gastro-oesophageal reflux disease (GORD) is both common and troubling with a prevalence of 20-40%. We assessed the utility of a scintigraphic reflux study to evaluate the oesophageal and extra-oesophageal manifestation of disease compared to the standard tests such as pH monitoring and manometry.

Methods: Patients were recruited into a prospective database of referrals to a tertiary referral center for either resistance to maximal medical therapy or extra-oesophageal symptoms of GORD. Data included 2 channel 24-hour pH monitoring and manometry results, as well as scintigraphic reflux data with late images assessing pulmonary aspiration of refluxate.

Results: Study population included 250 patients (155 F, 95 M) with an average age of 60 years. Patients were clinically classified as either GORD (n=72) or laryngopharyngeal reflux (LPR) (n=178). Pulmonary aspiration of the refluxate was detected significantly more commonly in LPR patients (58/178 compared with GORD 10/72). Strong correlations were found between the scintigraphic time-activity curves in the upper oesophagus and pharynx, and ineffective oesophageal motility and pulmonary aspiration. pH studies correlated with the scintigraphic studies but did not predict aspiration similar to other modalities when evaluated by ROC analysis.

Conclusion: Scintigraphic reflux studies offer a viable alternative test for GORD and extra-oesophageal manifestations of reflux disease. Strong correlations were found between measurable scintigraphic parameters and oesophageal motility and lung aspiration of refluxate. This may provide a more confident decision analysis in patients being considered for fundoplication for troubling extra-oesophageal symptoms.

Keywords: Gastro-oesophageal, reflux, scintigraphy, manometry, aspiration, pulmonary

Öz

Amaç: Gastro-özofageal reflü (GÖR) hastalığı %20-40 arası prevalansı ile sık görülen bir sorundur. Bu çalışmada hastalığın özofageal ve özofagus dışı belirtilerini değerlendirmek için sintigrafik reflü testinin yararını inceleyerek bunu pH monitorizasyonu ve manometri gibi standart testlerle karşılaştırdık.

Address for Correspondence: Hans Van Der Wall MD, University of Notre Dame, Sydney, Australia

Phone: +61297361040 E-mail: hvanderwall@gmail.com ORCID ID: orcid.org/0000-0003-4184-3330

Received: 14.04.2018 **Accepted:** 17.08.2018

©Copyright 2018 by Turkish Society of Nuclear Medicine
Molecular Imaging and Radionuclide Therapy published by Galenos Yayınevi.

Yöntem: Maksimal medikal tedavi veya GÖR özofagus-dışı belirtiler nedeniyle üçüncü basamak bir referans merkezine yönlendirilmiş hastalar prospektif veri tabanında toplandı. İki kanal 24-saat pH monitorizasyonu ve manometri sonuçları ile reflüksatin pulmoner aspirasyonunu değerlendiren geç görüntülerin dahil edildiği sintigrafik reflü verileri saptandı.

Bulgular: Çalışmaya ortalama 60 yaşında 250 hasta (155 K, 95 E) dahil edildi. Hastalar klinik olarak ya GÖR (n=72) ya da laringofaringeal reflü (LPR) (n=178) olarak ikiye ayrıldı. Reflüksatin pulmoner aspirasyonu LPR hastalarında GÖR hastalarına göre anlamlı olarak daha sık saptandı (58/178'e vs. 10/72). Üst özofagus ile farinkste sintigrafik zaman-aktivite eğrileri arasında ve inefektif özofageal motilite ve pulmoner aspirasyon arasında ciddi korelasyon saptandı. pH testleri sintigrafik incelemelerle uyumlu idi ancak diğer incelemeler gibi ROC analizi ile değerlendirildiğinde sintigrafisi de aspirasyonu öngöremedi.

Sonuç: Sintigrafik reflü incelemeleri GÖR ve reflü hastalığının özofagus dışı belirtileri için yararlı bir alternatif testtir. Ölçülebilir sintigrafik parametreler ile özofagus motilitesi ve reflüksatin akciğer aspirasyonu arasında ciddi korelasyon saptanmıştır. Bu inceleme, özofagus dışı semptomu olan ve fundoplikasyon için değerlendirilen hastalarda ilgili karar verme sürecine katkı sağlayabilir.

Anahtar kelimeler: Gastro-özofageal, reflü, sintigrafisi, manometri, aspirasyon, pulmoner

Introduction

Gastro-oesophageal reflux disease (GORD) is a common and troubling problem that has a prevalence of 20-40% in its various complex manifestations (1). Variability depends on the criteria utilized in the definition and has now been expanded to "a condition that develops when the reflux of stomach contents causes troublesome symptoms and/or complications" (Montreal definition, 2006) (2). A problem with the definition is that it encompasses many non-specific symptoms and requires confirmation by endoscopy or the application of a therapeutic trial with a clinical response to confirm the diagnosis. Endoscopy is necessary to confirm the presence of esophagitis and exclude sinister pathology. Even so, endoscopy will miss a high proportion of uncomplicated GORD (>50%) and between 25% and 40% of patients will remain unresponsive or refractory to such clinical trials (3).

These circumstances have led to the requirement for invasive testing such as 24-hour pH monitoring, manometry and impedance reflux measurements. Such testing will fundamentally assess the presence of acidic reflux, lower oesophageal sphincter (LOS) pressures/oesophageal clearance or non-acid reflux, respectively (4). However, the blind spot of these tests is in assessment of the extra-oesophageal manifestations of reflux such as cough, recurrent sinusitis, laryngitis or chronic recurrent chest symptoms, particularly in those subgroups who experience silent (or non-heartburn) GORD. Laryngopharyngeal reflux (LPR) and lung aspiration of refluxate are dangerous complications that often occur in the absence of oesophagitis or its primary symptom, heartburn (5). LPR complications have been reported in numerous publications and have been succinctly summarized by Koufman et al (5). These complications include laryngeal carcinoma, vocal cord nodules, laryngospasm and subglottic stenosis.

While there have been a number of scintigraphic reflux studies in the past (6,7,8), there has been no general acceptance of the technique due to the variability in technique and inconsistent results. We have validated

(9) and present a simple modification of the existing scintigraphic reflux testing and benchmark the findings against the current reference standards such as 24-hour pH monitoring and manometry. The comparison with impedance will be reported separately. We hypothesized that scintigraphic reflux testing is capable of assessing both the presence of oesophageal disease and its extra-oesophageal manifestations with good correlation with existing testing regimens.

Materials and Methods

Population and Clinical Data

A database of patients with either proven or suspected GORD/LPR [approved by the Institutional Ethics Committee (LNR/12 CRGH/248)] was maintained prospectively. Patients being investigated for suspected GORD/LPR disease with pH/manometry studies was extracted from the database. Patients were chosen for the study if they had mainly upper respiratory tract symptoms that remained undiagnosed after 8 weeks of investigation by appropriate specialists and classified according to the reflux symptom index criteria of Belafsky et al (10). Major upper respiratory tract symptoms documented included cough, sore throat, recurrent throat clearing, voice change, laryngospasm, aspiration, globus and regurgitation. A history of heartburn, regurgitation and dysphagia was routinely elicited. All patients had severe symptoms that were resistant to high-dose proton-pump inhibitor therapy and had been referred for consideration of fundoplication. Scintigraphy was used to prospectively evaluate extra-oesophageal refluxate and the possibility of pulmonary aspiration of refluxate. This is therefore a highly selected group of patients with a strong pre-test probability of GORD causing LPR. A large proportion had a long history of undiagnosed upper respiratory tract symptoms and were studied by scintigraphy in order to evaluate the possibility of reflux disease as a causation. Clinical data was prospectively collected using a standardized proforma and entered into a database.

pH Monitoring (2 Channel)

24-hour impedance reflux study with two channel 24-hour pH was performed on all patients. Following local anesthetic application, a trans-nasal catheter was introduced into the oesophagus. This consisted of 2 level impedance rings and 2 level pH electrodes connected to an external monitoring device and calibrated accordingly. Impedance rings were maneuvered to 5 and 15 cm above the upper border of the LOS (Zephyr device, catheter ZAI-BD31, Sandhill Co, Highlands Ranch, Colorado, USA). No dietary restrictions were made other than ingestion of acidic beverages. Catheter placement was checked by manometry with the lower pH electrode 5 cm above the upper border of the LOS and the upper, 15 mm higher. Patients returned the following day for removal of the assembly. Meal-times were included in the reporting analysis. Reports of 24-hour pH and 24-hour impedance reflux were generated by autoscans and manual review. Reflux was classified according to the consensus on impedance and pH monitoring (11). In summary, this is based on oesophageal pH during reflux detected by impedance monitoring. Acid reflux is defined as a fall in pH below 4, weakly acid reflux as a fall in pH which is ≥ 4 but < 7 and non-acid reflux where oesophageal pH increases ≥ 7 or remains ≥ 7 during reflux.

Manometry

Stationary manometry was obtained with a water perfused dent sleeve 8 channel catheter (Dent Sleeve International Mississauga, Ontario, Canada) using standard techniques. Data was recorded with a multichannel recording system (PC polygraph HR Medtronic, Synectics Medical, Minneapolis, Minnesota, United States) and analyzed using the PolyGram software program (Medtronic,

Synectics Medical, Minneapolis, Minnesota, United States). Oesophageal motility was graded by the modified method of Kahrilas et al. (11,12). Grades were reported as normal, mildly, moderately or severely ineffective oesophageal motility (IOM). LOS pressure was recorded in all patients.

Scintigraphy

Patients were fasted overnight and medications were ceased for 24 h prior to the test. Patients were positioned upright in front of a Hawkeye 4 gamma camera (General Electric, Milwaukee, United States) with the mandible and stomach in the field of view. They swallowed 40-60 MBq of Tc-99m DTPA diluted in 50 mL of water followed by an additional 50 mL of water to clear activity from the oropharynx and oesophagus.

Dynamic imaging was performed for a duration of 2 minutes at an interval of 15s per frame into a 64*64 matrix. Patients were then placed in a supine position and dynamic images obtained at a framing rate of 30s per frame for 30 minutes. After supine imaging, 40-60 MBq of phytate (colloid) was administered orally with a 50 mL flush of water. Delayed static imaging using a 256*256 matrix was obtained two hours later for assessment of lung aspiration of refluxate. Images were analyzed by regions of interest over the pharynx, upper, mid and lower oesophagus with a background region over the lateral chest. Time-activity curves were generated from each region (Figure 1) Grades was assigned to the time-activity curves as shown in Figure 2. Grade 1 was a declining curve, with grade 2 being flat and grade 3 a rising curve. Delayed images (Figure 3) were analyzed with a line profile for the assessment of aspiration into the main airways ($> 2 \times$ background).

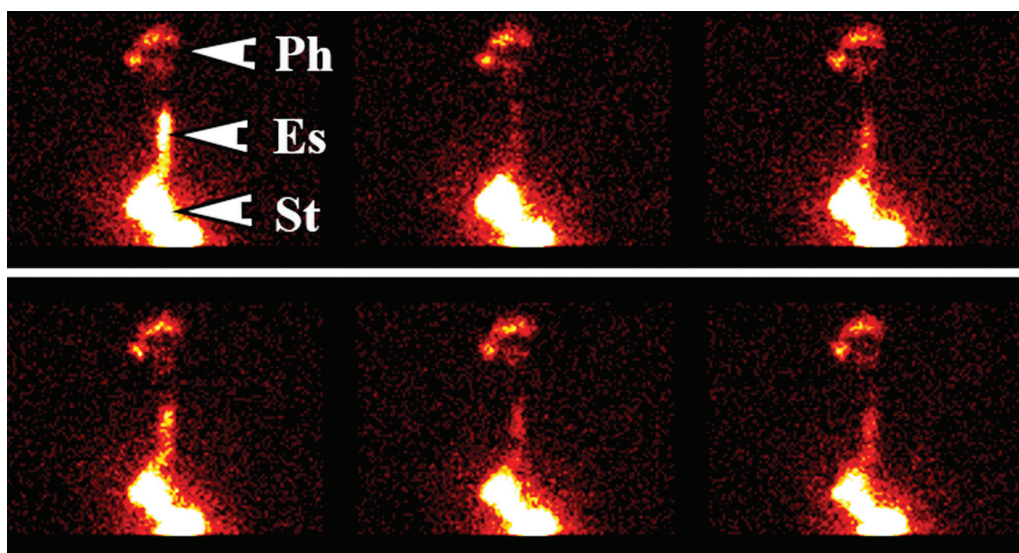


Figure 1. Dynamic sequence of the scintigraphic study showing full-column gastro-oesophageal reflux to the level of the pharynx. The oesophagus and stomach are labelled as Es and St, respectively

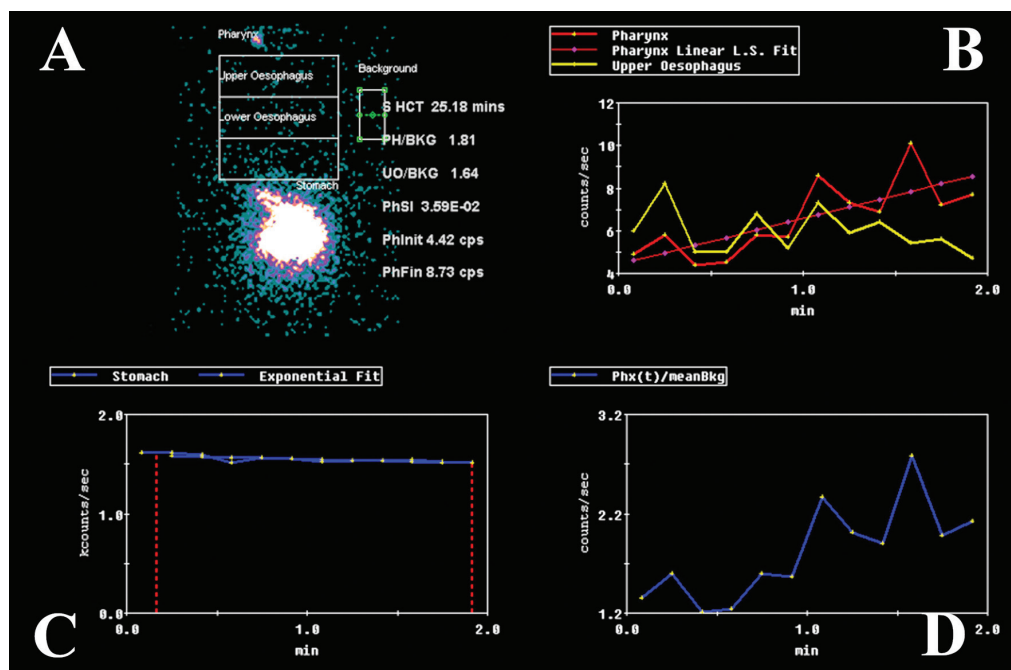


Figure 2. Graphical analysis of the dynamic study. Panel A shows the regions of interest for the pharynx, upper and lower oesophagus and the background regions as well as the relevant results. Panel B shows the time-activity curves for the pharynx (red) with its fitted curve (pink) and the curve for the upper oesophagus (yellow). Panel C is the gastric emptying curve with the time to half clearance being shown at 25.2 minutes in panel A. Panel D indicates the ratio of pharynx to background

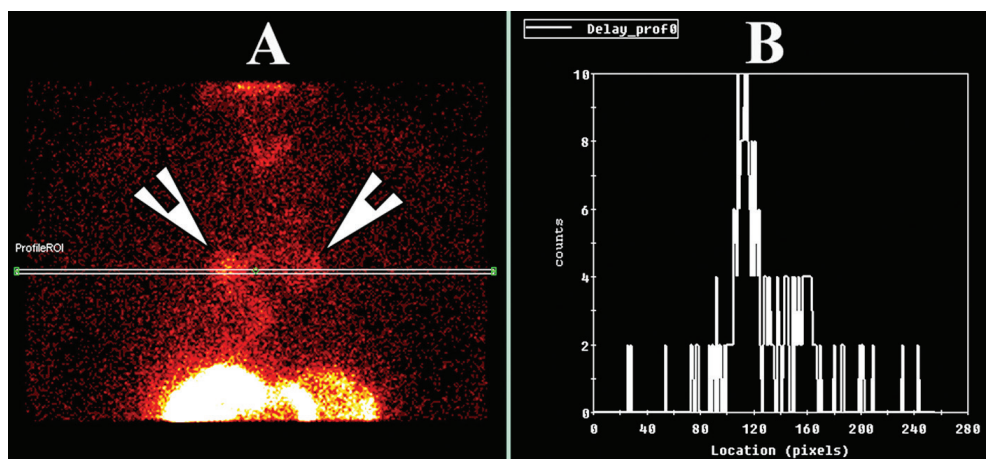


Figure 3. A) The delayed study at 2 hours demonstrates aspiration of tracer into both lungs with significant activity in the main airways (arrowheads). B) The line profile through the hilar regions shows the count densities in the lungs, which is 5 times higher than background activity

Statistical Analysis

Data was analyzed by nonparametric statistical methods as much of the analysis was of ordinal data with multiple studies for each patient. Standard ANOVA statistics, Wilcoxon matched pairs test, Student’s t-test and Pearson correlation coefficient (2 tails) with significance levels of 0.05 were utilized. Fisher’s exact test (two-tailed) and receiver operating characteristic (ROC) analysis was also undertaken where appropriate. Statistica V8 software

(Statsoft, Oklahoma, United States) package was used for data analysis.

Results

Population and clinical data. A total of 250 consecutive patients with complete data were studied (155 F, 95 M) over a period of 24 months. The average age was 60 years with a range of 20-85 years. Clinical history distinguished the patients clinically as predominantly GORD in 72

patients and LPR (\pm GORD) in 178. All patients underwent 24-hour pH monitoring and water perfused manometry. Scintigraphic studies were acquired within a 3-week period of the standard tests in all patients. A subset of 33 patients underwent laparoscopic fundoplication and these results have been reported elsewhere (9).

Two channel 24-hour pH monitoring. Twenty-four-hour pH studies were normal in 25 patients (pH >4), weakly acidic in 78 (pH >4 , <7) and abnormal in the rest (147). Results of the pH findings are shown in Table 1. In patients with scintigraphic evidence of aspiration, 14% (n=10) had normal proximal pH studies while 6% (n=5) had normal distal pH studies.

There was no significant difference in pH studies between patients with LPR and GORD ($p>0.05$). Moderate correlation was found between proximal and distal acid exposure (Pearson correlation coefficient=0.32, $p=0.001$).

Proximal and distal acid exposure had no significant correlation with either LOS pressure or oesophageal clearance by manometry ($p>0.05$). Correlation coefficients were poor (Pearson correlation coefficients ranging from 0.080 to 0.15).

No significant correlation was found between proximal and distal acid exposure and either scintigraphic clearance curves from the pharynx or upper oesophagus ($p>0.05$).

Manometry: The patients clinically classified as LPR, had severe IOM (35%); compared to the GORD group (17%). This was a significant difference by Fisher's exact test (two-tailed) with $p=0.0058$. Normal oesophageal motility was found in 27% with LPR symptoms and in 49% with GORD symptoms. This was a significant difference by Fisher's exact test (two-tailed) with $p=0.0021$.

The mean LOS pressure was 6.3 mmHg [median: 2.3, standard deviation: 8.4 (95% CI: 5.9-7.6) mmHg]. No significant difference was found between the LPR and GORD groups for mean LOS pressure ($p>0.01$).

Severe IOM was strongly associated with isotope aspiration in both groups [$p=0.00$ for LPR (Pearson correlation coefficients: 0.54)] and $p=0.04$ for GORD (Pearson correlation coefficients: 0.21).

There was a strong correlation between IOM and rising isotope curves in the pharynx when supine (Pearson correlation coefficients: 0.29, $p=0.003$) and upright (Pearson correlation coefficients: 0.38, $p=0.00$).

Table 1. pH study (% acidic reflux/24 hours)

Site	Mean	SD	Range
Proximal upright	6.0	6.8	1.0-34.0
Proximal supine	7.9	6.4	1.0-26.0
Distal upright	5.2	5.2	1.0-26.0
Distal supine	8.5	9.1	1.0-52.0

SD: Standard deviation

Scintigraphy: A total of 68 out of 250 patients demonstrated isotope aspiration into the lungs. There was significantly more pulmonary aspiration of refluxate in the group with LPR (58/178) symptoms than with a GORD profile (10/72) by Fisher's exact test ($p=0.0027$).

The time activity curves for the pharynx and upper oesophagus with the pulmonary aspiration data for each pattern of curve is shown in Table 2 and 3, respectively. The outstanding feature of these findings is the rarity of isotope aspiration in patients with a declining time activity curve (Grade 1) for the pharynx and upper oesophagus. No patient with a clinical GORD profile had lung aspiration in either the upright or supine position and only 3 of 63 patients with LPR symptoms showed evidence of aspiration. Similar findings were shown for declining time-activity curves for the upper oesophagus. This is in sharp contrast with a rising time activity curve, where a high proportion of patients had evidence of pulmonary aspiration. A declining time-activity curve in the pharynx and upper oesophagus has a negative predictive value (NPV) of 97% for aspiration. Rising curves at both sites have a positive predictive value (PPV) of 98% for aspiration. The results for the pharynx, regardless of the upper oesophageal clearance pattern, were NPV of 98% and PPV of 100%.

The ROC analysis demonstrated that the optimal tests for pulmonary aspiration of refluxate were the scintigraphic time activity curves for the pharynx and upper oesophagus, and the manometric marker of oesophageal clearance (Figure 4). Distal oesophageal total acid exposure and LOS pressures were not significant predictors of lung aspiration

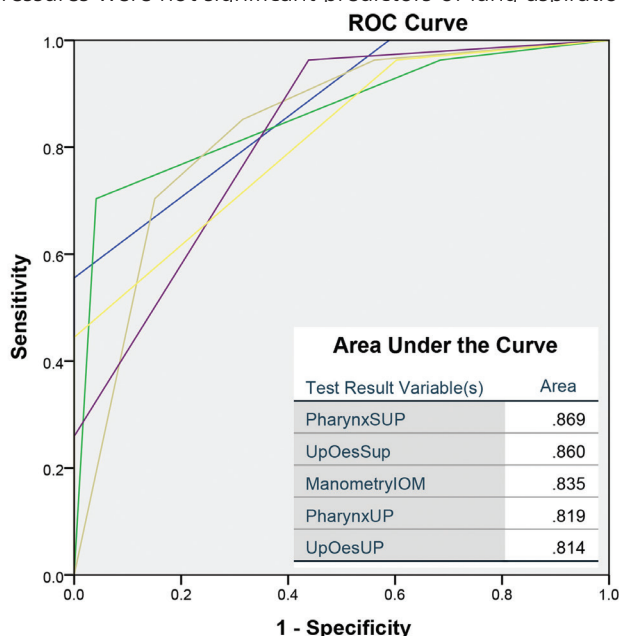


Figure 4. Receiver operating characteristic for the variables as predictors of lung aspiration of refluxate. The area under the curves is inset ROC: Receiver operating characteristic

Table 2. Pharyngeal time-activity curves for the scintigraphic studies according to symptom profile (laryngopharyngeal reflux versus gastro-oesophageal reflux disease)

Clinical	Grade 1	Aspiration	Grade 2	Aspiration	Grade 3	Aspiration
GORD upright	42	0 (0%)	30	10 (33%)	0	0 (0%)
GORD supine	20	0 (0%)	44	3 (7%)	8	8 (100%)
LPR upright	63	3 (5%)	97	38 (39%)	18	18 (100%)
LPR supine	55	0 (0%)	93	28 (30%)	30	30 (100%)

LPR: Laryngopharyngeal reflux, GORD: Gastro-oesophageal reflux disease

Table 3. Upper oesophageal time-activity curves for the scintigraphic studies according to symptom profile (laryngopharyngeal reflux versus gastro-oesophageal reflux disease)

Clinical	Grade 1	Aspiration	Grade 2	Aspiration	Grade 3	Aspiration
GORD upright	29	3 (10%)	40	5 (13%)	3	3 (100%)
GORD supine	15	0 (0%)	49	5 (10%)	8	5 (63%)
LPR upright	45	0 (0%)	105	30 (29%)	28	28 (100%)
LPR supine	45	3 (7%)	84	13 (15%)	49	43 (90%)

LPR: Laryngopharyngeal reflux, GORD: Gastro-oesophageal reflux disease

($p > 0.05$) with proximal total acid exposure just reaching significance ($p = 0.04$).

Discussion

This study indicates that scintigraphic reflux studies are a viable alternative to the current suite of testing for the establishment of a diagnosis of GORD. However, the group of patients enrolled in the current study are not a typical representation of how this disease presents in the general community. This is a highly selected group of patients, referred to a tertiary center for resistance to standard therapy or atypical symptoms of GORD. Perhaps the most important finding of this study is that attempting to clinically classify patients as either purely oesophageal disease (GORD) or extra oesophageal disease (LPR) is a futile exercise. A significant proportion of patients classified as GORD will demonstrate pulmonary aspiration of refluxate, which is clinically silent (Figure 3). This has been elegantly shown by similar scintigraphic techniques in 20% of patients with chronic respiratory disease but silent GORD. As little as 0.1 MBq of aspirated activity was detectable in the lungs of these patients (13).

While the scintigraphic reflux study is capable of demonstrating evidence of GORD at the oesophageal level (Figure 1), its other great advantage is the delineation of extra-oesophageal disease. This is clearly reflected at the level of the oropharynx, laryngopharynx and the lungs. These areas are not screened by the existing suite of testing such as manometry and pH and with some reservations by impedance monitoring. Refluxate contaminating the extra-oesophageal tissues can be visualized and although 27% of patients showed evidence of pulmonary aspiration of refluxate, this may in fact be an underestimate of the true

incidence of pulmonary aspiration in this type of patient cohort. Patients are supine for approximately 30 minutes and are essentially upright for the other 90 minutes prior to the delayed scan for pulmonary aspiration. This may in fact be significantly worse when the patient is supine and asleep at night (14).

Analysis of the scintigraphic time-activity curves for the pharynx and upper oesophagus showed a strong correlation with IOM, indicating that inability to adequately clear refluxate from the oesophagus is of significant importance in addition to the incompetence of the LOS tone in both GORD and LPR patients with pulmonary aspiration of refluxate. LOS tone was not a good discriminator as the majority of referred patients had poor tone with a mean of 6.3 mmHg (N~26 mmHg) (15). When analyzing the ROC curves, IOM was as useful as the scintigraphic time-activity curves in predicting aspiration of refluxate (Figure 4). This observation confirms that the scintigraphic technique is also useful in detecting dysmotility, as the time-activity curves will accurately reflect this. A rising curve is the end result of recurrent episodes of reflux and the inability of the oesophageal clearance mechanisms to remove the refluxate. Dysmotility is a key marker for LPR as has been shown by others, particularly in those with silent reflux and extra-oesophageal symptoms such as cough (16,17).

Earlier studies with 24-hour ambulatory pH monitoring have pointed erroneously out the importance of distal rather than proximal oesophageal pH as being important in patients with heart-burn and respiratory complications of GORD (18). Others have attempted to rationalize the disparity by suggesting that acid is neutralized during the ascent to the proximal oesophagus and may not register on the proximal pH probe (19). It is our contention that distal oesophageal pH does not fully emulate what is happening in the upper

oesophagus and pharynx which is essentially beyond the level of the pH probe and therefore, is fundamentally a blind spot. This verifies the hypothesis of a poor correlation between pH studies in the distal oesophagus and lung aspiration of isotope to be true. The ROC analysis shows a poor performance for total distal acid exposure [Area under the curve (AUC)=0.597, $p=0.179$] and a marginally better and barely significant finding with total proximal acid exposure (AUC=0.651, $p=0.036$) in patients with aspiration of refluxate. The scintigraphic variables and IOM were comparatively better performers in the prediction of pulmonary aspiration of refluxate (AUC~0.850).

It must however be acknowledged that the published data which validates 24-hour pH monitoring is fundamentally concerned with the typical symptoms of heartburn and acid regurgitation. This imposes a significant limitation and may subsequently lead to an under diagnosis, particularly in the group of patients with silent reflux. In this group of patients, pH testing may not be the optimal choice of test for diagnosis of the disease. Some theories suggest that neutral or basic pH is equally or more significant than acidic pH. Refluxate may contain pepsin and bile contents that have also been implicated in tissue injury in the laryngopharynx (20,21). The data presented here illustrates the poor correlation between positive distal pH and pulmonary aspiration (3). Some studies have demonstrated pepsin in the laryngeal epithelium after a reflux event and questions have been raised as to the potential damage which may be caused (20,21). Failure to identify this group of patients could subsequently lead to progression of the disease and the development of secondary manifestations (22,23) such as laryngeal carcinoma, vocal cord granulomas and pulmonary aspiration and its multiplicity of complications such as bronchiectasis, lung fibrosis etc. The major diagnostic issue is attempting to imply the presence of refluxate through indirect markers of pH monitoring and manometry. Scintigraphic studies allow direct visualization of activity in the laryngopharynx and lungs. Importance of the diagnostic algorithm for LPR versus GORD is that LPR requires more stringent medical therapy, which has a high failure rate and leads to earlier contemplation of fundoplication, particularly if there is lung aspiration of refluxate (5).

The negative and positive predictive values of the scintigraphic time-activity curves for the oesophagus and pharynx as predictors of pulmonary aspiration were very good at 97% and 98%, respectively. This was an unexpected finding and may prove to be of clinical value in patients with a high clinical suspicion of aspiration, but no scan evidence in the delayed study. It may inform the decision to undertake fundoplication for severe cases of reflux with a strong clinical suspicion of aspiration. It is also reassuring to physically see GORD in the dynamic studies and then refluxate in the lungs in the delayed phase of the study, particularly in silent (heartburn negative) disease

with manifest extra-oesophageal symptoms such as cough, globus etc.

The principal weakness of this study is the highly selected cohort of patients who already had a high pre-test probability of disease. It requires assessment in general community patients to ascertain its false positive rate. To this end, we have commenced a study in normal subjects with acquisition of reflux studies in 25 asymptomatic volunteers. Preliminary findings in 10 cases demonstrates low-grade gastroesophageal reflux in three and then to the mid-oesophagus when in the upright position only. The others showed no evidence of reflux. There was no pharyngeal reflux or lung aspiration of tracer.

Conclusion

We describe an innovative nuclear scintigraphic reflux test and its performance on a cohort of patients referred to a tertiary referral center for failure to respond to therapy of typical or atypical symptoms. This test has the potential to re-define the current understanding of GORD as it considers the broad definition of GORD. A strong correlation was found between scintigraphic parameters in the pharynx and upper oesophagus, and markers of ineffective oesophageal clearance consistent with dysmotility. These parameters were strongly predictive of pulmonary aspiration of the refluxate. pH studies were weakly correlated with these parameters and of little use in predicting laryngeal exposure and pulmonary aspiration.

Ethics

Ethics Committee Approval: Concord Hospital Institutional Ethics Committee (LNR/12 CRGH/248).

Informed Consent: Obtained in writing from all patients.

Peer-review: Externally and internally peer-reviewed.

Authorship Contributions

Surgical and Medical Practices: G.L.F., S.P., Concept: L.B., G.L.F., Design: G.L.F., H.V.D.W., Data Collection or Processing: L.B., H.V.D.W., M.C., Analysis or Interpretation: L.B., G.L.F., H.V.D.W., Literature Search: L.B., S.P., Writing: L.B., H.V.D.W., G.L.F., S.P., M.C.

Conflict of Interest: No conflict of interest was declared by the authors.

Financial Disclosure: No funding was received for the project.

References

1. Spechler SJ. Epidemiology and natural history of gastro-oesophageal reflux disease. *Digestion* 1992;51(Suppl 1):24-29.
2. Vakil N, van Zanten SV, Kahrilas P, Dent J, Jones R; Global Consensus Group. The Montreal definition and classification of gastroesophageal reflux disease: a global evidence-based consensus. *Am J Gastroenterol* 2006;101:1900-1920.

3. Richter JE. How to manage refractory GERD. *Nat Clin Pract Gastroenterol Hepatol* 2007;4:658-664.
4. De Giorgi F, Palmiero M, Esposito I, Mosca F, Cuomo R. Pathophysiology of gastro-oesophageal reflux disease. *Acta Otorhinolaryngol Ital* 2006;26:241-246.
5. Koufman J, Aviv JE, Casiano RR, Shaw GY. Laryngopharyngeal Reflux: Position Statement of the Committee on Speech, Voice, and Swallowing Disorders of the American Academy of Otolaryngology-Head and Neck Surgery. *Otolaryngol Head Neck Surg* 2002;127:32-35.
6. Caglar M, Volkan B, Alpar R. Reliability of radionuclide gastroesophageal reflux studies using visual and time-activity curve analysis: inter-observer and intra-observer variation and description of minimum detectable reflux. *Nucl Med Commun* 2003;24:421-428.
7. Kjellen G, Brudin L, Hakansson HO. Is scintigraphy of value in the diagnosis of gastroesophageal reflux disease? *Scand J Gastroenterol* 1991;26:425-430.
8. Shay SS, Abreu SH, Tsuchida A. Scintigraphy in gastroesophageal reflux disease: a comparison to endoscopy, LESp, and 24-h pH score, as well as to simultaneous pH monitoring. *Am J Gastroenterol* 1992;87:1094-1101.
9. Falk GL, Beattie J, Ing A, Falk SE, Magee M, Burton L, Van der Wall H. Scintigraphy in laryngopharyngeal and gastroesophageal reflux disease: a definitive diagnostic test? *World J Gastroenterol* 2015;21:3619-3627.
10. Belafsky PC, Postma GN, Koufman JA. Validity and reliability of the reflux symptom index (RSI). *J Voice* 2002;16:274-277.
11. Kahrilas PJ, Dodds WJ, Hogan WJ, Kern M, Arndorfer RC, Reece A. Esophageal peristaltic dysfunction in peptic esophagitis. *Gastroenterology* 1986;91:897-904.
12. Kahrilas PJ, Dent J, Dodds WJ, Hogan WJ, Arndorfer RC. A method for continuous monitoring of upper esophageal sphincter pressure. *Dig Dis Sci* 1987;32:121-128.
13. Ruth M, Carlsson S, Mansson I, Bengtsson U, Sandberg N. Scintigraphic detection of gastro-pulmonary aspiration in patients with respiratory disorders. *Clin Physiol* 1993;13:19-33.
14. Barish CF, Wu WC, Castell DO. Respiratory complications of gastroesophageal reflux. *Arch Intern Med* 1985;145:1882-1888.
15. Richter JE, Wu WC, Johns DN, Blackwell JN, Nelson JL, Castell DO. Esophageal manometry in 95 healthy adult volunteers. Variability of pressures with age and frequency of "abnormal" contractions. *Dig Dis Sci* 1987;32:583-592.
16. Agreus L. The epidemiology of functional gastrointestinal disorders. *Eur J Surg(Suppl)* 1998:60-66.
17. Kastelik JA, Redington AE, Aziz I, Buckton GK, Smith CM, Dakkak M, Morice AH. Abnormal oesophageal motility in patients with chronic cough. *Thorax* 2003;58:699-702.
18. Gastal OL, Castell JA, Castell DO. Frequency and site of gastroesophageal reflux in patients with chest symptoms. Studies using proximal and distal pH monitoring. *Chest* 1994;106:1793-1796.
19. Charbel S, Khandwala F, Vaezi MF. The role of esophageal pH monitoring in symptomatic patients on PPI therapy. *Am J Gastroenterol* 2005;100:283-289.
20. Gill G, Johnston N, Buda A, Pignatelli M, Pearson J, Dettmar PW, Koufman J. Laryngeal epithelial defenses against laryngopharyngeal reflux: investigations of E-cadherin, carbonic anhydrase isoenzyme III, and pepsin. *Ann Otol Rhinol Laryngol* 2005;114:913-921.
21. Johnston N, Knight J, Dettmar PW, Lively MQ, Koufman J. Pepsin and carbonic anhydrase isoenzyme III as diagnostic markers for laryngopharyngeal reflux disease. *Laryngoscope* 2004;114:2129-2134.
22. Khan AM, Hashmi SR, Elahi F, Tariq M, Ingrams DR. Laryngopharyngeal reflux: A literature review. *Surgeon* 2006;4:221-225.
23. Rathod NR. Extra-oesophageal presentation of gastro-oesophageal reflux disease. *J Indian Med Assoc* 2010;108:18-20.



I-131 mIBG Scintigraphy Curie Versus SIOOPEN Scoring: Prognostic Value in Stage 4 Neuroblastoma

I-131 mIBG Sintigrafisi Curie ve SIOOPEN Skorlarının Evre 4 Nöroblastomada Prognostik Değerinin Karşılaştırılması

✉ Saima Riaz¹, ✉ Humayun Bashir¹, ✉ Saadiya Javed Khan², ✉ Abid Qazi³

¹Shaukat Khanum Memorial Cancer Hospital and Research Centre, Clinic of Nuclear Medicine, Lahore, Pakistan

²Shaukat Khanum Memorial Cancer Hospital and Research Centre, Clinic of Pediatric Oncology, Lahore, Pakistan

³Canal Bank, Clinic of Surgery, Lahore, Pakistan

Abstract

Objective: I-131 mIBG scan semi-quantitative analysis with modified Curie and the International Society of Pediatric Oncology Europe Neuroblastoma (SIOOPEN) scoring systems is helpful in the evaluation of disease extent and has prognostic impact in stage 4 neuroblastoma.

Methods: Retrospective, cross-sectional analysis of baseline I-131 mIBG scans in 21 patients with stage 4 or 4S neuroblastoma diagnosed between January 2007 and December 2015. All scans were assessed for Curie and SIOOPEN scores. Distribution of scores was evaluated for risk factors i.e. age at diagnosis (>18 months) and early relapse (within 12 months). A curie score <2 and SIOOPEN score <4 at diagnosis were correlated with event-free survival (EFS) and overall survival (OS).

Results: The data set comprised of 12 (57%) males and 9 (43%) females. Patients with age >18 months (n=9) at diagnosis or early relapse (n=9) had higher Curie [mean 5+7.5 standard deviation (SD), p=0.004] and SIOOPEN (mean 5.2+10.8 SD, p=0.02) scores. Patients with a Curie score <2 and a SIOOPEN score of <4 had better EFS and OS than patients with higher scores. Curie: 5-year EFS=Curie <2 (79%) versus Curie >2 (33%) (p=0.03); 5-year OS=Curie <2 (56%) versus Curie >2 (36%) (p=0.01). SIOOPEN: 5-year EFS=SIOOPEN <4 (70%) versus SIOOPEN >4 (17%) (p=0.002); 5-year OS=SIOOPEN <4 (58%) versus SIOOPEN >4 (17%) (p=0.04). There was no statistically significant difference between the two scoring systems in terms of survival predictive value (Hazard ratio 2.38, 95% CI: 0.33-16.9, p=0.38).

Conclusion: I-131 mIBG Curie and SIOOPEN scores have prognostication value in stage 4 neuroblastoma and should be routinely applied. Higher scores predict unfavorable prognosis.

Keywords: I-131 mIBG scan, neuroblastoma, Curie scores, SIOOPEN scores

Öz

Amaç: I-131 mIBG sintigrafisinin modifiye Curie ve International Society of Pediatric Oncology Europe Neuroblastoma (SIOOPEN) skorlama sistemleri ile yarı-kantitatif analizi evre 4 nöroblastomda hastalığın yayılımını değerlendirmede yararlıdır ve prognostik etkisi bulunmaktadır.

Yöntem: Ocak 2007 ile Aralık 2015 tarihleri arasında, evre 4 veya 4S nöroblastom tanısıyla I-131 mIBG sintigrafisi yapılmış 21 hastanın retrospektif, kesitsel analizi yapıldı. Tüm tetkikler Curie ve SIOOPEN skoru ile değerlendirildi. Tanı yaşı (>18 ay) ve erken

Address for Correspondence: Saima Riaz MD, Shaukat Khanum Memorial Cancer Hospital and Research Centre, Clinic of Nuclear Medicine, Lahore, Pakistan
Phone: +923465938557 E-mail: saimarz.dr@gmail.com

Received: 05.05.2018 **Accepted:** 28.08.2018

©Copyright 2018 by Turkish Society of Nuclear Medicine
Molecular Imaging and Radionuclide Therapy published by Galenos Yayınevi.

nüks (12 ay içinde) gibi risk faktörlerine göre skor dağılımı değerlendirildi. Tanı anında Curie skoru <2 ve SIOPEN skoru <4 hastalısız (HGS) ve genel sağkalım (GS) ile ilişkili idi.

Bulgular: Çalışmaya 12 (57%) erkek ve 9 (43%) kadın dahil edildi. Tanı anında yaşı >18 ay olan hastalar (n=9) veya erken nüks edenlerde (n=9) Curie [ortalama 5+7,5 standart deviasyon (SD), p=0,004] ve SIOPEN (ortalama 5,2+10,8 SD, p=0,02) skorları daha yüksek bulundu. Curie skoru <2 ve SIOPEN skoru <4 olan hastaların HGS ve GS daha yüksek skorlu hastalardan daha iyiydi. Curie: 5-yıl HGS=Curie <2 (%79) vs Curie >2 (%33) (p=0,03); 5-yıl GS=Curie <2 (%56) vs Curie >2 (%36) (p=0,01). SIOPEN: 5-yıl HGS=SIOPEN<4 (%70) vs SIOPEN >4 (%17) (p=0,002); 5-yıl GS= SIOPEN <4 (%58) vs SIOPEN >4 (%17) (p=0,04). Her iki skortlama sistemi arasında sağkalım öngörücü değer açısından istatistik olarak anlamlı farklılık saptanmadı (Risk oranı: 2,38, %95 CI: 0,33-16,9, p=0,38).

Sonuç: I-131 mIBG Curie ve SIOPEN skorlarının evre 4 nöroblastomda prognostik öngörü değeri vardır ve rutin olarak kullanılmalıdır. Yüksek skorlar daha kötü prognozu göstermektedir.

Anahtar kelimeler: I-131 mIBG sintigrafi, nöroblastoma, Curie skoru, SIOPEN skoru

Introduction

Neuroblastoma is the most common extra-cranial solid malignant tumor in children. It originates from the sympathetic nervous system, most frequently from the adrenal medulla. The heterogeneous clinical behavior of neuroblastoma is dependent on numerous clinical as well as biological features (1). Neuroblastoma is diagnosed over a wide age range, from birth through young adulthood. Older age at diagnosis indicates a grim survival. Poor prognostic factors include: Age >18 months, NMYC amplification, poorly differentiated, advanced stage disease, and indistinguishable tumor histology (2). Approximately 70% of neuroblastoma patients present with metastatic disease (3). With the current treatment approaches, age at diagnosis has proven to be one of the most influential predictors of the outcome. In patients older than 1 year, the 5-year disease-free survival rates for stage 4 neuroblastoma have been reported to be 30-46% (4).

Treatment regimens including induction therapy, autologous stem cell transplantation, better radiotherapy techniques and immunotherapy have led to improvements in disease-free survival. Tailoring treatment to risk group stratification has improved outcome. The capacity to identify both biologic and clinical prognostic markers of response has the benefit of selecting treatment therapies (5).

Radioiodine labeled metaiodobenzylguanidine (mIBG) is an aralkylguanidine, structurally parallel to norepinephrine. Almost 90% of neuroblastoma concentrate mIBG within the marrow, soft-tissue sites of disease or cortical bone (6,7). Since I-123 labeled mIBG is not available in our part of the world, I-131 mIBG is used.

Materials and Methods

Retrospective data of baseline I-131 mIBG scans was analyzed in patients with stage 4 or 4S neuroblastoma registered between January 2007 and December 2015.

Our data set included 21 patients, aged 0.5 to 12 years. Twelve were males (57%) and 9 (43%) females.

This retrospective study has been approved by the Institutional Review Board of Shaukat Khanum Cancer Hospital and Research Centre, Lahore.

Imaging

Radiotracer dose in the range of 37 to 55 MBq I-131 mIBG was injected intravenously adjusted to patients' weight according to EANM recommendations. Scanning was acquired at 24 and 48 hours using Siemens Symbia T16 camera, 128x128 matrix for planar scan, bed movement 7-8 cm/min.

Semi-quantitative Analyses

Semi-quantitative evaluation of all scans was performed using the Curie and International Society of Pediatric Oncology Europe Neuroblastoma (SIOPEN) scoring methodology.

Initially developed in 1995, scoring is based on the presence of mIBG uptake in multiple anatomic regions (8,9). Ten different sites were scored, including 9 skeletal sites (head, chest, T-spine, L-spine, pelvis, upper arms, lower arms, femurs, and lower legs) and an additional tenth site for soft-tissue lesions.

The International Neuroblastoma Risk Group (INRG) Staging System (INRGSS) is an imaging defined staging and risk assessment system. According to the SIOPEN semi-quantitative scoring method, the skeleton was divided into 12 anatomical body segments as follows: the skull, the thoracic cage, the proximal right upper limb, the distal right upper limb, the proximal left upper limb, the distal left upper limb, the spine, the pelvis, the proximal right lower limb, the distal right lower limb, the proximal left lower limb and the distal left lower limb. The extent and pattern of skeletal mIBG involvement was scored using a 0-6 scale to discriminate between focal discrete lesions and patterns of more diffuse infiltration (10).

Distribution of scores was evaluated for two risk factors i.e. age at diagnosis (>18 months) and early relapse (within 12 months).

Statistical Analysis

The data were analyzed by the Kaplan-Meier method using IBM SPSS statistics 20 program. A Curie score <2 and SIOPEN score <4 (est defined cut-off) at diagnosis were correlated with event-free survival (EFS) and overall survival (OS) (11). Log-rank test with a p value of less than 0.05 was used to evaluate the differences between groups. Cox proportional hazards regression model applying the enter method was used to estimate hazards ratio (HR) for analysis.

Results

The data set included 12 (57%) males and 9 (43%) females (age range: 4 months to 12 years). All had stage 4 disease in terms of osteomedullary metastases (n=9), soft issue metastases (n=8) and cytological bone marrow involvement (n=4) (Table 1).

Out of total 21 patients, 12 (57%) were younger than 18 months, while 9 (43%) older than 18 months of age. Nine patients (57%) had either relapse within 12 months after diagnosis or primary progressive disease.

Semi-quantitative Scoring

Overall Curie score ranged from minimum 1 to a maximum score of 27 (average 5.9±7.9 S). SIOPEN scores ranged between 0 to a maximum score of 48 [average 6.1±11.6 standard deviation (SD)].

On Curie scores analysis, 10 patients had <2 and 11 had >2 Curie scores. SIOPEN score <4 was calculated in 15 and >4 in 6 patients.

Distribution of mIBG Score by Risk Factors

In patients with age <18 months at diagnosis, Curie scores were 2.7±4.2 SD and SIOPEN scores were 1.2±3.2 SD. For age >18 months, Curie scores were identified as 10.4±9.7 SD and SIOPEN scores 12.8±15.4 SD. On bivariate analysis, the scores were higher in age >18 months (p=0.002 for Curie and p=0.018 for SIOPEN scores).

In reference to relapse, patients with early relapse had Curies scores 9.8±10.2 SD, and SIOPEN scores were 14.0±10.8

SD. In comparison to this, patients who did not show early relapse, the Curie scores were 1.2±1.5 SD, while SIOPEN scores were 3.6±1.6 SD. The scores tended to be higher in patients with early relapse within 12 months in comparison to patients who did not show early relapse (p=0.004 for Curie and p=0.02 for SIOPEN scores). The details of these scores have been displayed in Figure 1.

Disease Outcome and Survival Analysis

Out of 10 patients with Curie score <2, 2 (20%) relapsed and 2 (20%) died, while with Curie score >2, 7 out of 11 (63.6%) relapsed and 6 (54.5%) died.

On analysis of SIOPEN scores, out of 15 patients with score <4, 4 (27%) relapsed and 4 (27%) died, while with scores >4, 5 out of 6 (83%) relapsed and 4 (67%) died.

Comparative analyses demonstrated that Curie score <2 and a SIOPEN score of <4, respectively, had better EFS and OS than patients with higher scores. 5-years EFS for Curie score <2 was 79% versus 33% for score >2 (p=0.03). 5-year OS was 56% for Curie score <2 versus 36% for score >2 (p=0.01).

Based on SIOPEN scoring, 5-year EFS was found to be 70% for score <4 as compared to 17% for score >4 (p=0.002). Similarly, 5-year OS for score <5 was 58% versus 17% for score >4 (p=0.04). The Kaplan-Meier disease-free survival

	Curie score		SIOPEN Score	
Age at Diagnosis				
<18 months	2.7 - SD4.2	P=0.02	1.2 - SD 3.2	P=0.018
>18 months	10.4 - SD9.7		12.8 -SD 15.4	
Tumor Relapse within 12 months				
No	1.2-SD 1.5	P=0.004	3.6 - SD 1.6	P=0.02
Yes	9.8 -SD 10.2		14.0- SD 10.8	

Figure 1. Distribution of Curie and International Society of Pediatric Oncology Europe Neuroblastoma scores with reference to risk factors
SD: Standard deviation

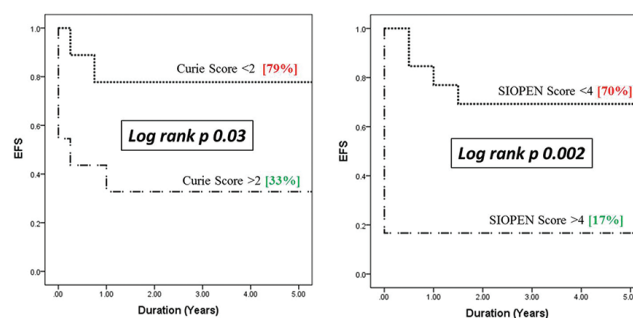


Figure 2. Curie and International Society of Pediatric Oncology Europe Neuroblastoma scores at diagnosis and event-free survival
SIOPEN: International Society of Pediatric Oncology Europe Neuroblastoma, EFS: Event-free survival

Table 1. Patient and disease characteristics	
n=21	
Gender	12 (57%) males 9 (43%) females
Age	Average: 2.7 years Range: 4 months to 12 years
Disease characteristics	Osteomedullary metastases: 9 Soft tissue metastases: 8 Cytological bone marrow: 4

distributions based on these low or high Curie and SIOPEN scores were significantly different (Figure 2, 3).

Comparing Curie and SIOPEN Scoring Systems in Predicting Prognosis

On bivariate analysis, there was no statistically significant difference between the two scoring systems in terms of survival predictive value [HR: 2.38, 95% confidence interval (CI): 0.33-16.9, $p=0.38$].

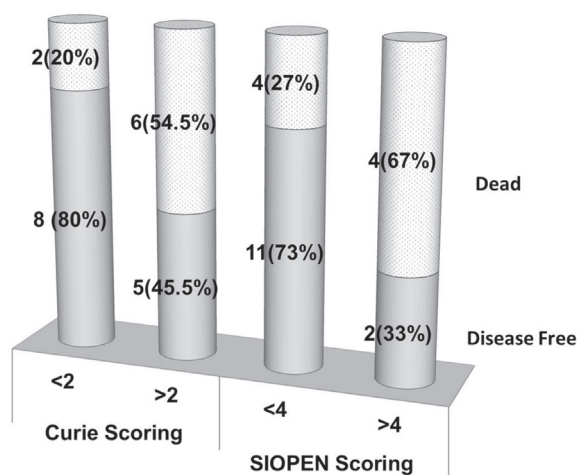


Figure 3. Curie and International Society of Pediatric Oncology Europe Neuroblastoma scores at diagnosis and overall survival
SIOPEN: International Society of Pediatric Oncology Europe Neuroblastoma

Discussion

Accurate disease staging is essential for an optimized treatment plan. The outcome is related to disease extent in stage 4 neuroblastoma. Radioiodine labeled mIBG semi-quantitative scoring systems are used to estimate disease burden. We selected two poor prognostic factors, age older than 18 months and early relapse, to evaluate the validity of mIBG scores (12).

In most of the earlier studies, age <12 months has been taken as the poor prognostic indicator. However, as shown by Moroz et al. (12,13), 18 months is a powerful indicator of unfavorable outcome as the cut off for age-of-diagnosis. Likewise, time to first relapse influences survival. London et al. (13), demonstrated that mortality risk is higher in patients who relapse early (14).

Scores tended to be higher in patients with age >18 months at diagnosis and early relapse. We found a statistically significant positive correlation between higher scores and poor prognostic factors. In this regard, radioiodine mIBG scan at baseline with high scores can be taken as an indicator of poor outcome. Various studies have shown different cut-off values for mIBG score systems (14,15), and there are several previous studies where no significant

prognostic impact of the initial mIBG score was reported (16,17).

However, Decarolis et al. (11), reported the best cut-off for the Curie score as 2 and that for the SIOPEN score as 4, which significantly discriminated between poor and more favorable outcomes. We evaluated the validity of these cut-off scores in our referral group. Patients who tended to have higher scores at baseline had higher frequencies of disease relapse and deaths. Outcome was significantly better in lower scores with better EFS and OS when compared with higher scores.

An INRG task force led by Matthay et al. (10) has examined both methodologies as a potential prognostic marker for outcome determination. The SIOPEN scoring methodology is currently being used in SIOPEN high risk neuroblastoma trials, with Curie scoring used in COG trials.

In a prior review of COG-A3973, COG investigators were unable to identify a mIBG (Curie) score at diagnosis that correlated with outcome (14). Ladenstein et al. (15) studied the baseline scores at diagnosis and reported SIOPEN mIBG score to be highly prognostic of outcome in two independent data sets, SIOPEN/HR-NBL1 and COG-A3973. In comparison, our data set comply with findings of Decarolis et al. (11). We found that the prognostic value of Curie and SIOPEN scores were similar. Although SIOPEN scores do not include soft tissue disease, both scoring systems were found to have similar prognostic significance with no statistically significant difference (HR: 2.38, 95% CI: 0.33-16.9, $p=0.38$).

Study Limitation

The limitation of this study is the limited number of follow-up I-131 mIBG scans, to provide statistically significant outcome analyses based on post-induction Curie and SIOPEN scores. Our data needs further extension with future prospect to report the validity of these scores in therapeutic response evaluation and to develop mIBG scoring systems based response criteria.

Conclusion

In conclusion, our study demonstrates the feasibility of mIBG scoring systems, which have prognostication value in stage 4 neuroblastoma. These scores are not used in routine clinical practice. However, with advancement in therapeutic options in stage 4 neuroblastoma, the implementation of mIBG scoring systems can be helpful in more precise prognostication based treatment.

Ethics

Ethics Committee Approval: The study was approved by Institutional Review Board Shaukat Khanum Memorial Cancer Hospital and Research Centre, Lahore, Pakistan.

Informed Consent: Consent form has been filled out by all authors.

Peer-review: Externally peer-reviewed.

Authorship Contributions

Surgical and Medical Practices: S.J.K., A.Q., Concept: S.R., Design: S.R., Data Collection or Processing: S.R., Analysis or Interpretation: S.R., Literature Search: S.R., H.B., Writing: S.R.

Conflict of Interest: No conflict of interest was declared by the authors.

Financial Disclosure: The authors declared that this study received no financial support.

References

- Matthay KK, Villablanca JG, Seeger RC, Stram DO, Harris RE, Ramsay NK, Swift P, Shimada H, Black CT, Brodeur GM, Gerbing RB, Reynolds CP. Treatment of high-risk neuroblastoma with intensive chemotherapy, radiotherapy, autologous bone marrow transplantation, and 13-cis-retinoic acid. Children's Cancer Group. *N Engl J Med* 1999;341:1165-1173.
- Cheung NK, Zhang J, Lu C, Parker M, Bahrami A, Tickoo SK, Heguy A, Pappo AS, Federico S, Dalton J, Cheung IY, Ding L, Fulton R, Wang J, Chen X, Becksfort J, Wu J, Billups CA, Ellison D, Mardis ER, Wilson RK, Downing JR, Dyer MA; St Jude Children's Research Hospital–Washington University Pediatric Cancer Genome Project. Association of age at diagnosis and genetic mutations in patients with neuroblastoma. *JAMA* 2012;307:1062-1071.
- Moroz V, Machin D, Faldum A, Hero B, Iehara T, Mosseri V, Ladenstein R, De Bernardi B, Rubie H, Berthold F, Matthay KK, Monclair T, Ambros PF, Pearson AD, Cohn SL, London WB. Changes over three decades in outcome and the prognostic influence of age-at-diagnosis in young patients with neuroblastoma: a report from the International Neuroblastoma Risk Group Project. *Eur J Cancer* 2011;47:561-571.
- Kreissman SG, Villablanca JG, Diller L, London WB, Maris JM, Park JR, Reynolds CP, Allmen DV, Cohn SL, Matthay KK. Response and toxicity to a dose-intensive multi-agent chemotherapy induction regimen for high risk neuroblastoma (HR-NB): a Children's Oncology Group (COG A3973) study. *J Clin Oncol* 2007;25:9505.
- Yu AL, Gilman AL, Ozkaynak MF, London WB, Kreissman SG, Chen HX, Smith M, Anderson B, Villablanca JG, Matthay KK, Shimada H, Grupp SA, Seeger R, Reynolds CP, Buxton A, Reisfeld RA, Gillies SD, Cohn SL, Maris JM, Sondel PM; Children's Oncology Group. Anti-GD2 antibody with GM-CSF, interleukin-2, and isotretinoin for neuroblastoma. *N Engl J Med* 2010;363:1324-1334.
- Wieland DM, Mangner TJ, Inbasekaran MN, Brown LE, Wu JL. Adrenal medulla imaging agents: a structure-distribution relationship study of radiolabeled aralkylguanidines. *J Med Chem* 1984;27:149-155.
- Claudiani F, Stimamiglio P, Bertolazzi L, Cabria M, Conte M, Villavecchia GP, Garaventa A, Lanino E, De Bernardi B, Scopinaro G. Radioiodinated meta-iodobenzylguanidine in the diagnosis of childhood neuroblastoma. *Q J Nucl Med* 1995;39(Suppl 4):21-24.
- Ady N, Zucker JM, Asselain B, Edeline V, Bonnin F, Michon J, Gongora R, Manil L. A new 123I-MIBG whole body scan scoring method: application to the prediction of the response of metastases to induction chemotherapy in stage IV neuroblastoma. *Eur J Cancer* 1995;31:256-261.
- Matthay KK, Edeline V, Lumbroso J, Tanguy ML, Asselain B, Zucker JM, Valteau-Couanet D, Hartmann O, Michon J. Correlation of early metastatic response by 123I-metaiodobenzylguanidine scintigraphy with overall response and event-free survival in stage IV neuroblastoma. *J Clin Oncol* 2003;21:2486-2491.
- Matthay KK, Shulkin B, Ladenstein R, Michon J, Giammarile F, Lewington V, Pearson AD, Cohn SL. Criteria for evaluation of disease extent by (123I)-metaiodobenzylguanidine scans in neuroblastoma: a report for the International Neuroblastoma Risk Group (INRG) Task Force. *Br J Cancer* 2010;102:1319-1326.
- Decarolis B, Schneider C, Hero B, Simon T, Volland R, Roels F, Dietlein M, Berthold F, Schmidt M. Iodine-123 metaiodobenzylguanidine scintigraphy scoring allows prediction of outcome in patients with stage 4 neuroblastoma: results of the Cologne interscore comparison study. *J Clin Oncol* 2013;31:944-951.
- Moroz V, Machin D, Faldum A, Hero B, Iehara T, Mosseri V, Ladenstein R, De Bernardi B, Rubie H, Berthold F, Matthay KK, Monclair T, Ambros PF, Pearson AD, Cohn SL, London WB. Changes over three decades in outcome and the prognostic influence of age-at-diagnosis in young patients with neuroblastoma: a report from the International Neuroblastoma Risk Group Project. *Eur J Cancer* 2011;47:561-571.
- London WB, Castel V, Monclair T, Ambros PF, Pearson AD, Cohn SL, Berthold F, Nakagawara A, Ladenstein RL, Iehara T, Matthay KK. Clinical and biologic features predictive of survival after relapse of neuroblastoma: a report from the International Neuroblastoma Risk Group project. *J Clin Oncol* 2011;29:3286-3292.
- Yanik GA, Parisi MT, Shulkin BL, Naranjo A, Kreissman SG, London WB, Villablanca JG, Maris JM, Park JR, Cohn SL, McGrady P, Matthay KK. Semiquantitative mIBG scoring as a prognostic indicator in patients with stage 4 neuroblastoma: a report from the Children's oncology group. *J Nucl Med* 2013;54:541-548.
- Ladenstein R, Lambert B, Pötschger U, Castellani MR, Lewington V, Bar-Sever Z, Oudoux A, Sliwińska A, Taborska K, Biassoni L, Yanik GA, Naranjo A, Parisi MT, Shulkin BL, Nadel H, Gelfand MJ, Matthay KK, Park JR, Kreissman SG, Valteau-Couanet D, Boubaker A. Validation of the mIBG skeletal SIOPEN scoring method in two independent high-risk neuroblastoma populations: the SIOPEN/HR-NBL1 and COG-A3973 trials. *Eur J Nucl Med Mol Imaging* 2018;45:292-305.
- Katzenstein HM, Cohn SL, Shore RM, Bardo DM, Haut PR, Olszewski M, Schmoldt J, Liu D, Rademaker AW, Kletzel M. Scintigraphic response by 123I-metaiodobenzylguanidine scan correlates with event-free survival in high-risk neuroblastoma. *J Clin Oncol* 2004;22:3909-3915.
- Messina JA, Cheng SC, Franc BL, Charron M, Shulkin B, To B, Maris JM, Yanik G, Hawkins RA, Matthay KK. Evaluation of semi-quantitative scoring system for metaiodobenzylguanidine (mIBG) scans in patients with relapsed neuroblastoma. *Pediatr Blood Cancer* 2006;47:865-874.



Diagnostic Value of ¹⁸F-FDG PET/CT in Patients with Carcinoma of Unknown Primary

Primeri Bilinmeyen Kanserlerde ¹⁸F-FDG PET/CT'nin Tanısal Değeri

Arzu Cengiz, Sibel Göksel, Yakup Yüreklı

Adnan Menderes University Faculty of Medicine, Department of Nuclear Medicine, Aydın, Turkey

Abstract

Objective: The aim of this study is to investigate the clinical role of ¹⁸F-fluorodeoxyglucose (¹⁸F-FDG) positron emission tomography/computed tomography (PET/CT) in patients with carcinoma of unknown primary (CUP).

Methods: One hundred twenty one patients with a diagnosis of CUP who underwent whole body ¹⁸F-FDG PET/CT imaging were included in this retrospective study. The final diagnoses were confirmed either histopathologically or by clinical follow-up.

Results: The ¹⁸F-FDG-PET/CT successfully detected the primary tumor in 59 out of 121 (49%) patients. The most common primary tumor as detected by ¹⁸F-FDG PET/CT was lung cancer (n=31). In a patient, two primary tumors (colon and prostate) were detected on PET/CT imaging. Bone marrow biopsy revealed prostate cancer in this patient and the colon cancer was accepted as a synchronous second primary tumor. ¹⁸F-FDG PET/CT findings were false-positive in 11 patients. ¹⁸F-FDG PET/CT could not detect any primary lesion in 51 patients, whose conventional work-up detected a primary tumor in 11 and thus considered as false-negative. The sensitivity, specificity rate and accuracy of ¹⁸F-FDG PET/CT in detection of primary tumor were identified as 84%, 78% and 82%, respectively.

Conclusion: Whole body ¹⁸F-FDG PET/CT is an effective method for detecting the primary tumor in patients with CUP. In addition to detecting the primary tumor, it can also help determine disease extent and contribute to patient management.

Keywords: Fluorodeoxyglucose, positron emission tomography/computed tomography, metastasis, unknown primary neoplasms

Öz

Amaç: Bu çalışmanın amacı, primeri bilinmeyen kanserlerde (PBK) ¹⁸F-florodeoksiglukoz (¹⁸F-FDG) pozitron emisyon tomografi/bilgisayarlı tomografinin (PET/CT) klinik rolünü araştırmaktır.

Yöntem: Bu retrospektif çalışmaya PBK tanısıyla tüm vücut ¹⁸F-FDG PET/CT yapılan 121 hasta dahil edildi. Sonuç tanı histopatolojik olarak veya klinik izleme doğrulandı.

Bulgular: ¹⁸F-FDG PET/CT, 121 hastanın 59'unda (49%) primer tümörü saptadı. PET/CT ile en çok saptanan tümör akciğer kanseri idi (n=31). Bir hastada iki primer tümör saptandı (kolon ve prostat). Bu hastada kemik iliği biyopsisi prostat kanseri metastazını gösterdiği için kolon kanseri senkron ikinci primer olarak kabul edildi. ¹⁸F-FDG PET/CT bulguları 11 hastada yanlış pozitif idi. PET/CT ile herhangi bir lezyon saptanmayan 51 hastanın 11 tanesinde konvansiyonel tetkiklerle primer tümör saptandı ve bu hastalar yanlış negatif olarak değerlendirildi. Primer tümör saptanmasında ¹⁸F-FDG PET/CT ile duyarlılık, özgüllük ve doğruluk sırasıyla %84, %78 ve %82 idi.

Address for Correspondence: Arzu Cengiz MD, Adnan Menderes University Faculty of Medicine, Department of Nuclear Medicine, Aydın, Turkey
E-mail: arzukincengiz@gmail.com ORCID ID: orcid.org/0000-0003-2110-4450

Received: 22.04.2018 **Accepted:** 04.09.2018

©Copyright 2018 by Turkish Society of Nuclear Medicine
Molecular Imaging and Radionuclide Therapy published by Galenos Yayınevi.

Sonuç: PBK olan hastalarda primer tümörün saptanmasında tüm vücut ^{18}F -FDG PET/BT etkin bir yöntemdir. Primer tümör saptanması yanında hastalığın yaygınlığını da belirleyerek hastaların izlemine katkıda bulunur.

Anahtar kelimeler: Florodeoksiglukoz, pozitron emisyon tomografi/bilgisayarlı tomografi, metastaz, primeri bilinmeyen neoplaziler

Introduction

Carcinoma of unknown primary (CUP) refers to the presence of metastatic disease for which the site of the primary lesion remains unidentified after conventional diagnostic procedures. CUP accounts for approximately 2.3-4.2% of cancer in both men and women (1,2). The mean survival is between 3-11 months, and only 25% of patients survive over one year (3,4). Several studies have shown that survival of patients in whom the primary tumor has been detected was higher than that of patients in whom the primary tumor has remained unknown (5,6). Various radiologic methods and serum tumor markers can be used for primary tumor detection. However, the primary tumor could be detected in less than 20% of patients with CUP (1). Although spontaneous regression or immune-mediated destruction of primary tumor or the small size of a primary tumor may be an explanation, it is not yet fully understood why primary tumors remain undetected (2,7,8).

Several studies reported that ^{18}F -fluorodeoxyglucose (FDG) positron emission tomography/computed tomography (PET/CT) has higher sensitivity than other imaging methods for detection of the primary tumor (9,10,11).

The aim of this retrospective study is to evaluate to primary tumor detection efficiency of ^{18}F -FDG PET/CT in patients with CUP.

Materials and Methods

Patient Population

All patients who have been referred to our department for ^{18}F -FDG PET/CT with a diagnosis of CUP from April 2013 to March 2016 were retrospectively evaluated. Patients who had inadequate medical records or irregular clinical follow-up data and who had chemotherapy before imaging were excluded. 121 patients (79 men, 42 women, age range 30-86 years, mean 63 ± 12 years) were analyzed finally in the study. Ninety five out of 121 patients were proved to have metastases histopathologically and 26 patients had highly suspicious metastases by conventional imaging [8 patients with multiple lung metastases detected by CT, 10 patients with multiple bone metastases detected by scintigraphy and/or magnetic resonance imaging (MRI), 5 patients with multiple liver metastases by MRI and/or US, and 3 patients with brain metastases detected by MRI]. Locations of the

metastatic foci that have been proven histologically were as follows; 36 in lymph nodes, (21 cervical, 6 supraclavicular, 4 axillary, 2 mediastinal, 2 inguinal, 1 retroperitoneal), 19 in liver, 13 in bone, 6 in brain, 3 in soft tissue, 1 in adrenal gland, 1 in lung, 9 patients had peritoneal implants or malignant ascites, 6 patients had malignant pleural effusion and 1 patient had malignant pericardial effusion.

The study were approved by the Adnan Menderes University of Local Ethics Committee (protocol number: 2017/1043).

^{18}F -FDG PET/CT Imaging

All patients underwent ^{18}F -FDG PET/CT imaging after 6-8 hours of fasting. Before injection of ^{18}F -FDG, the medical history, weight and blood sugar level of the patients were recorded. All patients' blood sugar levels were less than 180 mg/dL prior to imaging. Oral contrast was given to all patients. After intravenous administration of 270-370 MBq of ^{18}F -FDG, patients rested in a quiet room. Imaging was performed after a resting period of 60 minutes with (Siemens Biograph mCT 20 Excel) PET/CT scanner. Images were acquired from the head to the feet. The CT transmission scan was acquired with 140 kVp and 110 mA and 3 mm slice thickness. PET scan was acquired at 2-4 min per bed position. ^{18}F -FDG PET/CT images were evaluated both visually and semi-quantitatively by two nuclear medicine physicians. Abnormal ^{18}F -FDG uptake ($\text{SUV}_{\text{max}} \geq 2.5$) with an anatomical correlation in any tissue or organ other than the metastases sites was considered as the primary site. The final results were confirmed either histopathologically or by clinical follow up including other imaging methods.

Data Analysis and Statistical Evaluation

The final diagnosis was considered true-positive (TP) when ^{18}F -FDG PET/CT detected the primary tumor and it was confirmed histopathologically and/or by clinical follow up. If it was not confirmed to be malignant histopathologically then the result was considered as false-positive (FP). If ^{18}F -FDG PET/CT could not detect the primary tumor and it remained unknown in follow up, the result was considered true-negative (TN). When ^{18}F -FDG PET/CT did not suggest any primary tumor but it was diagnosed with conventional work-up or in the patient's follow-up, the result was considered as false-negative (FN).

Sensitivity, specificity rates and accuracy were calculated using standard statistical formulas:

Sensitivity=TP/(TP+FN), Specificity=TN/(TN+FP), Accuracy=(TP+TN)/(TP+FP+TN+FN).

Results

Primary tumors were correctly detected in 59 of 121 patients (49%) by ^{18}F -FDG PET/CT whole body imaging. The primary tumor locations were as follows; lung (n=31), breast (n=3), stomach (n=1), colon (n=4), pancreas (n=2), ovary (n=3), prostate (n=4), liver (n=2), endometrium (n=1), skin (n=2), thyroid (n=2), larynx (n=1), hypopharynx (n=1), salivary gland (n=1) and bone marrow (multiple myeloma; n=1). In a patient, two primary tumors (colon and prostate) were detected by PET/CT imaging both of which were confirmed histopathologically (Figure 1). In this patient, the bone marrow biopsy revealed metastatic prostate carcinoma thus the colon carcinoma was accepted as a synchronous second primary tumor. Fifty-nine TP results were selected for statistical evaluation. The SUV_{max} of the hyper-metabolic lesions were between 3 to 27 (mean 11.57 ± 6.1). TP results are reported in Table 1.

The sensitivity, specificity rates and accuracy of ^{18}F -FDG PET/CT in detection of primary tumor were identified as

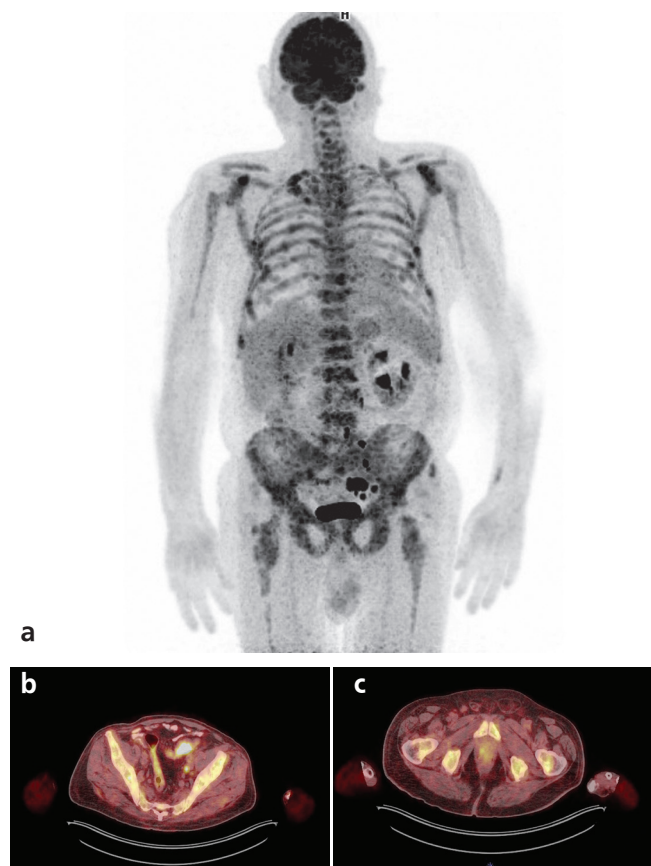


Figure 1. ^{18}F -FDG PET/CT images of a 72-year-old male patient with bone metastasis proven histopathologically. MIP (a), fusion (b and c) images showed hyper-metabolic focus in the prostate and wall-thickness on descending colon with pathologically increased ^{18}F -FDG uptake, which were later confirmed as prostate adenocarcinoma and colon adenocarcinoma by histopathology

84%, 78% and 82%, respectively. When 36 patients with lymph node metastases were evaluated separately, primary tumors were correctly identified in 14 out of 36 patients. In these cases, the sensitivity, specificity and accuracy were calculated as 66%, 75% and 70%, respectively.

There were eleven patients in whom primary tumors were reported incorrectly by ^{18}F -FDG PET/CT imaging. These results were accepted as false-positive (Table 2). A false-positive case is presented in Figure 2.

The primary tumor could not be identified in 51 (42%) patients. Forty of these patients were TN. The remaining 11 patients, ^{18}F -FDG PET/CT did not detect any lesion but the primary tumors were detected during clinical follow-up (mean 6.8 months, range: 2-30 months). These FN results are listed in Table 3.

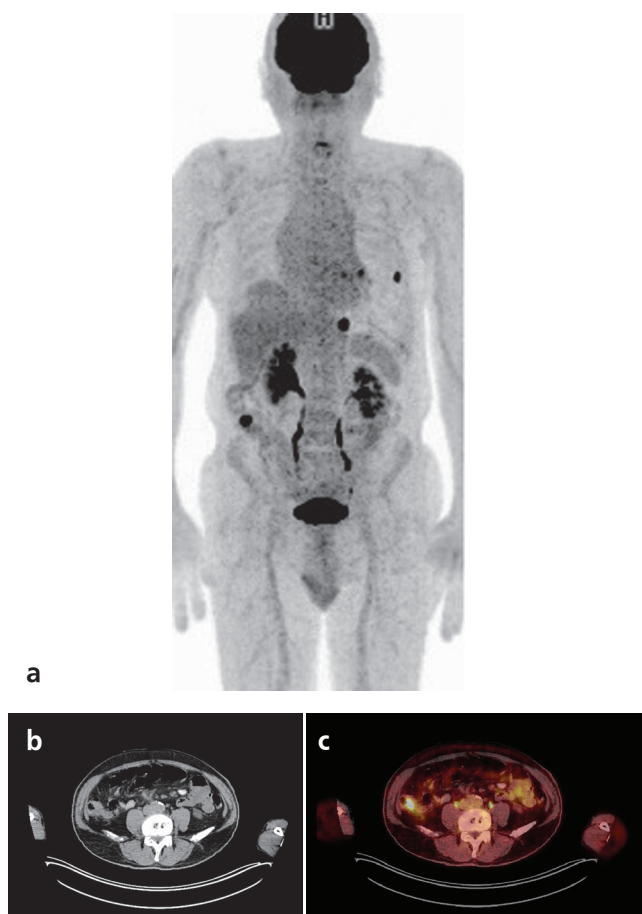


Figure 2. MIP (a), CT (b) and fusion (c) ^{18}F -FDG PET/CT images of a 64-year-old male patient. Cervical lymph node biopsy revealed adenocarcinoma metastasis. On PET/CT imaging, there were multiple hyper-metabolic mediastinal lymph nodes and mild hyper-metabolic infiltrations in both lungs suggesting infection. PET/CT imaging also demonstrates wall thickness on the ascending colon with abnormally increased ^{18}F -FDG uptake ($\text{SUV}_{\text{max}} : 5.0$), which was interpreted as a primary tumor. The histopathology examination revealed a hyperplastic polyp. The ^{18}F -FDG PET/CT result was false-positive

Table 1. There were fifty-nine patients with sixty true-positive results diagnosed by ¹⁸F-fluorodeoxyglucose positron emission tomography/computed tomography

	Age and gender	Location of metastases	Histopathologic/radiologic metastases	Primary tumor
1	68, M	Bone	Adenosquamous	Lung
2	70, M	Liver	Malignant epithelial tumor met.	Lung
3	49, M	Soft tissue	Malignant epithelial tumor met.	Lung
4	51, F	Bone	Carcinoma	Lung
5	65, F	Pleura	Signet-ring cell carcinoma	Lung
6	59, F	Liver	Malignant epithelial tumor met.	Lung
7	56, M	Bone	Adenocancer	Lung
8	46, F	Supraclavicular LN	Malignant epithelial tumor met.	Lung
9	60, F	Brain	Adenocancer	Lung
10	56, M	Liver	Adenocancer	Lung
11	68, M	Cervical LN	Neuroendocrine	Lung
12	59, F	Bone	Metastatic bone scintigraphy	Lung
13	46, M	Soft tissue	Adenocancer	Lung
14	59, M	Cervical LN	Squamous cell carcinoma	Lung
15	60, F	Bone	Metastatic bone scintigraphy	Lung
16	74, M	Cervical LN	Squamous cell carcinoma	Lung
17	75, F	Pleural effusion	Malignant	Lung
18	70, F	Bone	Malignant epithelial tumor met.	Lung
19	72, M	Liver	Malignant epithelial tumor met.	Lung
20	35, M	Liver	Adenocancer	Lung
21	53, M	Brain	Metastasis on brain MRI	Lung
22	39, M	Bone	Adenocancer	Lung
23	59, M	Adrenal	Neuroendocrine	Lung
24	75, M	Brain	Metastasis on brain MRI	Lung
25	52, M	Brain	Malignant epithelial tumor met.	Lung
26	74, M	Brain	Neuroendocrine	Lung
27	62, F	Liver	Malignant epithelial tumor met.	Lung
28	72, M	Liver	Small cell cancer	Lung
29	51, M	Liver	Malignant epithelial tumor met.	Lung
30	35, F	Pleural effusion	Malignant	Lung
31	58, M	Brain	Malignant epithelial tumor met.	Lung
32	58, M	Peritoneum	Adenocancer	Colon
33	30, M	Peritoneum	Mucinous adeno ca	Colon
34	54, M	Peritoneum	Adenocancer	Colon
35	63, M	Liver	Metastasis on CT	Colon
36	72, M	Bone	Malignant epithelial tumor met.	Colon and prostate
37	63, M	Bone	Metastasis on MRI	Prostate
38	64, M	Cervical LN	Adenocancer	Prostate
39	75, M	Bone	Metastasis on MRI	Prostate
40	67, F	Axillary LN	Malignant epithelial tumor met.	Breast
41	75, F	Bone	Malignant epithelial tumor met.	Breast
42	56, F	Bone	Metastatic bone scintigraphy	Breast
43	58, F	Cervical LN	Squamous cell carcinoma	Skin
44	86, M	Cervical LN	Squamous cell carcinoma	Skin

Table 1. Continue

45	69, M	Lung	Metastasis on thorax CT	Liver
46	79, F	Liver	Metastasis on MRI	Liver
47	75, F	Liver	Malignant epithelial tumor met.	Pancreas
48	77, F	Liver	Malignant epithelial tumor met.	Pancreas
49	66, F	Peritoneum	Malignant epithelial tumor met.	Ovary
50	64, F	Liver	Malignant epithelial tumor met.	Ovary
51	64, F	Peritoneum	Adenocancer	Ovary
52	72, M	Cervical LN	Papillary cancer	Thyroid
53	76, M	Supraclavicular LN	Malignant epithelial tumor met.	Thyroid
54	72, M	Cervical LN	Squamous cell carcinoma	Salivary gland
55	70, F	Peritoneum	Carcinomatosis	Stomach
56	46, F	Supraclavicular LN	Malignant epithelial tumor met.	Multiple myeloma
57	75, F	Lung	Metastasis on thorax CT	Endometrium
58	64, M	Cervical LN	Squamous cell carcinoma	Larynx
59	63, M	Cervical LN	Squamous cell carcinoma	Hypopharynx

LN: Lymph node, M: Male, F: Female, met: Metastasis, CT: Computed tomography, ¹⁸F-FDG: ¹⁸F-fluorodeoxyglucose, PET/CT: Positron emission tomography/computed tomography

Table 2. The eleven false-positive results diagnosed by ¹⁸F-fluorodeoxyglucose positron emission tomography/computed tomography

	Age and gender	Location of metastases	PET/CT diagnosis	Pathology of lesion	True primary site
1	46, M	Lung	Hypopharynx cancer	Cordoma	CUP
2	61, F	Inguinal LN	Endometrial cancer	Myoma uteri	CUP
3	44, M	Bone	Lung cancer	Pulmonary alveolar proteinosis	CUP
4	53, F	Cervical LN	Cervix cancer	Cervical polyp	Thyroid papillary cancer
5	48, M	Brain	Lung cancer	Lung hamartoma	CUP
6	80, M	Bone	Thyroid cancer	Benign nodule	CUP
7	85, M	Bone	Lung cancer	Lung inflammation	CUP
8	56, M	Liver	Sigmoid cancer	Diverticulitis	CUP
9	78, M	Malignant pleural effusion	Colon cancer	Polyp	Urinary bladder cancer
10	64, M	Cervical LN	Colon cancer	Polyp	Prostate cancer
11	50, F	Cervical LN	Thyroid cancer	Hashimoto thyroiditis	CUP

LN: Lymph node, M: Male, F: Female, CUP: Carcinoma of unknown primary, PET/CT: Positron emission tomography/computed tomography

Additional distant metastases were detected in 45 out of 59 (76%) patients whose primary tumors were detected correctly by ¹⁸F-FDG PET/CT. In patients with only lymph node metastases, additional solid organ metastases were detected in 5 patients out of 36 (14%) with PET/CT imaging.

Discussion

CT and MRI have been the imaging methods of choice in clinical practice in patients with CUP. Although they detect anatomical abnormalities with pathologic contrast enhancement, small or non-enhancing lesions can be overlooked (1). ¹⁸F-FDG PET/CT is gaining acceptance as an imaging method to be used in the management of

patients with CUP. Small lesions can be detected with higher sensitivity due to its high lesion-to-background contrast. Several studies reported that ¹⁸F-FDG PET/CT is more sensitive than CT and MRI in the imaging of CUP. In a study, Gutzeit et al. (12) have shown that CT alone indicated a primary tumor in only 8 of 45 patients (18%) while ¹⁸F-FDG PET/CT detected the primary site in 15 of 45 patients (33%). In another study, Roh et al. (13) have reported that the sensitivity rate of ¹⁸F-FDG PET/CT (87.5%) was significantly higher than that of CT (43.7%) for the primary tumor in patients with cervical metastases from unknown origin. In several studies, primary tumor detection rate ranged between 24.5-53% for ¹⁸F-FDG PET/CT in patients with CUP (11,14,15,16). Consistent with

Table 3. False-negative results of ¹⁸F-fluorodeoxyglucose positron emission tomography/computed tomography in patients with carcinoma of unknown primary

	Age and gender	Location of metastases	Final diagnosis	Pathology of primary tumor
1	71, M	Supraclavicular LN	Lung cancer	Neuroendocrine
2	64, F	Peritoneum	Ovarian cancer	Clinical Follow-up
3	78, M	Pleural fluid	Bladder cancer	Papillary urothelial low grade tumor
4	52, M	Cervical LN	Laryngeal cancer	ScC
5	65, M	Cervical LN	Laryngeal cancer	ScC
6	50, M	Brain	Lung cancer	Adenocarcinoma
7	60, F	Liver	Breast cancer	Invasive ductal
8	68, M	Axillary LN	Lung cancer	Neuroendocrine
9	65, M	Mediastinal LN	Lung cancer	Adenocarcinoma
10	60, F	Inguinal LN	Vulvar cancer	ScC
11	64, F	Cervical LN	Parotid tumor	Carcinoma ex pleomorphic adenoma

LN: Lymph node, M: Male, F: Female, ScC: Squamous cell carcinoma

the literature, in this study, primary tumors were correctly detected in 59 of 121 patients (49%) by ¹⁸F-FDG PET/CT whole body imaging. The sensitivity, specificity rates and accuracy of ¹⁸F-FDG PET/CT in detection of primary tumor were identified as 84%, 78% and 82%, respectively. Han et al. (17) reported the sensitivity, specificity and accuracy of ¹⁸F-FDG PET/CT in patients with CUP as 91.5%, 85.2% and 88.3%, respectively. In another study, the sensitivity, specificity and accuracy of ¹⁸F-FDG PET/CT in detection of primary tumor were reported as 80%, 74% and 78%, respectively (18). In our study, ¹⁸F-FDG PET/CT was the first imaging method used for detecting the primary in majority of the patients. Although the role of ¹⁸F-FDG PET/CT as the first line imaging of patients with CUP is yet to be established, it has significant advantages. Whole body imaging demonstrates disease extent in addition to detection of the primary tumor, eliminates the need for further imaging and other invasive procedures. Thus, it prevents delay in starting appropriate treatment (19,20).

Lung, oropharyngeal and pancreatic cancers were reported to be most common primary tumors in patients with CUP (21). In our study, lung (52%) and colon (8%) were the most common sites for primary tumors. Colorectal cancer is the third most common cancer in women and the fourth in men in our country (22). Although there were 21 patients with cervical lymph node metastases in our study, we detected 5 head and neck tumors as true-positive.

The most important limitation of ¹⁸F-FDG PET/CT is that it's not a specific tumor imaging technique. Inflammatory lesions or benign tumors with high tracer uptake are the most common causes of false-positive results. In our study, there were eleven false-positive results related to benign tumors or inflammation. In a meta-analysis, authors

reported that oropharynx and the lung are the two most common locations of false-positive ¹⁸F-FDG PET/CT results (21). Inflammatory lesions, pulmonary infarction and emboli have been reported as etiologies for false-positive results in the lung (2,12). In this study, 3 out of the 11 false-positive results were detected in the lung. Pulmonary alveolar proteinosis, hamartoma and inflammation were the final diagnosis in these patients. PET/CT diagnosed a false-positive colon cancer in three patients. The final diagnoses were polyps in two patients and diverticulitis in one patient, that were confirmed histopathologically. In a study, the authors concluded that if ¹⁸F-FDG PET/CT findings are positive, a confirmatory biopsy is necessary due to false-positive results (23).

In our study, ¹⁸F-FDG PET/CT could not detect the primary tumor in 42% of patients. Primary tumors were detected on follow-up in 11 out of 51 patients and were considered as FN. Small and low grade tumors with low ¹⁸F-FDG uptake may result in FN findings. Breast and oropharynx are the most common sites for FN ¹⁸F-FDG PET/CT imaging (21). In this study, a small primary breast cancer was detected by MRI and was histopathologically diagnosed as invasive ductal cancer following a FN ¹⁸F-FDG PET/CT imaging. In four patients, lung tumors with low ¹⁸F-FDG avidity caused FN results.

Whole body ¹⁸F-FDG PET/CT is also useful in detecting the extent of metastatic disease which may have important implications for clinical management. It is especially important in patients with initial lymph node metastases (2,24). We showed additional solid organ metastases in 5 out of 36 (14%) patients with CUP who presented with lymph node metastases on PET/CT imaging.

Conclusion

Whole body ¹⁸F-FDG PET/CT is an effective method for detecting the primary tumors in patients with CUP. Additionally, it can also determine disease extent and contribute significantly to clinical patient management.

Ethics

Ethics Committee Approval: The study were approved by the Adnan Menderes University of Local Ethics Committee (protocol number: 2017/1043).

Informed Consent: Consent form was filled out by all participants.

Peer-review: Externally peer-reviewed.

Authorship Contributions

Surgical and Medical Practices: A.C., S.G., Y.Y., Concept: A.C., Design: A.C., S.G., Y.Y., Data Collection or Processing: A.C., S.G., Y.Y., Analysis or Interpretation: A.C., Y.Y., Literature Search: A.C., Writing: A.C., Y.Y.

Conflict of Interest: No conflict of interest was declared by the authors.

Financial Disclosure: The authors declared that this study received no financial support.

References

- Pavlidis N, Fizazi K. Carcinoma of unknown primary (CUP). *Crit Rev Oncol Hematol* 2009;69:271-278.
- Kwee TC, Basu S, Cheng G, Alavi A. FDG PET/CT in carcinoma of unknown primary. *Eur J Nucl Med Mol Imaging* 2010;37:635-644.
- Pavlidis N, Briasoulis E, Hainsworth J, Greco FA. Diagnostic and therapeutic management of cancer of unknown primary. *Eur J Cancer* 2003;39:1990-2005.
- Chorost MI, Lee MC, Yeoh CB, Molina M, Ghosh BC. Unknown primary. *J Surg Oncol* 2004;15;87:191-203.
- Haas I, Hoffmann TK, Engers R, Ganzer U. Diagnostic strategies in cervical carcinoma of an unknown primary (CUP). *Eur Arch Otorhinolaryngol* 2002;259:325-333.
- Raber MN, Faintuch J, Abbruzzese JL, Sumrall C, Frost P. Continuous infusion 5-fluorouracil, etoposide and cisdiaminedichloroplatinum in patients with metastatic carcinoma of unknown primary origin. *Ann Oncol* 1991;2:519-520.
- Pentheroudakis G, Briasoulis E, Pavlidis N. Cancer of unknown primary site: missing primary or missing biology? *Oncologist* 2007;12:418-425.
- van de Wouw AJ, Jansen RL, Speel EJ, Hillen HF. The unknown biology of the unknown primary tumour: a literature review. *Ann Oncol* 2003;14:191-196.
- Sève P, Billotey C, Broussolle C, Dumontet C, Mackey JR. The role of 2-deoxy-2-[¹⁸F]fluoro-D-glucose positron emission tomography in disseminated carcinoma of unknown primary site. *Cancer* 2007;109:292-299.
- Rusthoven KE, Koshy M, Paulino AC. The role of fluorodeoxyglucose positron emission tomography in cervical lymph node metastases from an unknown primary tumor. *Cancer* 2004;101:2641-2649.
- Delgado-Bolton RC, Fernández-Pérez C, González-Maté A, Carreras JL. Meta analysis of the performance of 18F-FDG PET in primary tumor detection in unknown primary tumors. *J Nucl Med* 2003;44:1301-1314.
- Gutzeit A, Antoch G, Kühl H, Egelhof T, Fischer M, Hauth E, Goehde S, Bockisch A, Debatin J, Freudenberg L. Unknown primary tumors: detection with dual-modality PET/CT-initial experience. *Radiology* 2005;234:227-234.
- Roh JL, Kim JS, Lee JH, Cho KJ, Choi SH, Nam SY, Kim SY. Utility of combined (18)F-fluorodeoxyglucose-positron emission tomography and computed tomography in patients with cervical metastases from unknown primary tumors. *Oral Oncol* 2009;45:218-224.
- Lonneux M, Reffad A. Metastases from Unknown Primary Tumor. PET-FDG as Initial Diagnostic Procedure? *Clin Positron Imaging*. 2000;3:137-141.
- Rusthoven KE, Koshy M, Paulino AC. The role of fluorodeoxyglucose positron emission tomography in cervical lymph node metastases from an unknown primary tumor. *Cancer* 2004;101:2641-2649.
- Bohuslavizki KH, Klutmann S, Kröger S, Sonnemann U, Buchert R, Werner JA, Mester J, Clausen M. FDG PET detection of unknown primary tumors. *J Nucl Med* 2000;41:816-822.
- Han A, Xue J, Hu M, Zheng J, Wang X. Clinical value of 18F-FDG PET-CT in detecting primary tumor for patients with carcinoma of unknown primary. *Cancer Epidemiol* 2012;36:470-475.
- Riaz S, Nawaz MK, Faruqi ZS, Saeed Kazmi SA, Loya A, Bashir H. Diagnostic Accuracy of 18F-Fluorodeoxyglucose Positron Emission Tomography-Computed Tomography in the Evaluation of Carcinoma of Unknown Primary. *Mol Imaging Radionucl Ther* 2016;25:11-18.
- Pelosi E, Pennone M, Deandreis D, Douroukas A, Mancini M, Bisi G. Role of whole body positron emission tomography/computed tomography scan with 18F-fluorodeoxyglucose in patients with biopsy proven tumor metastases from unknown primary site. *Q J Nucl Med Mol Imaging* 2006;50:15-22.
- Wang G, Wu Y, Zhang W, Li J, Wu P, Xie C. Clinical value of whole-body F-18 fluorodeoxyglucose positron emission tomography/computed tomography in patients with carcinoma of unknown primary. *J Med Imaging Radiat Oncol* 2013;57:65-71.
- Kwee TC, Kwee RM. Combined FDG-PET/CT for the detection of unknown primary tumors: systematic review and meta-analysis. *Eur Radiol* 2009;19:731-744.
- Aykan N, Yalçın S, Turhal NS, Özdoğan M, Demir G, Özkan M, Yaren A, Camcı C, Akbulut H, Artaç M, Meydan N, Uygun K, Işıkdoğan A, Ünsal D, Özyılkan Ö, Arıcan A, Seyrek E, Tekin SB, Manavoğlu O, Özet A, Elkıran T, Dişçi R. Epidemiology of colorectal cancer in Turkey: A cross-sectional disease registry study (A Turkish Oncology Group trial). *Turk J Gastroenterol* 2015;26:145-153.
- Fletcher JW, Djulbegovic B, Soares HP, Siegel BA, Lowe VJ, Lyman GH, Coleman RE, Wahl R, Paschold JC, Avril N, Einhorn LH, Suh WW, Samson D, Delbeke D, Gorman M, Shields AF. Recommendations on the use of 18F-FDG PET in oncology. *J Nucl Med* 2008;49:480-508.
- Basu S, Alavi A. FDG-PET in the clinical management of carcinoma of unknown primary with metastatic cervical lymphadenopathy: shifting gears from detecting the primary to planning therapeutic strategies. *Eur J Nucl Med Mol Imaging* 2007;34:427-428.



Incidental ¹⁸F-FDG Uptake of the Pubic Ramus and Abdominal Muscles due to Athletic Pubalgia During Acute Prostatitis

Akut Prostatit Sırasında Ramus Pubis ve Abdominal Kaslarda Atletik Pubaljiye Bağlı İnsidental ¹⁸F-FDG Tutulumu

Oliver Rager¹, Marlise Picarra², Emmanouil Astrinakis², Valentina Garibotto¹, Gaël Amzalag¹

¹University Hospital of Geneva, Clinic of Nuclear Medicine, Geneva, Switzerland

²University Hospital of Geneva, Clinic of Radiology, Geneva, Switzerland

Abstract

A 23-year-old African native male patient presented with fever, lumbalgia and dysuria after returning from a trip to Togo. His physical examination revealed pain over the pubic symphysis and rectal tenderness on digital exam. The C-reactive protein (CRP) level was elevated along with positive blood and urinary cultures for methicillin-resistant *Staphylococcus aureus*. An magnetic resonance imaging that has been performed to rule out arthritis/osteomyelitis in the pubis revealed edema of the symphysis. An ¹⁸F-FDG positron emission tomography/computed tomography supported the diagnosis of prostate infection and showed a focal uptake of the pubic symphysis, with diffuse hyper-metabolism of the insertions of the rectus abdominis and longus adductor muscles, corresponding to athletic pubalgia. Fever and CRP responded rapidly to antibiotherapy.

Keywords: PET/CT, magnetic resonance imaging, athletic pubalgia, sports hernia, prostatitis

Öz

Yirmi üç yaşında Afrikalı erkek hasta Togo seyahati sonrası ateş, lumbalji ve disüri şikayetleri ile başvurdu. Fizik muayenede symphysis pubis üzeri ağrı ve rektal tuşede hassasiyet mevcuttu. C-reaktif protein (CRP) düzeyi yüksekti ve kan ve idrar kültürlerinde metisiline dirençli *Staphylococcus aureus* üremesi saptandı. Pubiste olası bir artrit/osteomyeliti ekarte etmek için istenen manyetik rezonans görüntüleme symphysisde ödem görüldü. ¹⁸F-FDG pozitron emisyon tomografisi/bilgisayarlı tomografi prostat enfeksiyonu tanısını doğruladı. Bununla birlikte atletik pubaljiye uyumlu olarak symphysis pubiste fokal tutulum ve rektus abdominis ve adductor longus kas insersiyolarında diffüz hipermetabolizm görüldü. Antibiyoterapi sonrası ateş ve CRP düzeyi hızla düzeldi.

Anahtar kelimeler: PET/CT, manyetik rezonans görüntüleme, atletik pubalji, sporcu hernisi, prostatit

Address for Correspondence: Olivier Rager MD, University Hospital of Geneva, Clinic of Nuclear Medicine, Geneva, Switzerland

Phone: +41 223727144 E-mail: olivier.rager@hcuge.ch ORCID ID: orcid.org/0000-0002-7030-2878

Received: 27.11.2017 **Accepted:** 10.03.2018

©Copyright 2018 by Turkish Society of Nuclear Medicine
Molecular Imaging and Radionuclide Therapy published by Galenos Yayınevi.

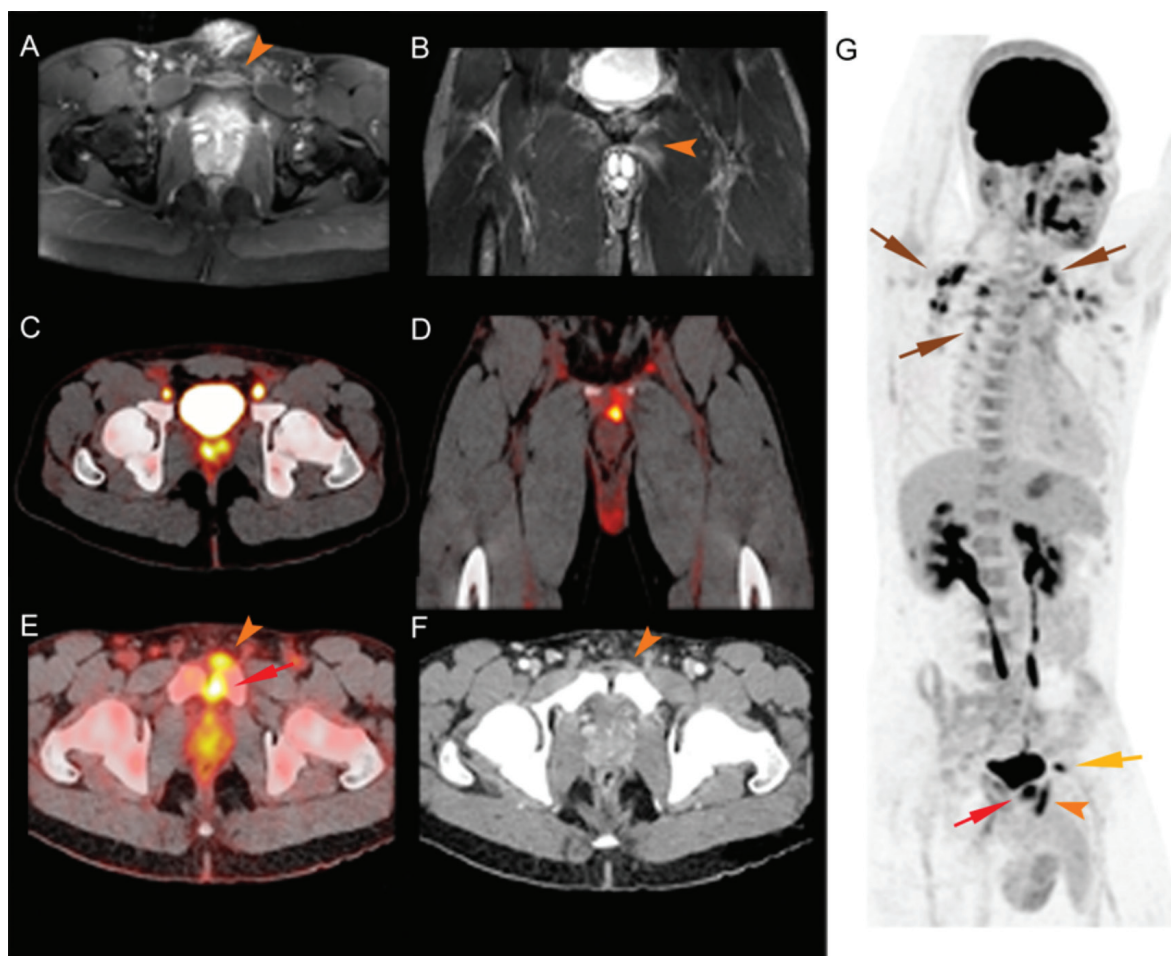


Figure 1. We present the case of a 23-year-old male African native patient presenting with fever, lumbalgia and dysuria after returning from a trip to Togo. The patient is a professional athlete (soccer player) with a known history of malaria during childhood. On palpation, there was pain over the pubic tubercle and the digital rectal exam was tender and sensitive. The blood formula was normal except elevated [C-reactive protein (CRP): 118 mg/L]. Recurrence of malaria had been excluded by repeated thick blood smears. Both blood and urinary cultures were positive for methicillin-resistant *Staphylococcus aureus*. Computed tomography (CT) with nephrographic contrast and dedicated ultrasound ruled out pyelonephritis. A pelvic magnetic resonance imaging (MRI) was performed to rule out arthritis and osteomyelitis that revealed a thickening of the aponeurosis of the left rectus abdominis muscle on T1-weighted axial sequence after injection of gadolinium (A, arrow head), a hyper-signal of the symphysis on the STIR-weighted sequence corresponding to marrow edema without articular effusion, and a hyper-signal corresponding to a strain of the left adductor longus muscle (B, arrow head) characteristic of athletic pubalgia (1,2). ^{18}F -FDG positron emission tomography/CT (PET/CT) found an increased prostatic tracer uptake along with bilateral external iliac lymph nodes hyper-metabolism (C), and also showed hyper-metabolism of the insertion of the left longus adductor (D) and of the left rectus abdominis (E and G, orange arrow) with a focal uptake in the pubic symphysis (E and G, red arrow) that were in concordance with the MRI findings. Increased ^{18}F -FDG uptake on the molecular inversion probe sequence (G) in the supraclavicular, latero-cervical and para-vertebral regions corresponded to activated brown adipose tissue (brown arrow), the yellow arrow corresponds to the left iliac node; the right iliac node and the prostate were masked by the bladder. The CT scan (F) with contrast media confirmed the findings (thickening of the aponeurosis of the left rectus abdominis, arrow head). A prostatic origin of the infection was presumed and antibiotic therapy was initiated (intravenous vancomycin, then co-trimoxazole per os). Regression of fever, normalization of CRP and clearing of the cultures were observed rapidly. Sports hernia/athletic pubalgia is an activity-related lower abdominal and proximal adductor-related pain seen in athletes (3,4,5,6). Symptoms are most often unilateral but are not uncommonly bilateral. This pattern with hyper-metabolism of the muscles associated with uptake in the pubic symphysis due to inflammation should be recognized on imaging not to be mistaken for a muscle abscess (7,8). To the best of our knowledge, this specific feature in ^{18}F -FDG PET/CT had not been previously described in the literature.

Ethics

Informed Consent: Consent form was filled out by all participants.

Peer-review: Externally and internally peer-reviewed.

Authorship Contributions

Surgical and Medical Practices: O.R., M.P., G.A., Concept: O.R., G.A., Design: O.R., G.A., Data Collection or Processing: M.P., E.A., V.G., Analysis or Interpretation: O.R., V.G., G.A.,

Literature Search: O.R., M.P., E.A., V.G., G.A., Writing: O.R., M.P., G.A.

Conflict of Interest: No conflict of interest was declared by the authors.

Financial Disclosure: The authors declared that this study received no financial support.

References

1. McArthur TA, Narducci CA, Lopez-Ben RR. The role of pubic symphyseal CT arthrography in the imaging of athletic pubalgia. *AJR Am J Roentgenol* 2014;203:1063-1068.
2. Brennan D, O'Connell MJ, Ryan M, Cunningham P, Taylor D, Cronin C, O'Neill P, Eustace S. Secondary cleft sign as a marker of injury in athletes with groin pain: MR image appearance and interpretation. *Radiology* 2005;235:162-167.
3. Larson CM. Sports hernia/athletic pubalgia: evaluation and management. *Sports Health* 2014;6:139-144.
4. Minnich JM, Hanks JB, Muschaweck U, Brunt LM, Diduch DR. Sports hernia: diagnosis and treatment highlighting a minimal repair surgical technique. *Am J Sports Med* 2011;39:1341-1349.
5. Munegato D, Bigoni M, Gridavilla G, Olmi S, Cesana G, Zatti G. Sports hernia and femoroacetabular impingement in athletes: A systematic review. *World J Clin Cases* 2015;3:823-830.
6. Ellsworth AA, Zoland MP, Tyler TF. Athletic pubalgia and associated rehabilitation. *Int J Sports Phys Ther* 2014;9:774-784.
7. Reyhan M. Post-traumatic psoas abscess diagnosed by 18F FDG PET/CT. *Rev Esp Med Nucl Imagen Mol* 2014;33:314-315.
8. Alqahtani SM, Jiang F, Barimani B, Gdalevitch M. Symphysis pubis osteomyelitis with bilateral adductor muscles abscess. *Case Rep Orthop* 2014;2014:982171.



Synchronous Hepatocellular Carcinoma and Cholangiocellular Carcinoma on ¹⁸F-FDG PET/CT

¹⁸F-FDG PET/BT'de Senkron Hepatosellüler Karsinoma ve Kolanjiosellüler Karsinoma

✉ Ezgi Başak Erdoğan¹, ✉ Hacı Mehmet Türk², ✉ Ertuğrul Tekçe³, ✉ Mehmet Aydın¹

¹Bezmialem Vakıf University Faculty of Medicine, Department of Nuclear Medicine, İstanbul, Turkey

²Bezmialem Vakıf University Faculty of Medicine, Department of Medical Oncology, İstanbul, Turkey

³Bezmialem Vakıf University Faculty of Medicine, Department of Radiation Oncology, İstanbul, Turkey

Abstract

A 43-year-old male patient presented with a mass lesion on the right liver lobe, segment 5, in radiological imaging and elevated alpha-fetoprotein levels (323 ng/mL) compatible with hepatocellular carcinoma (HCC). Positron emission tomography/computed tomography (PET/CT) images showed background level ¹⁸F-FDG uptake in the mass lesion. In addition, a secondary focus of increased ¹⁸F-FDG uptake was detected on the left liver lobe, segment 2, approximately 1,5 cm in diameter. Histopathological examination revealed HCC in the larger mass lesion with a lower ¹⁸F-FDG uptake, and cholangiocellular carcinoma in the smaller mass lesion with a higher ¹⁸F-FDG uptake. To our knowledge, this is the first case report of two histopathologically different primary malignant liver tumors in two distinct segments of the liver detected by PET/CT.

Keywords: Synchronous tumors, hepatocellular carcinoma, cholangiocellular carcinoma, ¹⁸F-FDG PET/CT

Öz

Radyolojik görüntüleme karaciğer sağ lob segment 5'de hepatosellüler karsinom (HCC) ile uyumlu kitle lezyonu saptanan ve alfa-fetoprotein yüksekliği (323 ng/mL) olan 43 yaşında erkek bir hasta kliniğimize başvurdu. ¹⁸F-FDG pozitron emisyon tomografi/bilgisayarlı tomografi (PET/BT) görüntüleri, kitle lezyonda fizyolojik seviyede ¹⁸F-FDG tutulumu gösterdi. Ek olarak, sol lob segment 2'de artmış ¹⁸F-FDG tutulumu olan, yaklaşık 1,5 cm çapında ikinci bir odak tespit edildi. Histopatolojik incelemede, daha düşük ¹⁸F-FDG tutan büyük kitle lezyonda HCC, daha yüksek ¹⁸F-FDG tutan küçük kitle lezyonda ise kolanjiosellüler karsinom saptandı. Bildiğimiz kadarıyla bu, PET/BT ile tanısı konulmuş karaciğerin farklı iki segmentinde histopatolojik olarak farklı iki primer malign karaciğer tümörünün bildirildiği ilk olgu sunumudur.

Anahtar kelimeler: Senkron tümörler, hepatosellüler karsinoma, kolanjiosellüler karsinoma, ¹⁸F-FDG PET/BT

Address for Correspondence: Ezgi Başak Erdoğan MD, Bezmialem Vakıf University Faculty of Medicine, Department of Nuclear Medicine, İstanbul, Turkey
Phone: +90 532 783 32 36 E-mail: erdogan_ezgi@yahoo.com.tr ORCID ID: orcid.org/0000-0002-6636-9324

Received: 06.11.2017 **Accepted:** 12.06.2018

©Copyright 2018 by Turkish Society of Nuclear Medicine
Molecular Imaging and Radionuclide Therapy published by Galenos Yayınevi.

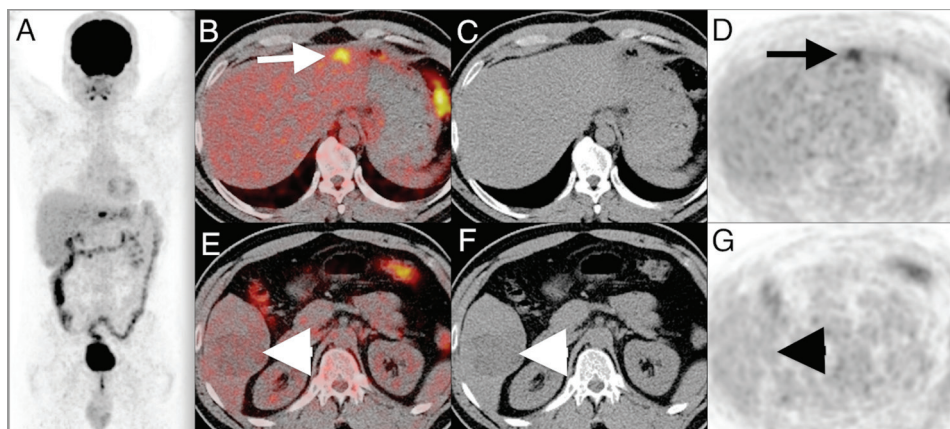


Figure 1. Positron emission tomography/computed tomography (PET/CT) images were acquired after a long period of fasting and 370 MBq (10 mCi) ¹⁸F-FDG administration. Maximum intensity projection (A) and axial slices of fusion (B, arrow), CT (C) and PET (D) images showed focal hyper-metabolic lesion in the left lobe, segment 2. A mass lesion, approximately 7 cm in diameter, with heterogeneous density at the right liver lobe segment 5 was detected, that displayed normal ¹⁸F-FDG uptake levels as the liver parenchyma (E arrowhead, F arrowhead, G). PET/CT did not reveal any other focus that was suspicious for malignancy. Hepatocellular carcinoma (HCC) and cholangiocellular carcinoma (CCC) are both primary malignant liver tumors originating from the hepatocytes and bile duct cells, respectively. The incidence of HCC and CCC together is extremely rare (lower than 1% of all primary malignant liver tumors) (1). Synchronous HCC and CCC cases, some of them on the same segment, detected with CT or magnetic resonance imaging (MRI) studies have previously been reported (2,3). Besides, both HCC and CCC components present in the same tumor and hepatic stem cells differentiating to hepatocytes or cholangio cells have also been reported (3). To our knowledge, this is the first case to report synchronous primary malignant liver tumors in two distinct segments detected by ¹⁸F-FDG PET/CT.

Cancer cell growth depends mainly on glucose metabolism. ¹⁸F-FDG uptake in malignant tumors is related to glucose transporter proteins (especially Glut1) and hexokinase type 2. Glut1 expression is low in HCC and high in CCC, while hexokinase 2 expression is elevated in HCC (4). ¹⁸F-FDG uptake is variable in HCC related to the degree of differentiation. Because glucose-6-phosphatase activity is high in well differentiated hepatocyte cells, intracellular ¹⁸F-FDG-6-phosphate is dephosphorylated to ¹⁸F-FDG, thus decreasing intracellular accumulation (5). Increased ¹⁸F-FDG uptake were reported in nearly half of the HCC cases. The higher ¹⁸F-FDG uptake of intrahepatic CCC and lower ¹⁸F-FDG uptake of hilar tumors is well known. CCC located in the hilum mostly originate from larger bile ducts, so obstructive symptoms are observed in the early periods. The low ¹⁸F-FDG uptake can thus be attributed to the small tumor size at diagnosis. Other reasons for the low ¹⁸F-FDG uptake by this tumor have been reported as mucin accumulation inside tumor cells or neoplastic glandular tissue lumen, and scattered settlement of malignant cells in fibrous stroma (6,7).

In our case, ¹⁸F-FDG uptake patterns of both tumors were quite different, so we considered two separate HCC lesions with two distinct degree of differentiation. Histopathologically, the mass lesion with low ¹⁸F-FDG uptake at the right liver lobe segment 5 was reported as clear cell HCC with micro-macro trabecular pattern, nuclear grade 2-3, while the tumor with higher ¹⁸F-FDG uptake at the left liver lobe segment 2 was identified as adenocarcinoma (CCC). The CCC was intrahepatic and therefore the ¹⁸F-FDG uptake was significantly higher.

Ethics

Informed Consent: Consent form was filled out by participant.

Peer-review: Externally peer-reviewed.

Authorship Contributions

Surgical and Medical Practices: H.M.T., Concept: E.B.E., H.M.T., E.T., M.A., Design: E.B.E., M.A., Data Collection or Processing: E.B.E., H.M.T., Analysis or Interpretation: E.B.E., M.A., Literature Search: E.B.E., Writing: E.B.E., E.T., M.A.

Conflict of Interest: No conflict of interest was declared by the authors.

Financial Disclosure: The authors declared that this study received no financial support.

References

- Hu J, Yuan R, Huang C, Shao J, Zou S, Wang K. Double primary hepatic cancer (hepatocellular carcinoma and intrahepatic cholangiocellular carcinoma) originating from hepatic progenitor cell: a case report and review of the literature. *World J Surg Oncol* 2016;14:218.
- Watanabe T, Sakata J, Ishikawa T, Shirai Y, Suda T, Hirono H, Hasegawa K, Soga K, Shibasaki K, Saito Y, Umezu H. Synchronous development of HCC and CCC in the same subsegment of the liver in a patient with type C liver cirrhosis. *World J Hepatol* 2009;31:103-109.
- Kanamoto M, Yoshizumi T, Ikegami T, Imura S, Morine Y, Ikemoto T, Sano N, Shimada M. Cholangiocellular carcinoma containing hepatocellular carcinoma and cholangiocellular carcinoma, extremely rare tumor of the liver: a case report. *J Med Invest* 2008;55:161-165.
- Lee JD, Yang WI, Park YN, Kim KS, Choi JS, Yun M, Ko D, Kim TS, Cho AE, Kim HM, Han KH, Im SS, Ahn YH, Choi CW, Park JH. Different glucose uptake and glycolytic mechanisms between hepatocellular carcinoma and intrahepatic mass-forming cholangiocellular carcinoma with increased (18)F-FDG uptake. *J Nucl Med* 2005;46:1753-1759.
- Weber G, Morris HP. Comparative biochemistry of hepatomas. III. carbohydrate enzymes in liver tumors of different growth rates. *Cancer Res* 1963;23:987-994.
- Fritscher-Ravens A, Bohuslavizki KH, Broering DC, Jenicke L, Schäfer H, Buchert R, Rogiers X, Clausen M. FDG PET in the diagnosis of hilar cholangiocellular carcinoma. *Nucl Med Commun* 2001;22:1277-1285.
- Jiang L, Tan H, Panje CM, Yu H, Xiu Y, Shi H. Role of 18F-FDG PET/CT imaging in intrahepatic cholangiocellular carcinoma. *Clin Nucl Med* 2016;41:1-7.



¹⁸F-FDG PET/CT Findings of Non-Hodgkin Lymphoma Involving the Whole Genitourinary System

Ürogenital Sistemin Tamamını Tutan Non-Hodgkin Lenfomada ¹⁸F-FDG PET/BT Bulguları

✉ Aylın Oral, ✉ Bülent Yazıcı, ✉ Özgür Ömür

Ege University Faculty of Medicine, Department of Nuclear Medicine, İzmir, Turkey

Abstract

A sixty-two-year-old male patient underwent orchiectomy and was diagnosed with diffuse large B-cell lymphoma in the testicle and spermatic cord. ¹⁸F-FDG positron emission tomography/computed tomography (PET/CT) scanning was performed for initial staging. ¹⁸F-FDG PET/CT scan revealed multiple hyper-metabolic lymphadenopathies, lung lesions and mass lesions in the adrenal glands and kidneys. In addition, diffuse increased ¹⁸F-FDG uptake suggesting lymphomatous infiltration on the right testicle, prostate and left testicular veins were detected. The genitourinary system involvement is extremely rare in extranodal lymphomas and to the best of our knowledge this is the first case in the literature having ¹⁸F-FDG accumulating lesions in all genitourinary system structures.

Keywords: Non-Hodgkin, extranodal, lymphoma, ¹⁸F-FDG, PET/CT, genitourinary system

Öz

Altmış iki yaşındaki erkek hasta, uygulanan orşiektomi sonucunda testis ve spermatik kordda diffüz büyük B-hücreli lenfoma tanısı aldı. Hastaya başlangıç evrelemesi amacıyla ¹⁸F-FDG pozitron emisyon tomografisi/bilgisayarlı tomografi (PET/BT) tetkiki yapıldı. Yapılan ¹⁸F-FDG PET/BT tetkikinde, hipermetabolik özellikte çok sayıda lenfadenopatiler, akciğer lezyonları, böbreklerde ve sürrenal bezlerde kitle lezyonları saptandı. Ek olarak, sağ testiste, prostat bezinde ve sol testiküler vende lenfoma tutulumu ile uyumlu diffüz özellikte artmış ¹⁸F-FDG tutuluşu izlendi. Lenfomada ürogenital sistem nadir ektranodal tutulum yerlerinden biri olup bu olgu bildiğimiz kadarıyla tüm ürogenital sistem yapılarında artmış ¹⁸F-FDG tutulumu gösteren lezyonlar izlenen literatürdeki ilk olgudur.

Anahtar kelimeler: Non-Hodgkin, ektranodal, lenfoma, ¹⁸F-FDG, PET/BT, ürogenital sistem

Address for Correspondence: Aylın Oral MD, Ege University Faculty of Medicine, Department of Nuclear Medicine, İzmir, Turkey
Phone: +90 505 265 62 77 E-mail: draylinoral@yahoo.com ORCID ID: orcid.org/0000-0001-8014-4327

Received: 06.04.2018 **Accepted:** 12.06.2018

©Copyright 2018 by Turkish Society of Nuclear Medicine
Molecular Imaging and Radionuclide Therapy published by Galenos Yayınevi.

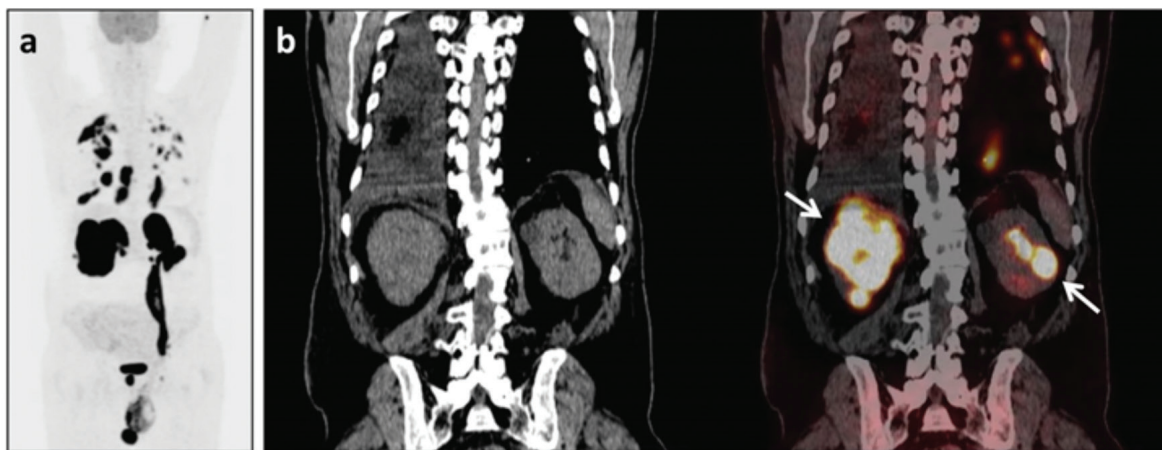


Figure 1. A sixty-two-year-old male patient suffering from swelling of the left testicle underwent orchiectomy and was diagnosed with diffuse large B-cell lymphoma in the testicle and spermatic cord. A) Maximum intensity projection image of the staging-intended ^{18}F -FDG positron-emission tomography/computed tomography (PET/CT) scan of the case revealed multiple hyper-metabolic lymphadenopathies in the cervical, thoracic and abdominopelvic regions (SUV_{max} : 34.8), hyper-metabolic lesions consistent with lymphatic/parenchymal infiltration in the lungs (SUV_{max} : 16.4-45.2), pleural involvements accompanied by rib invasion on the right thorax (SUV_{max} : 29.2), along with lymphoma infiltration of bilateral adrenal glands (SUV_{max} : 38.7-56.5), the kidneys (SUV_{max} : 40-53), the prostate gland (SUV_{max} : 40.4), the right testicle (SUV_{max} : 20.8) and the left testicular vein. B) Mass lesions in the kidneys are seen in selected coronal CT and fused PET/CT images.

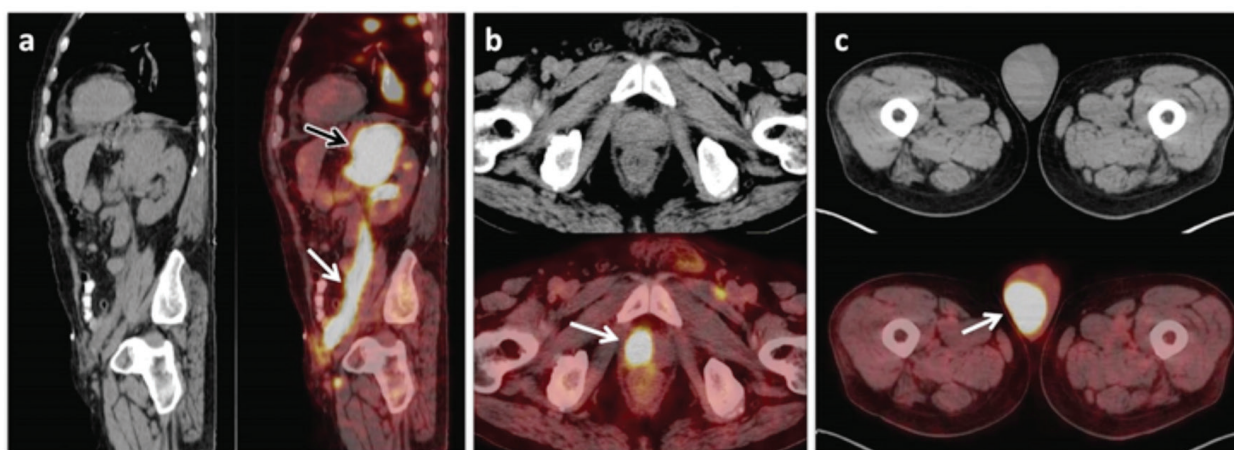


Figure 2. At sagittal CT and fused PET/CT images (A); mass lesion at the left adrenal gland (A; black arrow) and intense ^{18}F -FDG uptake (SUV_{max} : 36.8) along the left testicular vein (A; white arrow) are observed. At transaxial CT and fused PET/CT images (B, C); diffuse increased ^{18}F -FDG uptake without size or density changes at CT image suggesting diffuse lymphomatous infiltration on prostate (SUV_{max} : 40.4) (B) and right testicle (SUV_{max} : 20.8) (C) are also seen.

Although lymphomas generally originate from lymph nodes or lymphoid tissue, extranodal sites can also be involved. Extranodal lymphomas can arise in almost every organ. The most common extranodal involvement sites are gastrointestinal system, central nervous system, skin, Waldeyer's ring, spleen and more rarely kidneys, testicle, female genital organs and liver (1,2). The genitourinary system is an extremely rare extranodal infiltration area in lymphomas, the frequency is %1-2 for testicle and less than %1 for kidney, and the dominant histological subtype is diffuse B-cell lymphoma (1,3). To the best of our knowledge this is the first case in the literature having ^{18}F -FDG accumulating lesions on all of the structures of the genitourinary system. CT, the most common imaging modality at diagnosis and follow-up, is based on determining the size and the shape of lymphomatous lesions and their interface with adjacent structures. Identification of disease in normal-sized organs is difficult by anatomical imaging modalities. At this point the usefulness of the functional information provided by ^{18}F -FDG PET/CT comes forward (2,4,5). For the last decades, ^{18}F -FDG PET/CT has been widely used for disease staging, recurrence detection, and monitoring treatment response in patients with Hodgkin's disease and non-Hodgkin lymphoma (4,5,6,7). ^{18}F -FDG PET/CT with unenhanced CT is more sensitive and specific than contrast-enhanced CT for the detection of extralymphatic lymphomatous involvement (7). Also, ^{18}F -FDG PET/CT is superior to CT for determining diffuse lymphomatous infiltration in organs (8). In this case presentation, despite urinary excretion of ^{18}F -FDG, it is verified that ^{18}F -FDG PET/CT is superior to CT in determining genitourinary system involvement of lymphoma, especially in diffuse lymphomatous infiltration.

Ethics

Informed Consent: The subject in the study provided written informed consent.

Peer-review: Externally peer-reviewed.

Authorship Contributions

Surgical and Medical Practices: A.O., Ö.Ö., Concept: A.O., B.Y., Design: A.O., B.Y., Data Collection or Processing: A.O., Analysis or Interpretation: A.O., Ö.Ö., Literature Search: A.O., Writing: A.O.

Conflict of Interest: No conflict of interest was declared by the authors.

Financial Disclosure: The authors declared that this study received no financial support.

References

1. Zucca E, Roggero E, Bertoni F, Cavalli F. Primary extranodal non-Hodgkin's lymphomas. Part I: Gastrointestinal, cutaneous and genitourinary lymphomas. *Ann Oncol* 1997;8:727-737.
2. Chua SC, Rozalli FI, O'Connor SR. Imaging features of primary extranodal lymphomas. *Clin Radiol* 2009;64:574-588.
3. Çalışkan B, Peterson J, Henderson R. PET/CT Imaging of a Rare Presentation of Mantle Cell Lymphoma with Testicular Involvement. *Mol Imaging Radionucl Ther* 2015;24(Suppl 1):7-9.
4. Ömür Ö, Baran Y, Oral A, Ceylan Y. Fluorine-18 fluorodeoxyglucose PET-CT for extranodal staging of non-Hodgkin and Hodgkin lymphoma. *Diagn Interv Radiol* 2014;20:185-192.
5. Ilica AT, Kocacelebi K, Savas R, Ayan A. Imaging of extranodal lymphoma with PET/CT. *Clin Nucl Med* 2011;36:127-138.
6. Paes FM, Kalkanis DG, Sideras PA, Serafini AN. FDG PET/CT of extranodal involvement in non-Hodgkin lymphoma and Hodgkin disease. *Radiographics* 2010;30:269-291.
7. Schaefer NG, Hany TF, Taverna C, Seifert B, Stumpe KD, von Schulthess GK, Goerres GW. Non-Hodgkin lymphoma and Hodgkin disease: coregistered FDG PET and CT at staging and restaging-do we need contrast-enhanced CT? *Radiology* 2004;232:823-829.
8. Even-Sapir E, Lievshitz G, Perry C, Herishanu Y, Lerman H, Metser U. Fluorine-18 fluorodeoxyglucose PET/CT patterns of extranodal involvement in patients with Non-Hodgkin lymphoma and Hodgkin's disease. *Radiol Clin North Am* 2007;45:697-709.



Masking Effect of Radiopharmaceutical Dose Extravasation During Injection on Myocardial Perfusion Defects During SPECT Myocardial Perfusion Imaging: A Potential Source of False Negative Result

SPECT Miyokard Perfüzyon Sintigrafisi Sırasında Radyofarmasötik Doz Ekstravazasyonunun Miyokard Perfüzyon Defektlerini Maskeleyen Etkisi: Olası Bir Yanlış Negatif Sonuç Nedeni

© Mohsen Qutbi

Department of Nuclear Medicine, Taleghani Educational Hospital, School of Medicine, Shahid Beheshti University of Medical Sciences, Tehran, Iran

Abstract

Proper interpretation of SPECT myocardial perfusion imaging (MPI) is primarily based on strict adherence to standard procedural protocols from patient preparation to image processing and display. Inadvertent faulty injection of the radiopharmaceutical and, consequently, dose extravasation during SPECT MPI is a more important issue than that in any other diagnostic scintigraphic procedure. As it can be considered as a major source of false negative result, clinician's awareness of this problem during interpretation is of great importance. In some occasions, no local clinical signs or image findings may be available to the interpreter to be aware of dose extravasation to adopt a suitable approach. Herein, we present a case with dose extravasation during stress phase, which is repeated another day with the same protocol, and the potential effects of dose extravasation on SPECT myocardial perfusion images from different aspects and useful image findings as hints are provided.

Keywords: Masking effect, radiopharmaceutical dose extravasation, myocardial perfusion defect, SPECT, false negative

Öz

SPECT miyokard perfüzyon görüntülemenin (MPI) doğru yorumlanması hasta hazırlığından görüntü işlenmesine ve gösterilmesine kadar her aşamada standart protokollere katı bir şekilde uyulmasına bağlıdır. SPECT MPI'de radyofarmasötik için istemsiz olarak hatalı enjeksiyonu ve sonuç olarak doz ekstravazasyonu diğer herhangi bir tanısal sintigrafik işlemde olduğundan daha önemli bir konudur. Yanlış negatif sonucun ana kaynaklarından biri olarak değerlendirildiğinden, yorumlanma sırasında klinisyenin bu sorunun farkında olması büyük önem taşır. Bazı durumlarda, doz ekstravazasyonunun farkında olunmasını sağlayacak lokal belirtiler veya görüntüleme bulguları olmayabileceğinden yorum sırasında bu duruma uygun bir yaklaşım fırsatı olmayabilir. Burada stres fazında doz ekstravazasyonu olan bir hasta sunulmaktadır, görüntüleme aynı protokolle başka bir gün tekrarlanmıştır. Bu bulgular doğrultusunda doz ekstravazasyonunun SPECT MPI üzerinde olası etkileri farklı açılardan ele alınmış ve yararlı görüntüleme bulguları belirtilmiştir.

Anahtar kelimeler: Maskeleyen etkisi, radyofarmasötik doz ekstravazasyonu, miyokard perfüzyon görüntüleme, SPECT, yanlış negatif

Address for Correspondence: Mohsen Qutbi MD, Department of Nuclear Medicine, Taleghani Educational Hospital, School of Medicine, Shahid Beheshti University of Medical Sciences, Tehran, Iran Phone: +989197975902 E-mail: mohsen.qutbi@gmail.com ORCID ID: orcid.org/0000-0002-8347-605X

Received: 15.02.2018 **Accepted:** 24.07.2018

©Copyright 2018 by Turkish Society of Nuclear Medicine
Molecular Imaging and Radionuclide Therapy published by Galenos Yayınevi.

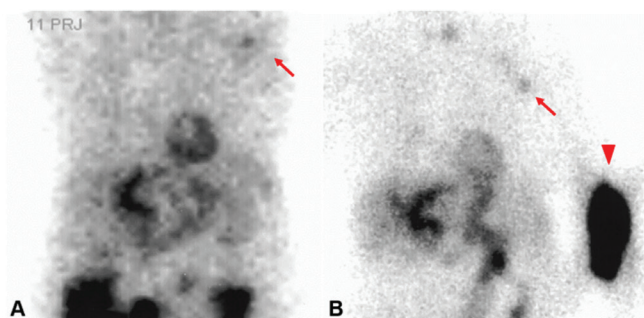


Figure 1. An 84-year-old female with a long history of asthma presented with an episode of chest pain and severe hypertension. The patient denied coronary angiography. Thus, a SPECT myocardial perfusion imaging (MPI) with dobutamine protocol was performed. Anterior projection of the raw cinematic image of stress SPECT MPI study (A) revealed a faint focal uptake in the region of left axilla (shown by arrow) as well as noticeably poor count statistics. In order to confirm the presence of tracer extravasation in the injection site, a planar anterior image with arms by the side (B) was obtained. As can be seen in B, considerable dose extravasation in the left forearm (shown by arrowhead) as well as a faintly hot axillary node ipsilateral to injection site were noted.

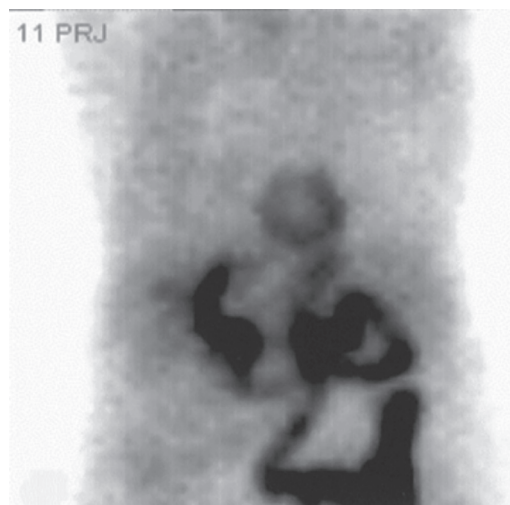


Figure 2. Anterior projection of the raw cinematic image of repeated stress study with the same protocol two days later demonstrated acceptable count statistics of the images without evidence of dose extravasation.

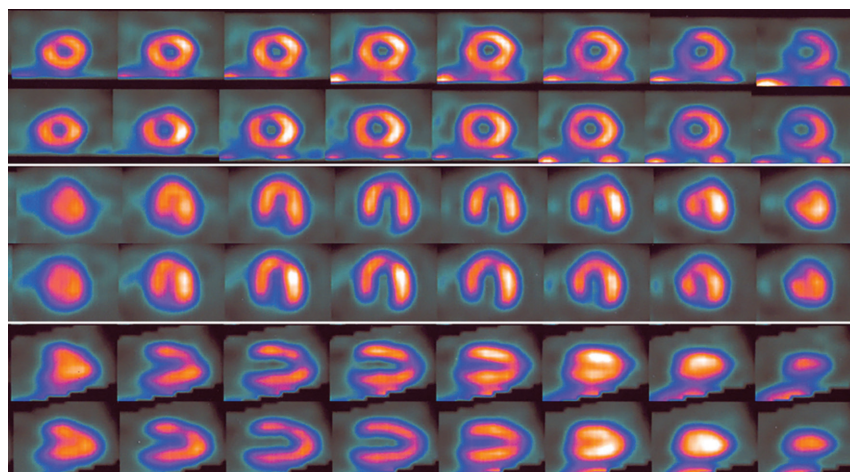


Figure 3. SPECT MPI of the initial study (upper row in each panel) and repeated study (lower row in each panel) showed a uniform tracer distribution in the initial study, but a mild perfusion defect in anterior and septal regions of left ventricular (LV) myocardium in the repeat study. From a technical viewpoint, the radiopharmaceutical with sufficient dose must be injected intravenously at peak stress during exercise or at target heart rate achieved by Dobutamine infusion. An injection with partly extravasated dose into the subcutaneous space effects the result, at least, in two possible ways. First, the amount of radioactivity entering into the circulation and then accumulating in the myocardium is insufficient that may cause a higher degree of noise in SPECT images (1). Second, which is even more troublesome, the extravasated dose gradually seeps out of the subcutaneous tissue into the circulation and then accumulates in the myocardium in the post-stress or resting condition. Therefore, the perfusion defects developing during peak stress may be attenuated or thoroughly masked (2). Moreover, the latter leads to a constantly high level of radioactivity in the background tissues. The added background counting rate and resultant higher scatter radiation are among the main factors of reducing contrast (i.e., myocardium-to-background ratio and defect-to-normal myocardium ratio). The added noise or decreased image information density as a result of lower radioactivity taken up by the myocardium contributes to impediments to visibility of defects, especially low-contrast defects (or mild perfusion defects) (3). As this issue may cause false negative interpretation and necessitates repeat of stress phase, the image should be carefully inspected for any evidence of extravasation. Although poor-count status (or grainy appearance) of the projection images and clumping of radioactivity in the myocardium (i.e., "sausage-string" pattern of LV walls) in tomographic slices (4) are considered as useful hints for dose extravasation, they are not invariably present and depend on the degree of extravasation. In patients with lower amount of extravasation, the decreased image count density might not be noticeable. Delayed images may show even better count statistics as a result of slow absorption of extravasated radioactivity (5). Another finding that implies dose extravasation is the visualization of hot axillary node ipsilateral to the injection site (6). But this is not a flawless way to discover extravasation. In some occasions, the axillary region may be out of the field-of-view and in other occasions, the node may be too faint to be readily visible. An easier and more certain way to realize possible extravasation is checking the injection site before imaging to avoid incorrect interpretation and repeating of the stress phase may be advisable.

Ethics

Informed Consent: Consent form was filled out by all participants.

Peer-review: Externally and internally peer-reviewed.

Financial Disclosure: The author declared that this study received no financial support.

References

1. Taillefer R. The clinical importance of accurate measurement of injected doses for radionuclide myocardial perfusion imaging. *J Nucl Cardiol* 2016;23:265-267.
2. Travin MI. Pitfalls and Limitations of Radionuclide and Hybrid Cardiac Imaging. *Semin Nucl Med* 2015;45:392-410.
3. Image quality in nuclear medicine. In: Cherry SR, Sorenson JA, Phelps ME (eds). *Physics in nuclear medicine*, Philadelphia, Elsevier Saunders, 2012;233-251.
4. Depuey EG. Image artifacts. In: Iskandrian AE, (ed). *Atlas of nuclear cardiology: imaging companion to Braunwald's heart disease*. Philadelphia, Elsevier Saunders, 2012;56-95.
5. Strauss HW, Miller DD, Wittry MD, Cerqueira MD, Garcia EV, Iskandrian AS, Schelbert HR, Wackers FJ. Procedure guideline for myocardial perfusion imaging. Society of Nuclear Medicine. *J Nucl Med* 1998;39:918-923.
6. Shih WJ, Collins J, Kiefer V. Visualization in the ipsilateral lymph nodes secondary to extravasation of a bone-imaging agent in the left hand: a case report. *J Nucl Med Technol* 2001;29:154-155.



Colonic Malignant Melanoma: ¹⁸F-FDG PET/CT Findings

Kolonda Malign Melanoma: ¹⁸F-FDG PET/CT Bulguları

© Eser Kaya, © Tamer Aksoy, © Ahmet Levent Güner, © Hakan Temiz, © Erkan Vardareli

Acıbadem Mehmet Ali Aydınlar University Faculty of Medicine, Department of Nuclear Medicine, İstanbul, Turkey

Abstract

Primary malignant melanoma occurs most often in the skin and much less frequently in the choroid layer of the eyes, in the leptomeninges, oral cavity, nasal mucosa, pharynx, esophagus, bronchus, under the nail and vaginal or anorectal mucosa. Primary melanoma of the gastrointestinal tract has been confirmed for lesions occurring in the esophagus, stomach, small bowel, and anorectum through several published reports, as these are the areas where melanocytes normally exist. The occurrence of primary malignant melanoma in the colon is relatively rare, because melanocytes are embryologically absent in the large bowel. Herein we report a patient whose colonic malignant melanoma was diagnosed and disseminated metastatic lesions were revealed with ¹⁸F-FDG PET/CT scan. There were multiple nodular lesions showing increased ¹⁸F-FDG uptake in both lungs. There was a soft tissue lesion with slightly increased ¹⁸F-FDG uptake, which extended to the intraluminal region of the thoracic esophagus. Increased metabolic activity was detected in the asymmetric stomach wall thickening site and in a soft tissue lesion located on the gall bladder wall that was filling the lumen. Multiple hypodense/hyper-metabolic lesions were identified in the liver. Multiple hyper-metabolic polypoid soft tissue lesions were visualized in almost the entire colonic segments. Multiple hyper-metabolic peritoneal implants were noted in all abdominal quadrants. Increased ¹⁸F-FDG uptake was detected at the right surrenal gland soft tissue lesion. There was a hyper-metabolic soft tissue lesion on the posterior wall of the rectum. Hyper-metabolic lytic lesions were seen at the thoracic and lumbar vertebrae, left scapula, left iliac bone, sacrum and left femur. There was no evidence of ¹⁸F-FDG avid skin lesions in both attenuation corrected and non-corrected images.

Keywords: Colon, malignant melanoma, ¹⁸F-FDG PET/CT

Öz

Primer malign melanom sıklıkla deride ortaya çıkmaktadır, daha az sıklıkla da, gözün koroid tabakasında, leptomeninkslerde, oral kavitede, nazal mukozada, farinkste, özefagusta, bronşlarda, tırnak altında, vagende ve anorektal mukozada izlenmektedir. Primer gastrointestinal sistem melanomu, melanositlerin normal olarak bulunduğu yerlerden özofagus, mide, ince barsakta ve anorektumda bildirilmiştir. Melanositler embriyolojik olarak kalın barsakta bulunmadığından, kolonda primer malign melanom oluşumu nadirdir. Bu makalede kolon malign melanoma tanısı alan ve ¹⁸F-FDG PET/CT taramasında dissemine metastatik lezyonları olan bir hastayı sunuyoruz. Her iki akciğerde artmış ¹⁸F-FDG tutulumu gösteren multipl nodüler lezyonlar vardı. Özefagus torakal segmentte, intraluminal alana taşan ılımlı düzeyde ¹⁸F-FDG tutulumu gösteren yumuşak doku lezyonu vardı. Asimetrik mide duvar kalınlaşmasında ve safra kesesi duvarında lümeni dolduran yumuşak doku lezyonlarında artmış metabolik aktivite görüldü. Karaciğerde multipl hipodens/hipermetabolik lezyonlar görüldü. Hemen tüm kolon segmentlerinde multipl hipermetabolik polipoid/yumuşak doku lezyonları görüldü. Tüm abdominal kadrantlarda multipl hipermetabolik peritoneal implantlar saptandı. Sağ sürrenal bez yumuşak doku lezyonunda artmış ¹⁸F-FDG tutulumu tespit edildi. Rektumun arka duvarında hipermetabolik yumuşak doku lezyonu vardı. Torakal ve lomber vertebralarda, sol skapulada, sol iliak kemikte, sakrumda ve sol femur boynunda hipermetabolik litik lezyonlar görüldü. Atenuasyon düzeltmesi yapılan ve yapılmayan görüntülerde, ¹⁸F-FDG tutulumu olan deri lezyonu lehine bulgu yoktu.

Anahtar kelimeler: Kolon, malign melanom, ¹⁸F-FDG PET/CT

Address for Correspondence: Eser Kaya MD, Acıbadem Kayseri Hospital, Clinic of Nuclear Medicine, Kayseri, Turkey

Phone: +90 352 207 39 76/77 E-mail: esermd@yahoo.com ORCID ID: orcid.org/0000-0003-2931-9974

Received: 06.02.2018 **Accepted:** 13.07.2018

©Copyright 2018 by Turkish Society of Nuclear Medicine
Molecular Imaging and Radionuclide Therapy published by Galenos Yayınevi.

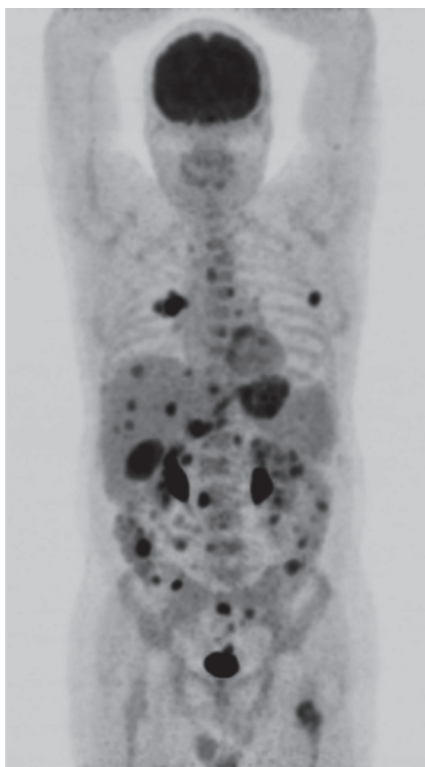


Figure 1. ^{18}F -FDG maximum intensity projection image. Colonoscopy examination of a 51-year-old man, whose only complaint was severe rectal bleeding, revealed multiple, large necrotic polypoid lesions in all colonic segments. Excisional biopsy has been performed from the sigmoid region. Histopathologic findings and immunohistochemistry analyses including S-100, HMB45 and vimentin were positive and all these findings strongly suggested colonic malignant melanoma. Ophthalmologic, dermatologic and ear-nose-throat examinations were negative for primary melanoma or any melanocytic lesion, thus the case was diagnosed as a colonic malignant melanoma. Melanomas within the gastrointestinal (GI) tract are usually metastatic in origin (1). However, some colonic melanomas are true primary tumors. The probable genesis of such tumors involves a concept of “ectodermal differentiation” - that ectodermal cells are capable of differentiation into multiple cell lines and may variably migrate into the colon during embryologic stages to develop into melanocytes (2). Primitive stem cells localized within the GI tract wall may also give rise to heterotopic melanocytes in the colon (3).

Ethics

Informed Consent: Consent form was filled out by all participants.

Peer-review: Externally and internally peer-reviewed.

Authorship Contributions

Surgical and Medical Practices: E.K., T.A., A.L.G., H.T., E.V., Concept: E.K., T.A., Design: E.K., Data Collection or Processing: E.K., Analysis or Interpretation: E.K., T.A., E.V., Literature Search: E.K., Writing: E.K., T.A.

Conflict of Interest: No conflict of interest was declared by the authors.



Figure 2. Markedly increased ^{18}F -FDG uptake is seen in soft tissue lesions of the colonic hepatic flexure, which was the largest lesion in this patient.

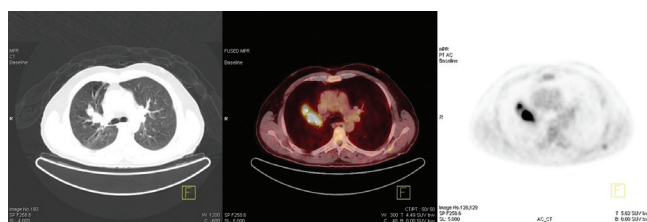


Figure 3. Increased ^{18}F -FDG uptake is detected in the lobulated contoured mass lesion at the right upper lung lobe anterior segment.



Figure 4. Hyper-metabolic soft tissue lesion located in the gallbladder wall and the entire lumen is viewed.

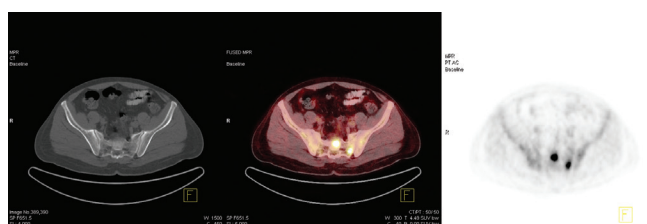


Figure 5. Hyper-metabolic, lytic lesions are visualized at the sacrum.

Financial Disclosure: The authors declared that this study has received no financial support.

References

- Serin G, Doğanavşargil B, Calışkan C, Akalin T, Sezak M, Tunçyürek M. Colonic malignant melanoma, primary or metastatic? Case report. *Turk J Gastroenterol* 2010;21:45-49.
- Takahashi-Monroy T, Vergara-Fernandez O, Aviles A, Morales JM, Gatica E, Suarez E. Primary melanoma of the colon presenting as ileocecal intussusception. *Am J Gastroenterol* 2006;101:676-677.
- Hazzan D, Reissman P, Halak M, Resnick MB, Lotem M, Shiloni E. Primary rectal malignant melanoma: report of two cases. *Tech Coloproctol* 2001;5:51-54.



Lung Perfusion Imaging in Tetralogy of Fallot: A Case Report

Fallot Tetralojisinde Akciğer Perfüzyon Görüntüleme: Bir Olgu Sunumu

Artor Niccoli Asabella, Alessandra Cimino, Corinna Altini, Valentina Lavelli, Giuseppe Rubini
Bari University Aldo Moro, Unit of Nuclear Medicine, Bari, Italy

Abstract

Congenital heart diseases, such as tetralogy of fallot (TOF), are the most common human birth defects that may cause pulmonary diseases. Lung perfusion scintigraphy (LPS) has an important role in evaluating pulmonary involvement in patients with these defects, both as part of the diagnostic work-up and for follow-up to guide best therapeutic strategy. Herein, we report a 10-year-old female patient with TOF who underwent LPS two years after cardiac surgery. The scan showed hypoperfusion of the left respect to the right lung and abnormal uptake of Tc-99m-macroaggregated albumin in the kidneys and spleen, revealing the presence of a right-to-left shunt, and the necessity for further cardiac surgery. This case is a demonstrative example of the usefulness of LPS in patients with TOF, allowing an accurate evaluation of the best therapeutic strategy with the benefits of low radiation exposure, lack of side effects, reproducibility, management ease and good patient compliance.

Keywords: Lung scintigraphy perfusion, congenital heart disease, tetralogy of fallot, right-to-left shunt

Öz

Fallot tetralojisi (TOF) gibi konjenital kalp hastalıkları, pulmoner hastalıklara neden olabilecek en yaygın doğumsal kusurlardandır. Akciğer perfüzyon sintigrafisi (LPS), bu hastalarda akciğer yükünün değerlendirilmesinde, en iyi tedavi stratejisini belirlemede ve takip sürecinde önemli bir role sahiptir. Bu yazıda 10 yaşında kardiyak cerrahiden iki yıl sonra LPS uygulanan TOF'lu bir kız hasta bildirilmektedir. Sağ akciğer sol altta hipo-perfüzyon ile birlikte böbreklerde ve dalakta anormal Tc-99m-makro albümin tutulumu, sağdan sola şant varlığını ve ileri kardiyak cerrahinin gerekliliğini ortaya koydu. Bu olgu, LPS'nin TOF hastalarında yararının bir örneği olup, bu teknik düşük radyasyon maruziyeti, yan etkisinin olmaması, tekrarlanabilirliği, kolay yöntemi ve iyi hasta uyumu ile en iyi tedavi stratejisinin doğru olarak değerlendirilmesini sağlar.

Anahtar kelimeler: Akciğer perfüzyon sintigrafisi, konjenital kalp hastalığı, fallot tetralojisi, sağdan-sola şant

Address for Correspondence: Artor Niccoli Asabella MD, Bari University Aldo Moro, Unit of Nuclear Medicine, Bari, Italy
Phone: +390805592913 E-mail: artor.niccoliasabella@uniba.it ORCID ID: orcid.org/0000-0002-1227-029X

Received: 18.07.2017 **Accepted:** 13.07.2018

©Copyright 2018 by Turkish Society of Nuclear Medicine
Molecular Imaging and Radionuclide Therapy published by Galenos Yayınevi.

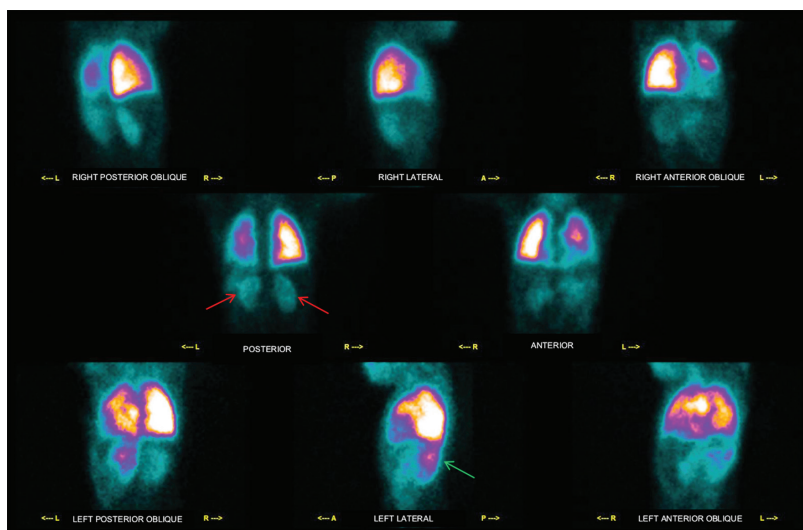


Figure 1. Congenital Heart diseases (CHD), such as tetralogy of fallot (TOF), are the most common human birth anomalies with severity depending on the anatomical defect with subsequent different clinical impact and management (1).

CHD may be associated with pulmonary hemodynamic defects so it is important to know lung perfusion status, since its asymmetry is a predictor of exercise capacity and outcome (2). Lung perfusion scintigraphy (LPS) is the gold standard for qualitative and semi-quantitative evaluation of pulmonary perfusion in patients with CHD (3). We report a case of a 10-year-old female patient with cyanotic spells, hypoxia and squatting episodes since birth that progressively increased during the years. A computed tomography angiography performed with a presumptive diagnosis of CHD revealed a cardiac anatomy as in TOF and the patient was admitted to pediatric cardiac surgery clinic according to the European Society of Cardiology guidelines. Her post-operative second year follow-up physical examination revealed clubbing and hypoxia as well as continuous murmur over the chest. Her abdomen was soft with normal bowel sounds and no organ enlargement. The chest X-ray suggested lung inflammatory interstitial disease without focal lesions, pleural effusion or cardiomegaly, her blood work-up revealed Hb: 10.5 gr/dL (normal values 11-13 g/dL), Htc: 36.8% (normal values 35-42%), and fibrinogen protein: 630 mg/dL (normal values 150-400 mg/dL). The patient underwent LPS by intravenous injection of 111 MBq Tc-99m-macroaggregated albumin to evaluate pulmonary hemodynamics and impairment. This figure depicts images of the thorax-abdomen acquired in all the 8 executable planar projections (i.e. right posterior oblique, right lateral, right anterior oblique, posterior, anterior, left posterior oblique, left lateral, left anterior oblique). LPS showed 80% radiopharmaceutical uptake in the lungs and the remnant 20% in the kidneys (red arrows) and spleen (green arrows). This finding supported the presence of a right-to-left shunt, and the patient was kept in close follow-up to be scheduled for further cardiac surgery.

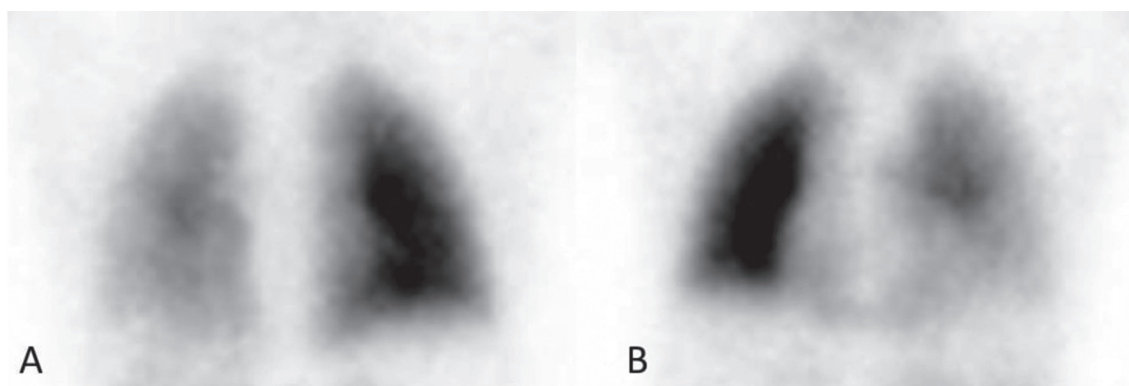


Figure 2. LPS is a functional diagnostic tool that records the distribution of pulmonary arterial blood flow. The most common clinical indications for LPS are to detect pulmonary embolism, to quantify differential pulmonary perfusion before surgery or in chronic disorders, to evaluate the cause of pulmonary hypertension and assessment for lung transplantation.

In patients with CHD, LPS evaluates the co-existence of congenital heart and lung hemodynamic defects such as cardiac shunt, pulmonary arterial stenosis, arteriovenous fistula and their treatment (4). LPS can depict normal symmetrical perfusion, unilateral absent or decreased perfusion, or multiple segmental abnormalities in patients with CHD. It allows to define the presence of a right to left shunt due to the presence of aortic-pulmonary collateral vessels, associated with cyanogenic CHDs such as TOF (5). This LPS figure shows the thorax in detail, in the posterior (A) and anterior (B) projections, which clearly depicts hypo-perfusion of the left lung as compared to the right.

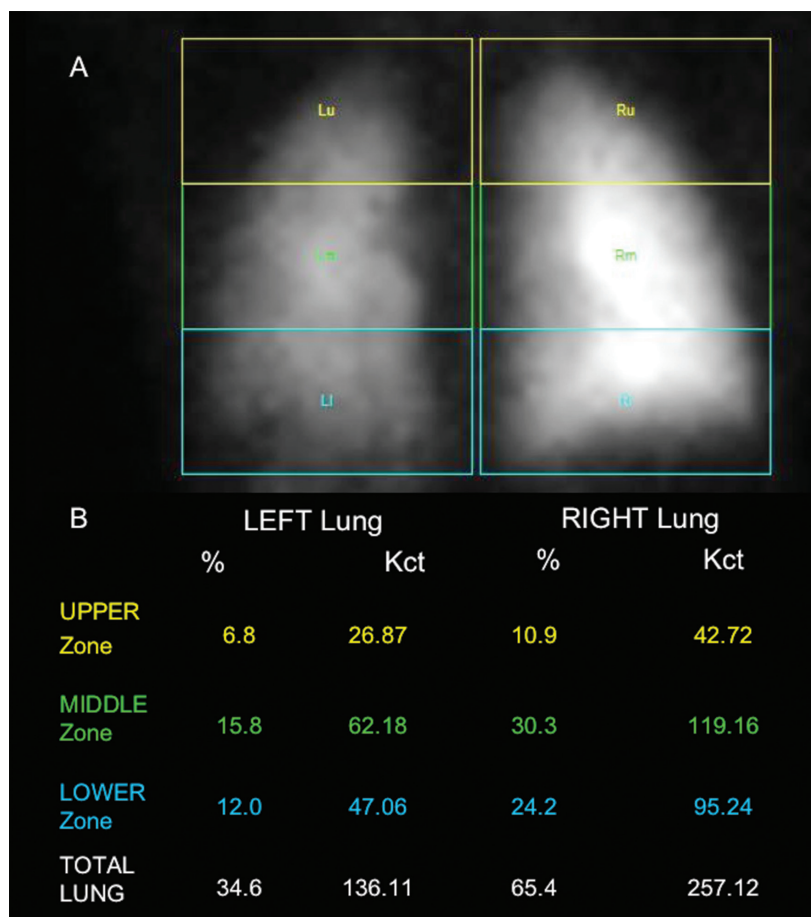


Figure 3. Semi-quantitative analysis identified significant reduction of radiopharmaceutical uptake in the upper, middle and lower regions of the left lung with respect to the right (A) and confirmed left lung hypo-perfusion (B), thus requiring further surgery. LPS has an important role in the diagnosis, as part of work-up for better patient management, and during follow-up to confirm surgery or therapy success in patients with CHD (6). Our case is a demonstrative example of LPS usefulness in the evaluation of lung hemodynamic effects in pediatric patients with TOF, allowing an accurate evaluation of the best therapeutic strategy with benefits of low radiation exposure, lack of adverse effects, reproducibility, management ease and good patient compliance.

Acknowledgements

Dino Rubini for graphic support in preparing the figures.

Ethics

Informed Consent: Consent form was filled out by all participants.

Peer-review: Externally and internally peer-reviewed.

Authorship Contributions

Surgical and Medical Practices: A.N.A., G.R., Concept: C.A., A.C., Design: A.C., V.L., Analysis or Interpretation: A.N.A., G.R., Literature Search: A.C., Writing: C.A., A.C.

Conflict of Interest: No conflict of interest was declared by the authors.

Financial Disclosure: The authors declared that this study received no financial support.

References

- Hoffman JI, Kaplan S, Liberthson RR. Prevalence of congenital heart disease. *Am Heart J* 2004;147:425-439.
- Zeng Z, Zhang H, Liu F, Zhang N. Current diagnosis and treatments for critical congenital heart defects. *Exp Ther Med* 2016;11:1550-1554.
- Sun R, Liu M, Lu L, Zheng Y, Zhang P. Congenital heart disease: Causes, diagnosis, symptoms, and treatments. *Cell Biochem Biophys* 2015;72:857-860.
- Fathala A. Quantitative Lung Perfusion Scintigraphy in Patient with Congenital Heart Disease. *Heart Views* 2010;11:109-114.
- Parker JA, Coleman RE, Grady E, Royal HD, Siegel BA, Stabin MG, Sostman HD, Hilson AJ; Society of Nuclear Medicine. SNM Practice Guideline for Lung Scintigraphy 4.0. *J Nucl Med Technol* 2012;40:57-65.
- Niccoli Asabella A, Stabile Ianora AA, Di Palo A, Rubini D, Pisani AR, Ferrari C, Notaristefano A, Rubini G. Lung perfusion scintigraphy in pediatric patients with congenital malformations. *Recenti Prog Med* 2013;104:442-445.

Affirmation of Originality and Assignment of Copyright

This form must be filled in thoroughly and uploaded to the website during the submission

The author(s) hereby affirms that the manuscript entitled:

is original, that all statement asserted as facts are based on author(s) careful investigation and research for accuracy, that the manuscript does not, in whole or part, infringe any copyright, that it has not been published in total or in part and is not being submitted or considered for publication in total or in part elsewhere.

In signing this form, each author acknowledge that he/she participated in the work in a substantive way and is prepared to take public responsibility for the work.

In signing this form, each author further affirms that he or she has read and understands the "Ethical Guidelines for Publication of Research".

The author(s), in consideration of the acceptance of the above work for publication, does hereby assign and transfer to the Molecular Imaging and Radionuclide Therapy all of the rights and interest in and the copyright of the above titled work in its current form and in any form subsequently revised for publication and/or electronic dissemination.

All authors must sign in the order in which each is listed in the authorship.

	Date	Name (print)	Signature
1.
2.
3.
4.
5.
6.
7.
8.
9.
10.

Disclosure Form for Potential Conflicts of Interest

Information about the support of this work under consideration for publication.

Did you or your institution at any time receive payment or support in kind for any aspect of the submitted work (including but not limited to grants, data monitoring board, study design, manuscript preparation, statistical analysis, etc...)?

Name	No	Yes (Specify nature of compensation)
1.	<input type="checkbox"/>	<input type="checkbox"/>
2.	<input type="checkbox"/>	<input type="checkbox"/>
3.	<input type="checkbox"/>	<input type="checkbox"/>
4.	<input type="checkbox"/>	<input type="checkbox"/>
5.	<input type="checkbox"/>	<input type="checkbox"/>
6.	<input type="checkbox"/>	<input type="checkbox"/>
7.	<input type="checkbox"/>	<input type="checkbox"/>
8.	<input type="checkbox"/>	<input type="checkbox"/>
9.	<input type="checkbox"/>	<input type="checkbox"/>
10.	<input type="checkbox"/>	<input type="checkbox"/>

Information about relevant financial relationships outside the submitted work.

Please specify if you have financial relationships (regardless of amount of compensation) with any entities that have an interest related to the submitted work like board membership, consultancy, employment, expert testimony, gifts, grants, honoraria, payment for manuscript preparation, patents, royalties, payment for development of educational presentations including service on speakers' bureaus, travel/accommodations expenses covered or reimbursed, stock/stock options, others.

Name	No	Yes (Specify the nature and the entity)
1.	<input type="checkbox"/>	<input type="checkbox"/>
2.	<input type="checkbox"/>	<input type="checkbox"/>
3.	<input type="checkbox"/>	<input type="checkbox"/>
4.	<input type="checkbox"/>	<input type="checkbox"/>
5.	<input type="checkbox"/>	<input type="checkbox"/>
6.	<input type="checkbox"/>	<input type="checkbox"/>
7.	<input type="checkbox"/>	<input type="checkbox"/>
8.	<input type="checkbox"/>	<input type="checkbox"/>
9.	<input type="checkbox"/>	<input type="checkbox"/>
10.	<input type="checkbox"/>	<input type="checkbox"/>